



DOCTORAL DISSERTATION

**Technological applications for human health
and performance across different environments**

By:

Konstantinos Mantzios

Supervisors:

Dr. Andreas D. Flouris

*A thesis submitted in fulfillment of the requirements
for the degree of Doctor of Philosophy in the*

Department of Physical Education and Sport Science, University of Thessaly

June 15, 2023

Members of the examination committee (in alphabetical order).

Full name	University	Information
Andreas D. Flouris	University of Thessaly	Supervisor
Ioannis Koutentakis	University of Thessaly	UTH committee
Athanasios Jamurtas	University of Thessaly	UTH committee
Ioannis Giakas	University of Thessaly	UTH committee
Dimitrios E. Tsaopoulos	Centre for Research and Technology – Hellas	External examining committee
Spyros Panagiotakis	Hellenic Mediterranean University	External examining committee
Costas Panagiotakis	Hellenic Mediterranean University	External examining committee

Declaration

I, Konstantinos Mantzios, hereby declare that this thesis has not been previously submitted in this University or any other University for the award of any degree, diploma, associateship, fellowship, or other similar titles of recognition.

Thesis title: Technological applications for human health and performance across different environments.
Pages: 203
Words: 42,493
Figures: 65
Tables: 15

PhD candidate: Konstantinos Mantzios
Signed by: Konstantinos Mantzios
Date: June 15, 2023

Plagiarism Disclaimer

I declare that this thesis is based on a total of five studies/papers of which four (Chapter 2, Chapter 3, Chapter 4 and Chapter 5) have been published and one is in preparation. These papers are referred to and cited in the thesis chapters (with specification in the intro to each chapter of the study/paper referenced).

Published articles

- Chapter 2** ¹ Effects of Weather Parameters on Endurance Running Performance: Discipline-specific Analysis of 1258 Races
- Chapter 3** ² Risk assessment for heat stress during work and leisure
- Chapter 4** ³ Towards model-based online monitoring of cyclist's head thermal comfort: smart helmet concept and prototype
- Chapter 5** ⁴ Night-Time Heart Rate Variability during an Expedition to Mt Everest: A Case Report

Articles in preparation

- Chapter 6** Free Web Tool for Heat Strain Mitigation: Aligning with ISO 7933:2018 Standards

PhD candidate: Konstantinos Mantzios
Signed by: Konstantinos Mantzios
Date: june15, 2023

Dedicated to my loving family.

Acknowledgments

During my PhD, I've been lucky to travel a lot and meet many different people. They all helped me grow academically and personally. My advisor, Dr. Andreas D. Flouris, has been really patient and supportive. His guidance, insightful feedback, and wealth of knowledge have not only shaped my research but also inspired me to reach new heights in my field.

I gratefully acknowledge that this work was supported by funding from the European Union's Horizon 2020 research and innovation programme under the grant agreements no. 645770 (Smart HELMET project) and no. 668786 (HEAT-SHIELD project). Also, some of the studies conducted have received funding from the International Labour Organization (Contract Number: 40262271 / 1).

I was part of the FAME Lab team for seven great years. I'm really thankful to all the team members for their continuous support and the memories we've made.

My family has been really important in this journey. Their constant love, support, and belief in me helped me during hard times.

Last but certainly not least, my partner, Zoe. Her love, understanding, and faith in me have always motivated and inspired me to persevere and reach new heights throughout my PhD journey.

Table of Contents

Abstract.....	15
Περίληψη.....	17
General Introduction.....	20
Chapter 1	23
1. Smart Helmet.....	24
2. Sweat Rate System	29
3. Portable Temperature Logger	33
4. Web Thermometer Tracker	38
5. GPS Tracker.....	42
6. Task Analysis App	45
7. Questionnaire App.....	47
8. FL-WebPHS	48
Chapter 2	50
Abstract	51
Introduction.....	52
Methods.....	53
Performance data.....	53
Weather data	54
Data management and statistical analysis.....	55
Results	57
Weather data and cross-validity	57
Performance impacts of weather parameters	59
Discussion	64
Methodological considerations	66
Acknowledgments.....	69
Chapter 3	70
Abstract	71
Introduction.....	72
Factors affecting the risk for heat strain	74
1. Acclimatization	74
2. Aging.....	74
3. Anthropometrics	75
4. Clothing.....	79
5. Cultural habits	79
6. Diet	80

7. Disabilities.....	81
8. Drugs and addictions.....	81
9. Environmental stress.....	83
10. Ethnicity	84
11. Heat mitigation	85
12. Medical conditions.....	86
13. Metabolic demands	86
14. Physical fitness	87
15. Sex.....	87
16. Sleep deprivation	88
17. Work duration.....	89
18. Work experience	89
Concluding remarks.....	91
Chapter 4	93
Abstract	94
Introduction.....	95
Materials and Methods	98
Development of General Thermal Comfort Predictive Model.....	99
Experimental Setup and Test Subjects	99
Pretest Experiments	100
Thermal Comfort and Variable Screening Experimental Protocol.....	101
General Linear Regression (LR) Model Identification and Offline Parameter Estimation.....	103
Development of Smart Helmet Prototype	104
Testing the Developed Smart Helmet Prototype.....	105
Test Subjects.....	105
Experimental Design and Protocol.....	106
Results	107
Pretest Experiments.....	107
Development of Offline (General) Thermal Comfort Model.....	108
Testing the SmartHelmet Prototype and Validation of the Developed General Model.....	114
Introduction of Online Personalisation and Adaptive Modelling Algorithm	117
Offline Linear Regression Model.....	119
Streaming Data.....	119
Online Parameter Estimation Algorithm	119
Conclusions	121

Acknowledgments.....	122
Chapter 5	123
Abstract	124
Introduction.....	125
Materials and Methods	126
Results	130
Discussion	131
Conclusions	133
Acknowledgments.....	133
Chapter 6	134
Abstract	135
Introduction.....	136
Methods.....	137
Development of the FL-WebPHS.....	137
FL-WebPHS optimization.....	139
Unlimited different time periods:.....	139
Unit conversion flexibility:.....	140
Expanded results and export capabilities:	140
Validating FL-WebPHS for athletes	140
Results	142
Discussion	145
General Conclusions	148
Future Directions	151
Limitations	152
Epilogue	153
References.....	154
Appendixes	170
Appendix A: Detailed Visualization and Functional Description of the FL-WebPHS Software Components	170
Appendix B: Effects of weather parameters on endurance running performance: discipline specific analysis of 1258 races.....	177
Annexes	197
Annex A: Ethics	197
Annex B: Student’s Contribution in Paper	200

List of Figures

Figure 1.1.1 Smart Helmet Prototype.	24
Figure 1.1.2 Schematic of Smart Helmet.	25
Figure 1.1.3 Smart Helmet code representation.	26
Figure 1.1.4 Snapshot of the Smart Helmet App in action.	28
Figure 1.2.1 Schematic of Sweat Rate System.....	29
Figure 1.2.2 Sweat Rate System.	30
Figure 1.2.3 Sweat Rate code representation.....	31
Figure 1.3.1 Portable Temperature Logger.....	33
Figure 1.3.2 Schematic of Portable Temperature Logger	34
Figure 1.3.3 Portable Temperature Logger code representation.....	35
Figure 1.3.4 Snapshot of the Portable Temperature Logger App in action.....	37
Figure 1.4.1 Web Thermometer Tracker prototype.	38
Figure 1.4.2 Schematic of Web Thermometer Tracker	39
Figure 1.4.3 Web Thermometer Tracker code representation.....	40
Figure 1.4.4 Snapshot of the Web Thermometer Tracker software in action.....	41
Figure 1.5.1 Schematic of GPS Tracker.	42
Figure 1.5.2 GPS Tracker code representation.	43
Figure 1.6.1 Infographic Demonstrating the Task Analysis App in use.	45
Figure 1.6.2 Task Analysis App.....	46
Figure 1.7 Questionnaire App.....	47
Figure 1.8 FL-WebPHS.	48
Figure 2.1 Endurance Events and Heat Stress.....	58
Figure 2.2 Decision tree classification.	60
Figure 2.3 Feature importance scores.....	61
Figure 2.4 WBGT Performance decrement.	62
Figure 2.5 Heat Stress and Marathon Performance.	63

Figure 3.1 Graphical illustration of the factors affecting the risk for experiencing heat strain.	73
Figure 3.2 Decision tree classifying.	78
Figure 3.3 Differences in the physiological.	83
Figure 3.4 Differences in work activities.	91
Figure 4.1 Schematic diagram of the smart helmet prototype.	98
Figure 4.2 Representation of customized wind tunnel.	100
Figure 4.3 Power values of pretest.	108
Figure 4.4 The recorded measurements of the different variables obtained from test subject 1.	109
Figure 4.5 Model prediction traces.	111
Figure 4.6 Average values of RPE, TC, and TS.	115
Figure 4.7 Obtained data during the TT.	116
Figure 4.8 Personalisation algorithm.	118
Figure 5.1 40-day Mt Everest expedition.	128
Figure 5.2 Results for the HRV values.	131
Figure 6.1 FL-WebPHS main screen.	139
Figure 6.2 Linear relationship.	143
Figure 6.3 Average observed and predicted values.	144
Figure 6.4 95% limits of agreement.	144
Figure 6.5 Violin plot.	145
Figure A.1 Component based on ISO 7933:2018.	170
Figure A.2 Covered Body Surface Area.	171
Figure A.3 Reflection Coefficients.	171
Figure A.4 Clothing Insulation.	172
Figure A.5 Metabolic Rate.	173
Figure A.6 FL-WebPHS Results.	174
Figure A.7 Raw data table.	175

Figure A.8 ISO 7933:2018 Results.....	176
Figure B.1 Performance decrement (competition’s standing record)	185
Figure B.2 Performance decrement (event’s world record).....	186
Figure B.3 Percentage and number of races for 1258 races held between 1936 and 2019.....	187
Figure B.4 Decision tree (50km race-walk).....	188
Figure B.5 Decision tree (20km race-walk).....	189
Figure B.6 Decision tree (10,000m).....	190
Figure B.7 Decision tree (5,000m).....	191
Figure B.8 Decision tree (3,000m-steeplechase).....	192
Figure B.9 Impact of heat stress on 50km race-walk.....	193
Figure B.10 Impact of heat stress on 20km race-walk.....	194
Figure B.11 Impact of heat stress on 10,000m.....	195
Figure B.12 Impact of heat stress on 5,000m.....	196

List of Tables

Table 1 Overview of developed technologies during PhD research.	23
Table 4.1 The applied values for each variable.	101
Table 4.2 Thermal comfort scale introduced by Gagge et al. ¹⁸⁸ , excluding the cold sensation votes.	102
Table 4.3 Experimental design	103
Table 4.4 The mean average power output, pedalling cadence and 30 km time-trial (TT) obtained from all test subjects.	107
Table 4.5 Estimation results.	110
Table 4.6 Estimation results.	112
Table 6.1 FL-WebPHS software.	137
Table B1 Official websites of each competition.	177
Table B2 Summary of best hyperparameters and testing estimations for each event.	178
Table B3 Cross validity statistics.	179
Table B4 Competition statistics.	180
Table B5 World Athletics Gold Label Races.	182
Table B6 Decision tree analysis.	183
Table B7 Regression equations.	184

Abstract

The aim of this thesis was to explore the intersection of technology and its application in optimizing human performance and protecting health under various environmental conditions. Comprising six chapters, the research investigated the use of wearables, artificial intelligence, and data analytics in varying scenarios, from challenging work environments to endurance sports in extreme conditions. The first study utilized machine learning algorithms to analyze the impact of weather parameters on peak performance during endurance running events. It established that weather conditions significantly influence performance and recommended thorough evaluation of weather parameters and adoption of heat mitigation strategies. Using similar machine learning techniques, the research delved into assessing the critical factors that contribute to the risk of heat strain during work and leisure activities. The analysis identified work duration and body mass index as significant factors influencing individuals' exposure to heat stress. The thesis further delved into improving the comfort of bicyclists by developing an adaptive model for monitoring head thermal comfort in helmets. A SmartHelmet prototype, equipped with sensors, was created to ensure continuous data streaming and precise comfort prediction. In a move to more extreme conditions, a case report analyzing the impact of high altitude on sleep quality and heart rate variability in a Mt. Everest climber revealed a progressive reduction in sleep quality and heart rate variability at altitudes above 5500m. Finally, a new web tool was developed, complying with ISO 7933:2018 standards, to estimate heat strain under various environmental conditions. In summary, this thesis significantly enhanced the understanding of how technological innovations can optimize human performance and protect health in diverse environmental conditions, laying the groundwork for future research and technological advancements in these domains.

Keywords: Technology; Performance; Health; Extreme Conditions; Machine Learning; Heat Mitigation

Περίληψη

Στόχος της παρούσας διατριβής ήταν να εξερευνήσει τη συμβολή της τεχνολογίας στη προάσπιση της υγείας και την βελτίωση της απόδοσης των ανθρώπων κατά την έκθεση σε διάφορες περιβαλλοντικές συνθήκες. Αποτελείται από έξι κεφάλαια, που αναλύουν την εφαρμογή των φορητών συσκευών, της τεχνητής νοημοσύνης και της ανάλυσης δεδομένων σε διάφορες καταστάσεις και ομάδες, όπως εργαζόμενοι και αθλητές. Στην αρχική μελέτη, η μηχανική μάθηση χρησιμοποιήθηκε για να αναλύσει την επίδραση των καιρικών παραμέτρων στην αθλητική απόδοση κατά τη διάρκεια μεγάλων αθλητικών διοργανώσεων σε δρομικά αγωνίσματα αντοχής. Διαπιστώθηκε ότι ο καιρός επηρεάζει σημαντικά την απόδοση των αθλητών και συνιστάτε η αξιολόγηση όλων των παραμέτρων του καιρού και η υιοθέτηση στρατηγικών μετριασμού της ζέστης κατά την διοργάνωση μεγάλων αθλητικών διοργανώσεων. Στη συνέχεια, η έρευνα χρησιμοποιώντας αντίστοιχες τεχνικές μηχανικής μάθησης, διερεύνησε τους κρίσιμους παράγοντες που συνεισφέρουν στον κίνδυνο εμφάνισης θερμικού στρες κατά τη διάρκεια της εργασίας. Από τα αποτελέσματα προέκυψε πως η διάρκεια της εργασίας και ο δείκτης μάζας σώματος αποτελούν τους πιο σημαντικούς παράγοντες εμφάνισης θερμικού στρες κατά την εργασία. Μετέπειτα, οι ερευνητικές προσπάθειες στράφηκαν στην χρήση αισθητήρων, ειδικότερα στη βελτίωση της θερμικής άνεσης των ποδηλατών μέσω της ανάπτυξης ενός μοντέλου για την παρακολούθηση της θερμοκρασίας στο κεφάλι. Για αυτόν τον σκοπό, δημιουργήθηκε ένα πρωτότυπο "έξυπνο" κράνος, εξοπλισμένο με αισθητήρες, που διασφαλίζει την συνεχή παρακολούθηση με στόχο την ακριβή πρόβλεψη της θερμικής άνεσης. Μεταβαίνοντας σε πιο ακραίες συνθήκες, μια περιπτώσιολογική μελέτη διερεύνησε την επίδραση του υψόμετρου στην ποιότητα του ύπνου και την μεταβλητότητα του καρδιακού παλμού κατά την διάρκεια αναρρίχησης στο βουνό Έβερεστ. Τα ευρήματα έδειξαν ότι σε υψόμετρα πάνω από 5500 μέτρα, η ποιότητα του ύπνου και η

μεταβλητότητα του καρδιακού παλμού σταδιακά μειώνονται. Ολοκληρώνοντας, αναπτύχθηκε ένα διαδικτυακό εργαλείο το FL-WebPHS. Ακολουθώντας τα πρότυπα ISO 7933:2018 είναι σε θέση να εκτιμήσει το θερμικό στρες σε διάφορες περιβαλλοντικές συνθήκες. Συνοπτικά, αυτή η διατριβή βελτίωσε σημαντικά την κατανόηση του πώς διάφορες τεχνολογίες μπορούν να βελτιστοποιήσουν την ανθρώπινη απόδοση και να προστατεύσουν την υγεία σε διάφορες περιβαλλοντικές συνθήκες, δημιουργώντας τα θεμέλια για μελλοντική έρευνα και τεχνολογικές εξελίξεις γύρω από αυτούς τους τομείς.

Λέξεις-κλειδιά: Τεχνολογία; Απόδοση; Υγεία; Ακραία Περιβάλλοντα; Μηχανική Μάθηση; Μετρισμός Θερμότητας

General Introduction

Technological applications for human health and performance across different environments

Currently, the global landscape is characterized by a growing technological increment aimed at improving human health and performance⁵⁻⁹. The 21st century is marked by progressive technological innovations that have reshaped our existence, leaving a significant impact on a wide array of sectors, ranging from sports^{10,11} to work^{7-9,12-14}. At the same time, the world is seeing environmental changes that are creating challenges for people's health and performance.^{15,16} Climate change, leading to more frequent and intense heatwaves, extreme weather events, and shifts in temperature patterns,^{17,18} has direct implications for human well-being, including physical and cognitive performance^{19,20}.

The daily routines of individuals involve a wide range of activities, including occupational tasks, that take place in diverse and often demanding environments^{21,22,23}. Many are confronted with the need to work in extreme conditions, such as workplaces located at high-altitudes or with extreme temperatures^{24,25}. These challenging work environments can strain human capabilities and expose workers to physical, cognitive, and environmental stressors^{26,27}, requiring innovative solutions to optimize performance and ensure safety. Innovative technologies like wearable devices, artificial intelligence, and data analytics have emerged as vital tools for increasing human capacities every day^{8,24,28-30}.

The impact of these technological advancements extends beyond the workplace, influencing our activities and exercises ³¹⁻³⁵. From everyday tasks to physical exercise, individuals are frequently exposed to diverse environmental conditions, including intense heat, cold temperatures, or high humidity. These varying conditions can affect their performance and well-being, as well as the efficiency of regular exercise regimens ³⁶⁻³⁸. Activities such as high-altitude training, outdoor endurance competitions, and adventure sports have been gaining popularity among individuals seeking unique challenges and experiences ³⁹⁻⁴¹.

Therefore, this PhD thesis comprises six chapters aiming to explore the intersection of these technological developments and their application in optimizing human performance and protecting health under various environmental conditions. It delves into how these tools can be connected to understand and mitigate the impact of challenging environments on human health and performance, and how they can be used to develop strategies and solutions that increase safety, productivity, performance, and overall wellbeing. **Chapter 1** introduces a series of technologies developed during the PhD research, setting the stage for a deeper exploration of the research and findings in following chapters. In **Chapter 2**, the focus shifts to a detailed investigation of endurance races. It presents an in-depth analysis of how different weather parameters influence human performance. Leveraging machine learning methods, the study employs a decision tree regressor algorithm to examine the impact of weather factors on athletic performance, and it demonstrates the specific weather conditions associated with peak performance. **Chapter 3** extends this exploration by employing similar analytical techniques to conduct a thorough risk assessment for heat stress during work and leisure activities, highlighting the need to understand and mitigate heat-related risks for optimal performance. The next two chapters shift focus towards wearable technology, applying insights from the previous chapters about the weather parameters influencing human performance. **Chapter 4** introduces the Smart

Helmet, a cyclist helmet embedded with physiological and environmental sensors, crafted to increase performance and safety in diverse conditions. Building upon the themes of extreme conditions and wearable technology, **Chapter 5** explores the use of such devices for physiological monitoring in high-altitude environments such as Mt Everest. The final chapter, **Chapter 6**, introduces a free web tool aligned with ISO 7933:2018 standards for heat strain mitigation, showcasing the practical application of the research in human health and performance.

Chapter 1

Developing innovative technologies for enhancing human health and performance in diverse environments

This chapter presents a series of technologies that have been developed during years of PhD research. Detailed in table 1, these technologies are the outcome of efforts to develop technological solutions that can enhance people's health and performance. This introductory chapter sets the stage for the following chapters, which delve deeply into the research and findings of these technologies. It demonstrates their direct relevance and connection to the scope of the researcher's work. This chapter focuses on the process of creating these technologies, highlighting their design principles, development, and the rationale behind their development.

Table 1 | Overview of developed technologies during PhD research.

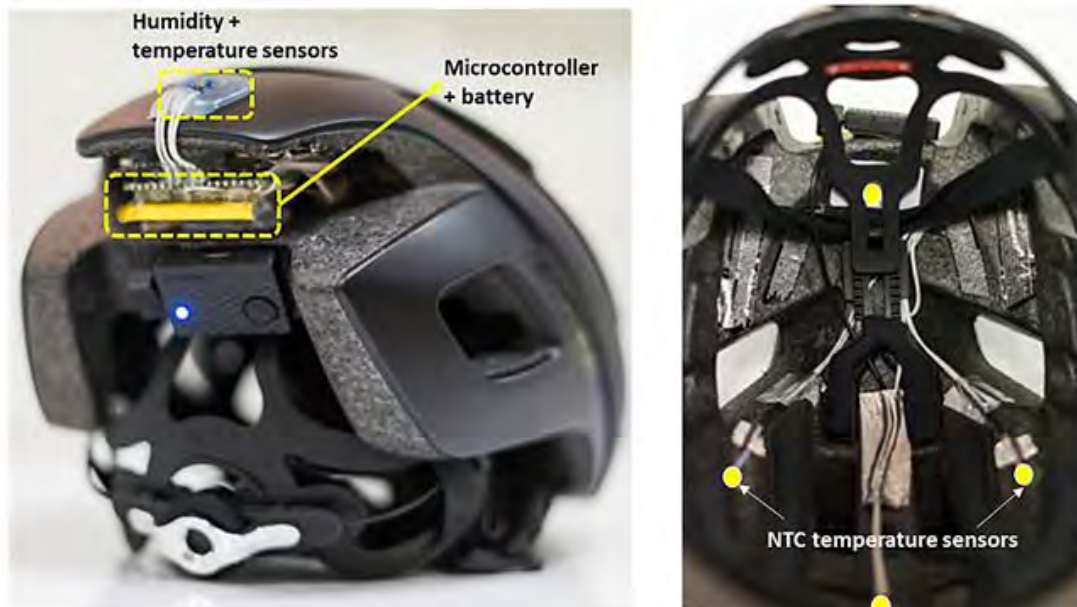
No	Name	Short description	Technology type	Application
1	Smart Helmet	Monitors real-time temperature and heart rate during physical activity	Sensors, Mobile App	Health, Fitness
2	Sweat Rate System	Monitors sweat rate at various body points using a ventilated capsule system	Sensors, Desktop App	Health, Research
3	Portable Temperature Logger	Real-time temperature monitoring with a mobile, portable device	Sensors, Mobile App	Health, Research
4	Web Thermometer Tracker	Real-time temperature monitoring system through a web application	Sensors, Web App	Health, Research
5	GPS Tracker	Track location, elevation, and speed during extreme outdoor conditions	Sensors	Health, Performance
6	Task Analysis	Mobile app for real-time monitoring and analysis of work-related behaviors	Mobile App	Health, Productivity
7	Questionnaire App	Collects user health information, and asses health status and productivity	Mobile App	Health, Productivity
8	FL-WebPHS	Online web software for Predicted Heat Strain	Web App	Health, Productivity, Performance

1. Smart Helmet

In the development of the smart helmet prototype, a standard cyclist helmet (Lazer Bullet 1.0, Lazer Sport, Antwerp, Belgium) was employed as the basis, initially weighing 312 grams. The design process involved integrating a range of sensors to track the athlete's physiological values and conditions of the environment. The helmet was equipped with a Lifebeam heart rate sensor (Lazer Sport, Antwerp, Belgium; Figure A.1) for continuous heart rate monitoring and a high-accuracy digital humidity and temperature sensor (CJMCU-1080 HTC1080, Texas Instruments, Dallas, Texas;) to assess ambient air conditions. To obtain an in-depth understanding of the helmet's internal temperature distribution, four Negative-Temperature-Coefficient (NTC) temperature sensors (100 k Ω at 25°C; Figure 1.1.1) were placed at the front, back, right, and left regions of the helmet's inner structure.

Figure 1.1.1 | Smart Helmet Prototype.

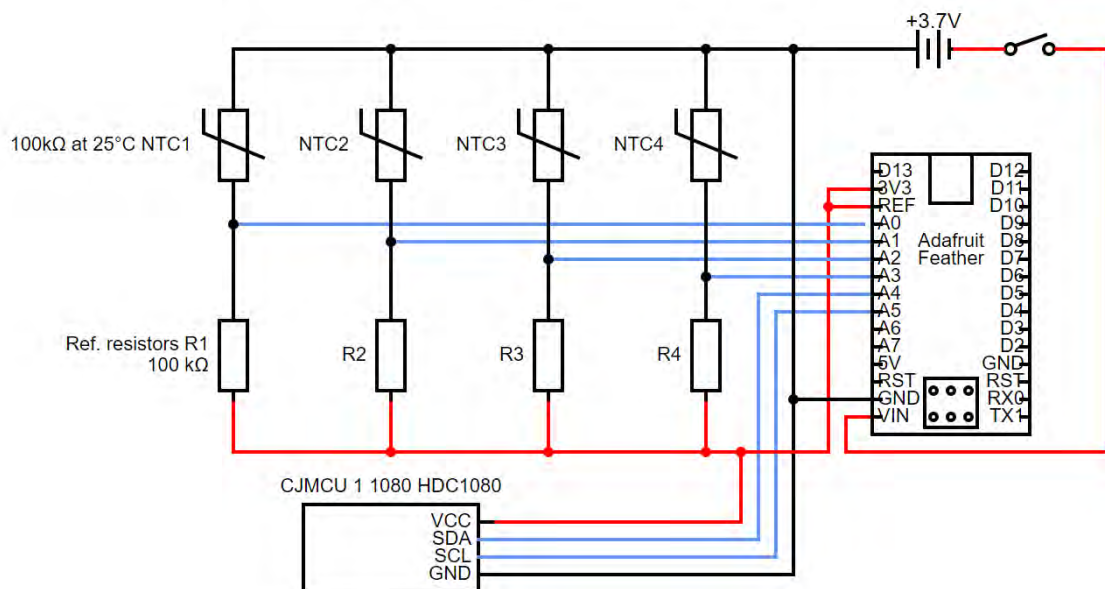
Display of the Smart Helmet prototype with microcontroller, humidity, and temperature sensor on the back (left image) and four NTC temperature sensors within the helmet's interior (right image)



The integration of these sensors increased the overall weight to 358 grams, a 14.7% rise from the original weight, without compromising the geometric and aerodynamic properties of the helmet. A tiny microcontroller Adafruit Feather 32u4 Bluefruit (Adafruit Industries, New York, NY, USA) was utilized to interface all the sensors, transmitting the collected data to a smartphone app via Bluetooth. The system was powered by a 3.7 V Li-polymer rechargeable battery (LP-523450-1S-3), providing up to 10 hours of continuous operation. A comprehensive circuit diagram illustrating the interconnections between the electronics and sensors is shown in Figure 1.1.2.

Figure 1.1.2 | Schematic of Smart Helmet.

Representation of the sensors system integrated into the Smart Helmet prototype.



The Adafruit microcontroller was programmed using the Arduino Integrated Development Environment (IDE). Figure 1.1.3 illustrates the source code visualization, which provides a clear representation of the code structure and the relationship between different functions and variables.

Figure 1.1.3 | Smart Helmet code representation.

A visual representation of the Arduino-based source code structure for programming the Smart Helmet sensors.

```
1 #include <Arduino.h>
2 #include <SPI.h>
3 #include "Adafruit_BLE.h"
4 #include "Adafruit_BluefruitLE_SPI.h"
5 #include "Adafruit_BluefruitLE_UART.h"
6 #include "BluefruitConfig.h"
7 #include <Wire.h>
8 #include "ClosedCube_HDC1080.h"
9
10 #if SOFTWARE_SERIAL_AVAILABLE
11 #include <SoftwareSerial.h>
12 #endif
13
14 #define FACTORYRESET_ENABLE 1
15 #define MINIMUM_FIRMWARE_VERSION "0.6.6"
16 #define MODE_LED_BEHAVIOUR "MODE"
17
18 #define THERMISTORNOMINAL 10000
19 #define TEMPERATURENOMINAL 25
20 #define BCOEFFICIENT 3950
21 #define SERIESRESISTOR 10000
22
23 Adafruit_BluefruitLE_SPI ble(BLUEFRUIT_SPI_CS, BLUEFRUIT_SPI_IRQ, BLUEFRUIT_SPI_RST);
24 ClosedCube_HDC1080 hdc1080;
25
26 String sensorData1 = "";
27 String sensorData2 = "";
28 String sensorData3 = "";
29
30 void error(const __FlashStringHelper* err) {
31   Serial.println(err);
32   while (1);
33 }
34
35 void setup() {
36   delay(500);
37   setupBluefruit();
38   analogReference(EXTERNAL);
39   hdc1080.begin(0x40);
40 }
41
42 void loop() {
43   readSensorsValues();
44   sendDataToBluefruit();
45   delay(1000);
46 }
47
48 void setupBluefruit() {
49   Serial.print(F("Initialising the Bluefruit LE module: "));
50   if (!ble.begin(VERBOSE_MODE)) {
51     error(F("Couldn't find Bluefruit, make sure it's in CoMmanD mode & check wiring?"));
52   }
53   Serial.println(F("OK!"));
54
55   if (FACTORYRESET_ENABLE) {
56     Serial.println(F("Performing a factory reset: "));
57     if (!ble.factoryReset()) {
58       error(F("Couldn't factory reset"));
59     }
60   }
61
62   Serial.println(F("Setting device name to 'SmartHelmet': "));
63   if (!ble.sendCommandCheckOK(F("AT+GAPDEVNAME=SmartHelmet"))) {
64     error(F("Could not set device name?"));
65   }
66
67   ble.echo(false);
68   ble.verbose(false);
69 }
```

```

70 while (!ble.isConnected()) {
71     delay(500);
72 }
73
74 if (ble.isVersionAtLeast(MINIMUM_FIRMWARE_VERSION)) {
75     Serial.println(F("Change LED activity to " MODE_LED_BEHAVIOUR));
76     ble.sendCommandCheckOK("AT+HWModeLED=" MODE_LED_BEHAVIOUR);
77 }
78
79 Serial.println(F("Switching to DATA mode!"));
80 ble.setMode(BLUEFRUIT_MODE_DATA);
81 }
82
83 void sendDataToBluefruit() {
84     ble.print(sensorData1);
85     delay(1000);
86     ble.print(sensorData2);
87     delay(1000);
88     ble.print(sensorData3);
89     delay(1000);
90 }
91
92 float readTemperature(float resistance) {
93     float temperature;
94     temperature = resistance / THERMISTORNOMINAL;
95     temperature = log(temperature);
96     temperature /= BCOEFFICIENT;
97     temperature += 1.0 / (TEMPERATURENOMINAL + 273.15);
98     temperature = 1.0 / temperature;
99     temperature -= 273.15;
100    return temperature;
101 }
102
103 void readSensorsValues() {
104     float resistances[4];
105     float temperatures[4];
106
107     for (int i = 0; i < 4; i++) {
108         resistances[i] = analogRead(A0 + i);
109         resistances[i] = 1023 / resistances[i] - 1;
110         resistances[i] = SERIESRESISTOR / resistances[i];
111         temperatures[i] = readTemperature(resistances[i]);
112     }
113
114     float hdcTemperature = hdc1080.readTemperature();
115     float hdcHumidity = hdc1080.readHumidity();
116
117     sensorData1 = ("%f" + String(hdcTemperature) + ";" + String(hdcHumidity) + ";");
118     sensorData2 = ("##" + String(temperatures[0]) + ";" + String(temperatures[1]) + ";");
119     sensorData3 = ("##" + String(temperatures[2]) + ";" + String(temperatures[3]) + ";");
120 }

```

Following the programming of sensors, the Android-based application, "SmartHelmet App" (Figure 1.1.4), was developed to establish real-time communication with both the Adafruit Feather microcontroller and the Lifebeam heart rate monitor using a Bluetooth communication protocol. The SmartHelmet App, designed with the AppyBuilder online platform (App Inventor, Massachusetts Institute of Technology, Cambridge, Massachusetts, USA), facilitated the real-time reception, display, and storage of data from the smart helmet at a 0.2 Hz sampling rate. Additionally, the app allows users to save and export the collected data in a CSV file format for further analysis and processing.

Figure 1.1.4 | Snapshot of the Smart Helmet App in action.

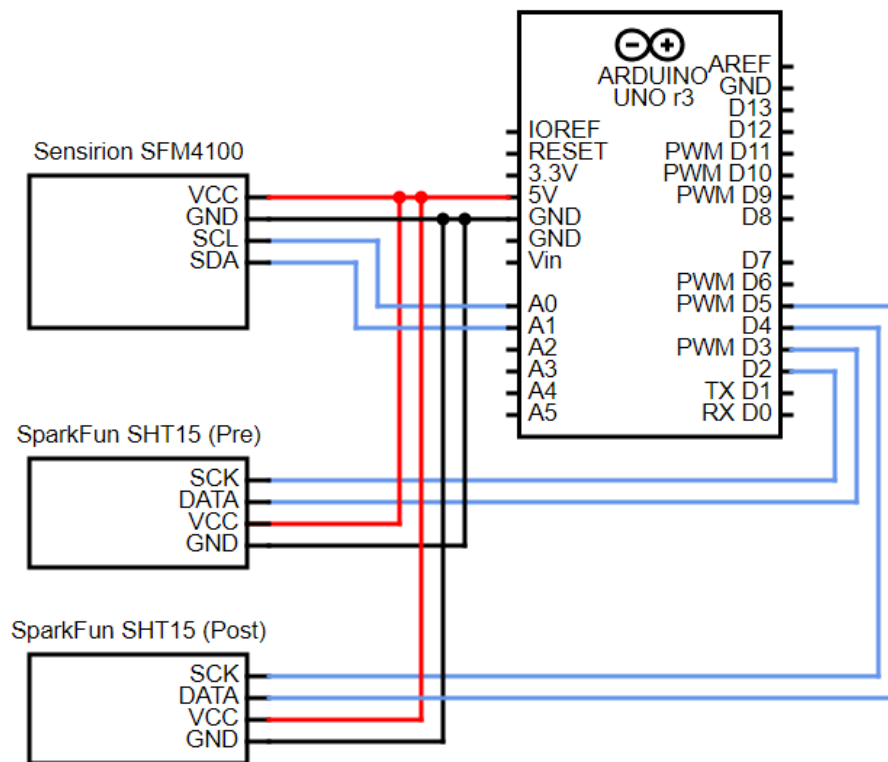


2. Sweat Rate System

The Sweat Rate System, initially developed as part of my bachelor's thesis ⁴², integrates an array of sensors and components for accurate measurement of sweat rate. The two primary sensors used are the airflow sensor (Sensirion SFM4100, Staefa, Switzerland) to precisely measure airflow volume, and the relative humidity and temperature sensor (Sensirion SHT15, Staefa, Switzerland) to assess ambient air conditions (Figure 1.2.1).

Figure 1.2.1 | Schematic of Sweat Rate System.

Representation of the Independent Sensor System Integrated into the Sweat Rate System.



The system utilizes an Arduino Uno Rev3 microcontroller (Ivrea, Italy) to interface all the sensors, transmitting the collected data to a custom computer application developed with the Visual Basic 6 programming package (Figure 1.2.2). The software allows users to select from various sample rates for data collection (ranging from 10 to

60 seconds), enabling real-time data monitoring and the ability to track sweat rate changes as they occur. Figure 1.2.3 illustrates the source code visualization, which provides a clear representation of the code structure and the relationship between different functions and variables.

Figure 1.2.2 | Sweat Rate System.

The Sweat Rate System software interface, which has been optimized to run on a tablet.

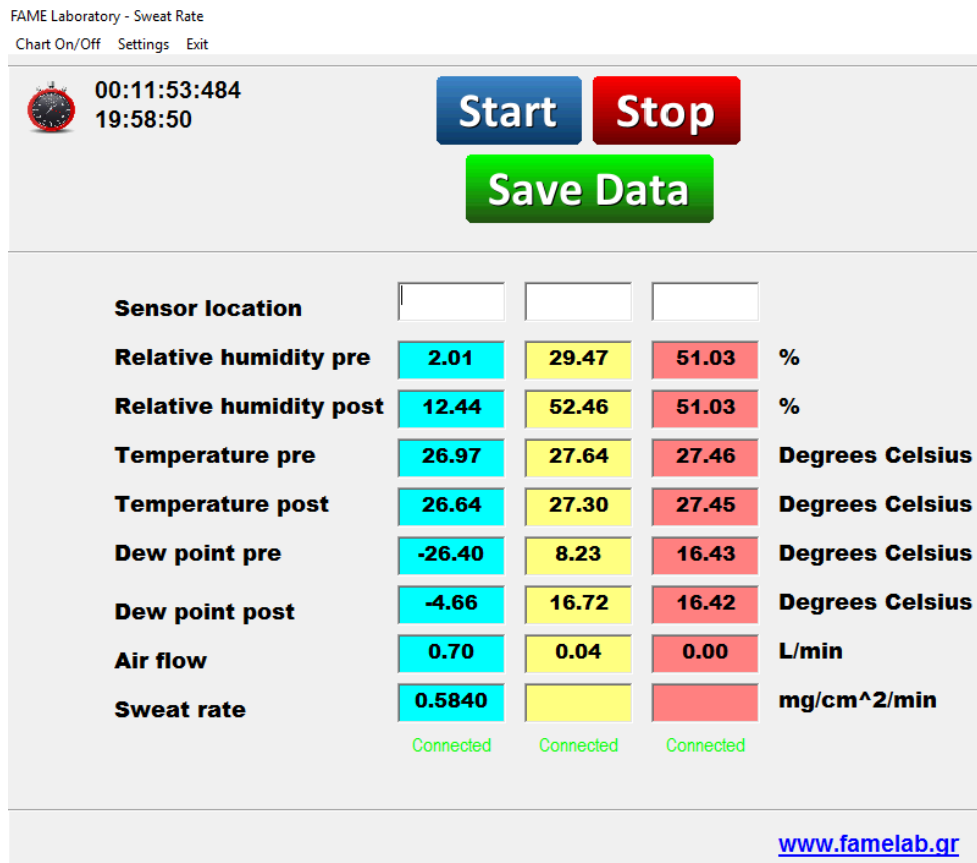


Figure 1.2.3 | Sweat Rate code representation

A visual representation of the Arduino-based source code structure for programming the Sweat Rate System sensors.

```
1 #include <Wire.h>
2 #include <sensirionflow.h>
3 #include "cactus_io_SHT15.h"
4
5 SensirionFlow airFlow(0x81);
6
7 const int SHT_DataBefore = 2;
8 const int SHT_ClockBefore = 3;
9 const int SHT_DataAfter = 4;
10 const int SHT_ClockAfter = 5;
11
12
13 SHT15 sensorAfter(SHT_DataAfter, SHT_ClockAfter);
14 SHT15 sensorBefore(SHT_DataBefore, SHT_ClockBefore);
15
16 void setup() {
17   Wire.begin();
18   Serial.begin(9600);
19   airFlow.init();
20   delay(1000);
21 }
22
23 void loop() {
24   float flowResult = airFlow.readSample() / 1000;
25
26   sensorAfter.readSensor();
27   sensorBefore.readSensor();
28
29   float humidityAfter = sensorAfter.getHumidity();
30   float humidityBefore = sensorBefore.getHumidity();
31
32   if (humidityBefore < 0.006) {
33     humidityBefore = 0.006;
34   }
35   Serial.print(humidityBefore);
36   Serial.print(" ");
37
38   if (humidityAfter < 0) {
39     humidityAfter = 0;
40   }
41   Serial.print(humidityAfter);
42   Serial.print(";");
43
44   Serial.print(sensorBefore.getTemperature_C());
45   Serial.print(";");
46   Serial.print(sensorAfter.getTemperature_C());
47   Serial.print(";");
48
49   Serial.print(sensorBefore.getDewPoint());
50   Serial.print(";");
51   Serial.print(sensorAfter.getDewPoint());
52   Serial.print(";");
53
54   if (flowResult < 0) {
55     flowResult = 0;
56   }
57   Serial.print(flowResult);
58   Serial.println();
59
60   delay(1000);
61 }
62
```

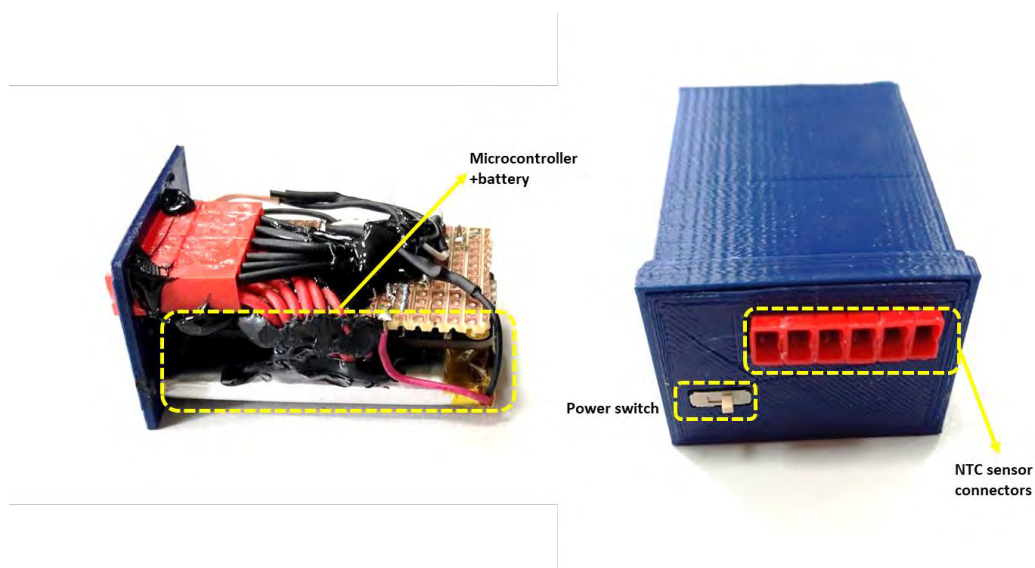
As part of the ongoing research in the current PhD program, a significant modification to the original Sweat Rate System was introduced. Instead of using dry-air from an industrial gas bottle, the new approach generates dry-air from room air using a silica gel technique. To achieve this, air pumps pass room air through a system containing silica gel, effectively dehydrating the air. This generated dry air is then measured by the Sensirion SHT15 sensor before passing through the sweat rate capsules to collect sweat from the skin. Afterward, the air is measured again by the Sensirion SHT15 sensor. The data from these measurements is used in the sweat rate calculations, improving the system's practicality by reducing the dependency on external sources of dry air and streamlining the measurement process. Additionally, the software used in the Sweat Rate System has been updated to improve its portability. While the original software was designed to run on a desktop computer, the updated version has been optimized to run on a tablet (Figure 1.2.2). The incorporation of the silica gel technique and the software update not only improve the Sweat Rate System but also offers several benefits. By generating dry air from room air using silica gel, the cost to perform a study is reduced, as there is no need to rely on industrial bottle dry air. Furthermore, the system becomes more portable, making it easier to transfer to different locations and laboratories for conducting measurements. This increased ease of use, cost-effectiveness, and portability contribute to the overall efficiency and practicality of the sweat rate measurement system.

3. Portable Temperature Logger

In the development of the Portable Temperature Logger prototype, a lightweight, and portable design was prioritized to ensure ease of use, and efficient temperature monitoring. The device was equipped with six Negative-Temperature-Coefficient (NTC) temperature sensors (100 k Ω at 25°C; Figure 1.3.1). A tiny microcontroller Bluefruit nRF52 Feather (Adafruit Industries, New York, NY, USA) was utilized to connect all the sensors and transmit the data to smartphone app through a Bluetooth connection. A Li-polymer 3.7 V, 800 mAh rechargeable battery with dimensions of 50 x 33 x 4.5 mm was used, providing up to 15 hours of continuous operation, making it ideal for extended data collection periods in the field. The device's cover was 3D printed, offering a lightweight and customizable solution for housing the NTC temperature sensors, microcontroller, and battery. This approach allowed for rapid prototyping and easy design adjustments.

Figure 1.3.1 | Portable Temperature Logger.

Illustration of the Portable Temperature Logger prototype: the left image displays the device without the 3D-printed cover, while the right image presents the prototype with the cover, highlighting the six NTC temperature sensor connectors.



A comprehensive circuit diagram illustrating the interconnections between the electronics and sensors is shown in Figure 1.3.2. The Bluefruit nRF52 Feather microcontroller was programmed using the Arduino Integrated Development Environment (IDE). Figure 1.3.3 illustrates the source code visualization, which provides a clear representation of the code structure and the relationship between different functions and variables.

Figure 1.3.2 | Schematic of Portable Temperature Logger

Schematic representation of the independent sensor system integrated into the Portable Temperature Logger

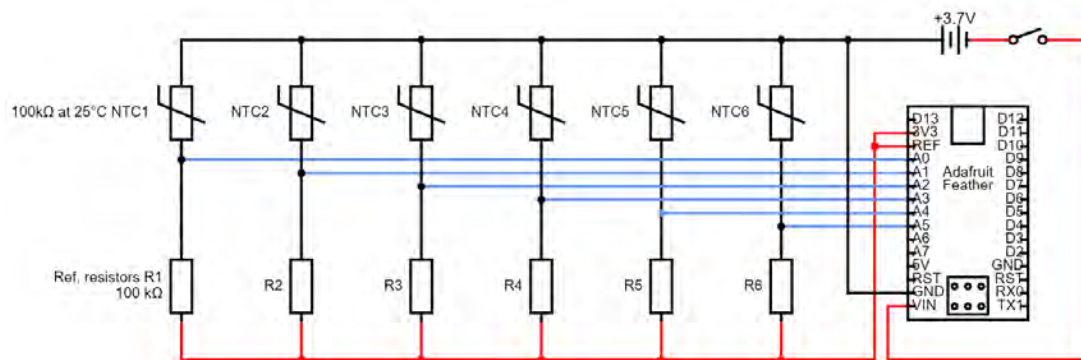


Figure 1.3.3 | Portable Temperature Logger code representation

A visual representation of the Arduino-based source code structure for programming the Portable Temperature Logger.

```
1 #include <bluefruit.h>
2 #include <Adafruit_LittleFS.h>
3 #include <InternalFileSystem.h>
4
5 BLEDFU bleDFU;
6 BLEDIS bleDIS;
7 BLEUART bleUART;
8 BLEBAS bleBATTERY;
9
10 #define THERMISTOR_NOMINAL 83005
11 #define TEMPERATURE_NOMINAL 25
12 #define NUM_SAMPLES 5
13 #define B_COEFFICIENT 4000
14 #define SERIES_RESISTOR 100000
15
16 String dataTemp1, dataTemp2, dataTemp3, dataTemp4, dataTemp5, dataTemp6;
17
18 void setup() {
19   Serial.begin(115200);
20   #if CFG_DEBUG
21   while (!Serial) yield();
22   #endif
23   Bluefruit.autoConnLed(true);
24   Bluefruit.configPrphBandwidth(BANDWIDTH_MAX);
25   Bluefruit.begin();
26   Bluefruit.setTxPower(4);
27   Bluefruit.setName("DataLogger");
28
29   bleDFU.begin();
30   bleDIS.setManufacturer("FAME Laboratory");
31   bleDIS.setModel("Portable Temperature Logger");
32   bleDIS.begin();
33
34   bleUART.begin();
35   bleBATTERY.begin();
36   bleBATTERY.write(100);
37
38   startAdv();
39 }
40
41 void startAdv(void) {
42   Bluefruit.Advertising.addFlags(BLE_GAP_ADV_FLAGS_LE_ONLY_GENERAL_DISC_MODE);
43   Bluefruit.Advertising.addTxPower();
44   Bluefruit.Advertising.addService(bleUART);
45   Bluefruit.ScanResponse.addName();
46
47   Bluefruit.Advertising.restartOnDisconnect(true);
48   Bluefruit.Advertising.setInterval(32, 244);
49   Bluefruit.Advertising.setFastTimeout(30);
50   Bluefruit.Advertising.start(0);
51 }
52
53 void loop() {
54   readSensorValues();
55
56   bleUART.println(dataTemp1);
57   delay(1000);
58   bleUART.println(dataTemp2);
59   delay(1000);
60   bleUART.println(dataTemp3);
61   delay(1000);
62   bleUART.println(dataTemp4);
63   delay(1000);
64   bleUART.println(dataTemp5);
65   delay(1000);
66   bleUART.println(dataTemp6);
67   delay(1000);
68 }
69
```

```
70 void readSensorValues() {
71   float resistances[6];
72   float temperatures[6];
73
74   for (int i = 0; i < 6; i++) {
75     resistances[i] = analogRead(A0 + i);
76     resistances[i] = 1023 / resistances[i] - 1;
77     resistances[i] = SERIES_RESISTOR / resistances[i];
78     temperatures[i] = readTemperature(resistances[i]);
79   }
80
81   dataTemp1 = "$1$" + String(temperatures[0]);
82   dataTemp2 = "$2$" + String(temperatures[1]);
83   dataTemp3 = "$3$" + String(temperatures[2]);
84   dataTemp4 = "$4$" + String(temperatures[3]);
85   dataTemp5 = "$5$" + String(temperatures[4]);
86   dataTemp6 = "$6$" + String(temperatures[5]);
87 }
88
89 float readTemperature(float resistance) {
90   float temperature;
91   temperature = resistance / THERMISTOR_NOMINAL;
92   temperature = log(temperature);
93   temperature /= B_COEFFICIENT;
94   temperature += 1.0 / (TEMPERATURE_NOMINAL + 273.15);
95   temperature = 1.0 / temperature;
96   temperature -= 273.15;
97
98   return temperature;
99 }
100
```

Following the programming of sensors, the Android-based application, "Temperature BLE Datalogger" (Figure 1.3.4), was developed to establish real-time communication with the Bluefruit nRF52 Feather microcontroller using a Bluetooth communication protocol. The Temperature BLE Datalogger App, designed with the AppyBuilder online platform (App Inventor, Massachusetts Institute of Technology, Cambridge, Massachusetts, USA), enables users to monitor temperature data in real time and facilitates the reception, display, and storage of data from the Portable Temperature Logger at a sampling rate of 10 seconds. In addition to real-time monitoring, the app allows users to save and export the collected data in a CSV file format for further analysis and processing. This feature provides researchers and professionals with a convenient way to analyze data and generate insights, enhancing the overall utility of the Portable Temperature Logger in various field applications.

Figure 1.3.4 | Snapshot of the Portable Temperature Logger App in action.

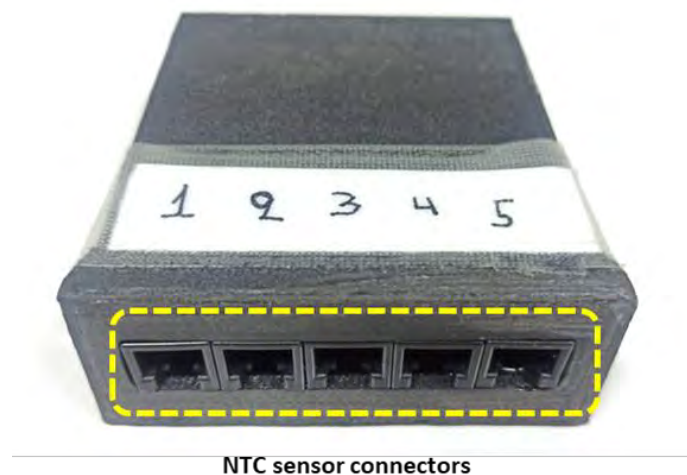


4. Web Thermometer Tracker

In the development of the Web Thermometer Tracker prototype, a compact design was conceived by integrating an array of sensors for monitoring temperature. This device was specifically created with the aim of providing highly accurate temperature measurements in laboratory studies, including those that involve immersion in water or activities that generate sweat, resulting in wet skin. The device was equipped with five water-resistant skin temperature sensors (2 k Ω at 25°C; NOVAMED, USA) for accurate and continuous temperature tracking. An Arduino Uno R3 microcontroller (Arduino, Somerville, MA, USA) was utilized to interface all the sensors, transmitting the collected data to a browser-based software platform via USB. The device was housed in a custom 3D printed cover designed to protect the sensors and electronics (Figure 1.4.1).

Figure 1.4.1 | Web Thermometer Tracker prototype.

Illustration of the Web Thermometer Tracker prototype. Image displays the device with the 3D-printed cover, displaying the five NTC temperature sensor connectors.



A comprehensive circuit diagram illustrating the interconnections between the electronics and sensors is shown in Figure 1.4.2. The Arduino microcontroller was programmed using the Arduino Integrated Development Environment (IDE). Figure 1.4.3 illustrates the source code visualization, which provides a clear representation of the code structure and the relationship between different functions and variables.

Figure 1.4.2 | Schematic of Web Thermometer Tracker

Schematic representation of the independent sensor system integrated into the Web Thermometer Tracker.

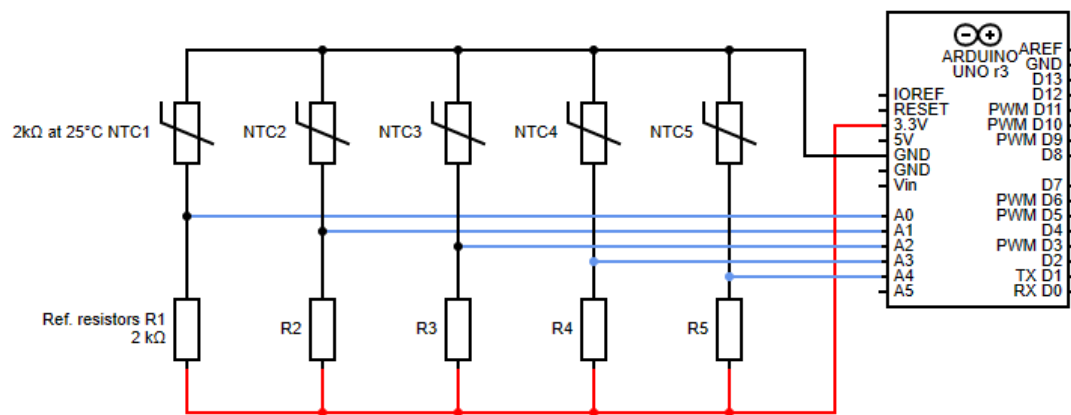


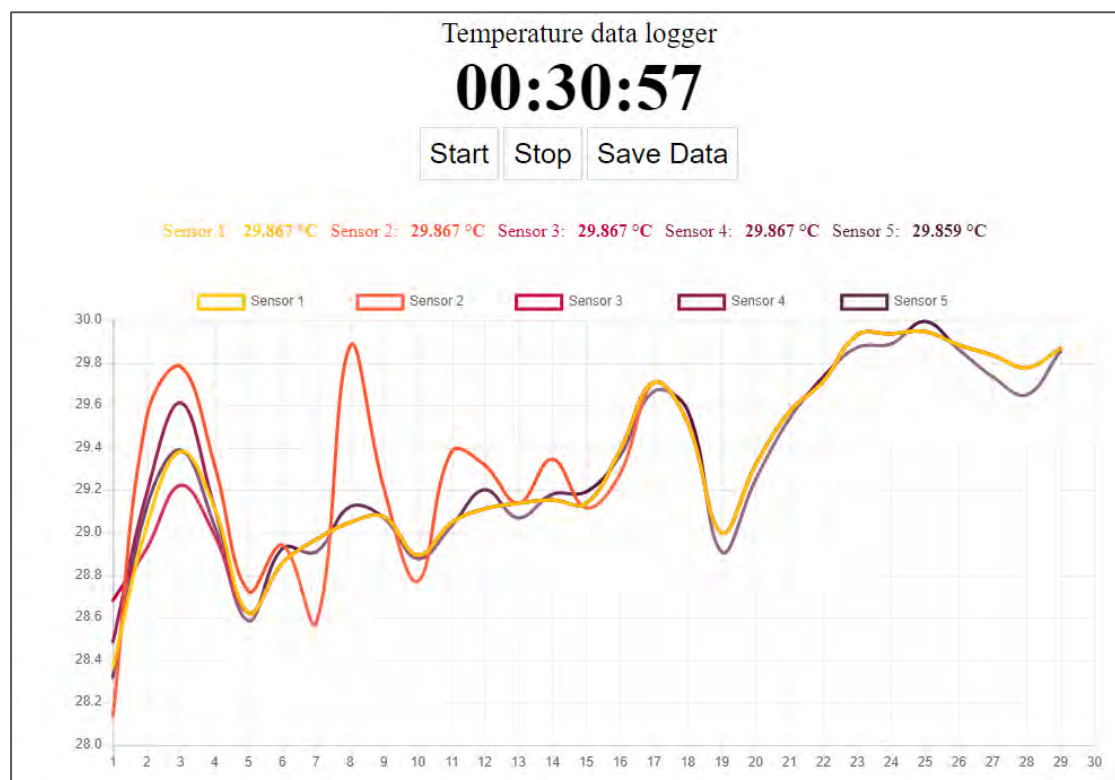
Figure 1.4.3 | Web Thermometer Tracker code representation.

A visual representation of the Arduino-based source code structure for programming the Web Thermometer Tracker.

```
1 #define THERMISTOR_NOMINAL 200
2 #define TEMPERATURE_NOMINAL 25
3 #define B_COEFFICIENT 4800
4 #define SERIES_RESISTOR 200
5
6 String inputString;
7 int analogPin = 0;
8
9 void setup() {
10   Serial.begin(115200);
11 }
12
13 void loop() {
14   while (Serial.available()) {
15     delay(3);
16     char receivedChar = Serial.read();
17     inputString += receivedChar;
18   }
19
20   inputString.trim();
21
22   if (inputString.length() > 0) {
23     for (int i = 1; i <= 5; i++) {
24       if (inputString == "S" + String(i)) {
25         delay(10);
26         analogPin = i;
27         readTemperature(analogPin);
28       }
29     }
30     inputString = "";
31   }
32 }
33
34 void readTemperature(int pin) {
35   float resistance;
36   int average = 0;
37
38   for (int i = 0; i < 10; i++) {
39     average += analogRead(pin);
40   }
41
42   resistance = static_cast<float>(average) / 10;
43   resistance = 1023 / resistance - 1;
44   resistance = SERIES_RESISTOR / resistance;
45
46   float temperature;
47   temperature = resistance / THERMISTOR_NOMINAL;
48   temperature = log(temperature);
49   temperature /= B_COEFFICIENT;
50   temperature += 1.0 / (TEMPERATURE_NOMINAL + 273.15);
51   temperature = 1.0 / temperature;
52   temperature -= 273.15;
53
54   Serial.print(temperature);
55 }
56
```


The software for the Web Thermometer Tracker is browser-based and was developed using HTML, CSS, and JavaScript (Figure 1.4.4). It is compatible with various operating systems, including macOS, Linux, and Windows, allowing for real-time reception, display, and storage of data from the device at a 10-second sampling rate. The software stores all recorded data in the browser cache, ensuring data persistence even after the browser is closed. Users can also save and export the collected data in a .csv file format for further analysis and processing.

Figure 1.4.4 | Snapshot of the Web Thermometer Tracker software in action.

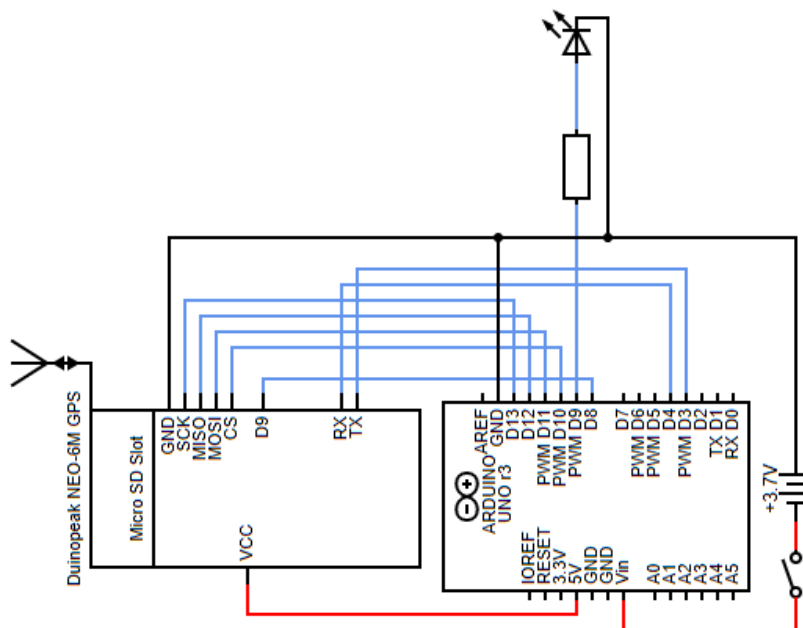


5. GPS Tracker

The GPS Tracker prototype was developed with focus to ensure durability and protection against harsh environmental conditions. It was specifically engineered to track climbers' locations in extreme environments, such as the Everest expedition ⁴. An Arduino Uno R3 microcontroller (Arduino, Somerville, MA, USA) was utilized as part of the system, and it was fitted with a NEO-6M GPS antenna (Somerville, MA, USA) to enable accurate navigation and positioning. The NEO-6M GPS is an Arduino GPS Shield that includes a microSD card slot and an active antenna with a frequency of 1575.42 MHz. Figure 1.5.1 showcases a detailed circuit diagram, highlighting the interconnections between the microcontroller and the GPS antenna.

Figure 1.5.1 | Schematic of GPS Tracker.

Schematic representation of the independent sensor system integrated into the GPS Tracker.



The Arduino Uno R3 microcontroller was programmed using the Arduino Integrated Development Environment (IDE). Figure 1.5.2 displays the source code visualization, which clearly illustrates the code's structure and the relationships between various functions and variables.

Figure 1.5.2 | GPS Tracker code representation.

A visual representation of the Arduino-based source code structure for programming the GPS Tracker.

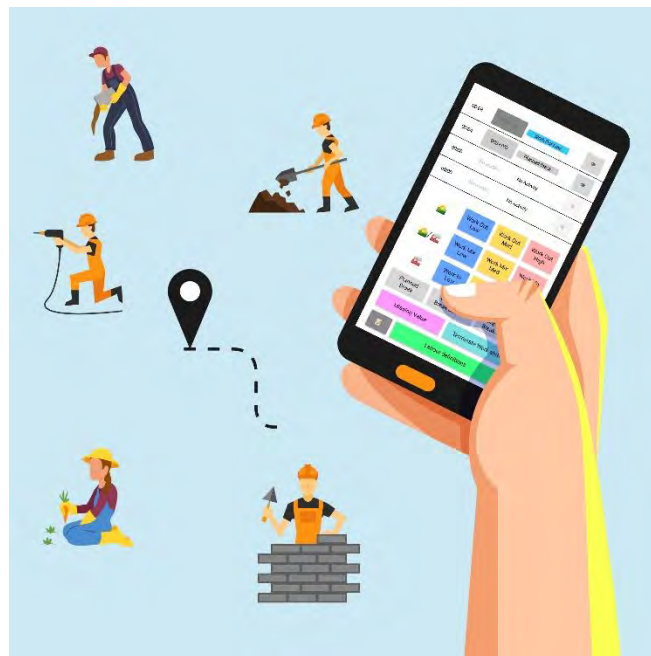
```
1 #include <SPI.h>
2 #include <SD.h>
3 #include <TinyGPS++.h>
4 TinyGPSPlus gps;
5 #include <SoftwareSerial.h>
6 SoftwareSerial gpsSerial(3, 4);
7 #define GPS_PORT gpsSerial
8 #define SERIAL_MONITOR Serial
9 const int ledPin = 9;
10 const int chipSelectPin = 8;
11
12 void setup() {
13   SERIAL_MONITOR.begin(9600);
14   pinMode(ledPin, OUTPUT);
15   digitalWrite(ledPin, HIGH);
16   GPS_PORT.begin(9600);
17 }
18
19 void loop() {
20   digitalWrite(ledPin, HIGH);
21
22   if (!SD.begin(chipSelectPin)) {
23     SERIAL_MONITOR.println("Card failed, or not present");
24     while (1);
25   }
26
27   SERIAL_MONITOR.println("Card initialized.");
28
29   if (gps.location.isUpdated()) {
30     if (logGPSData()) {
31       SERIAL_MONITOR.println("GPS logged.");
32       digitalWrite(ledPin, LOW);
33       delay(900000);
34       digitalWrite(ledPin, HIGH);
35     }
36   }
37
38   while (GPS_PORT.available()) {
39     gps.encode(GPS_PORT.read());
40   }
41 }
42
43 byte logGPSData() {
44   File dataFile = SD.open("datalog.txt", FILE_WRITE);
45   if (dataFile) {
46     dataFile.print(gps.location.lng(), 6);
47     dataFile.print(',');
48     dataFile.print(gps.location.lat(), 6);
49     dataFile.print(',');
50     dataFile.print(gps.altitude.feet(), 1);
51     dataFile.print(',');
52     dataFile.print(gps.speed.mph(), 1);
53     dataFile.print(',');
54     dataFile.print(gps.course.deg(), 1);
55     dataFile.print(',');
56     dataFile.print(gps.date.value());
57     dataFile.print(',');
58     dataFile.print(gps.time.value());
59     dataFile.print(',');
60     dataFile.print(gps.satellites.value());
61     dataFile.println();
62     dataFile.close();
63     return 1;
64   }
65
66   return 0; // If we failed to open the file, return fail
67 }
68
```

To ensure durability and protection against the extreme environments climbers may encounter, the GPS tracker cover was custom-made using neoprene materials. Additionally, a specially designed 9-volt lithium battery, featuring added protection for cold temperatures, powers the GPS Tracker, guaranteeing its proper functioning even in the most demanding expedition conditions.

6. Task Analysis App

The Task Analysis App (Figure 1.6.1) is a mobile productivity assessment tool that specializes in categorizing work tasks according to various factors such as work environment and the associated metabolic rate. It is designed for researchers and industry professionals, providing valuable insights into the unique characteristics of a wide range of work tasks. This Android-based application was developed using the AppyBuilder online platform (App Inventor, Massachusetts Institute of Technology, Cambridge, Massachusetts, USA).

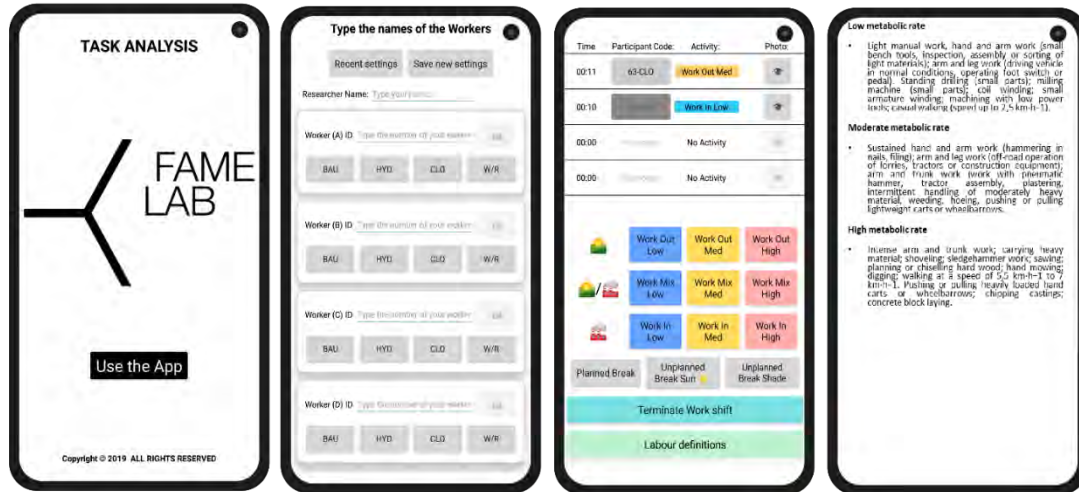
Figure 1.6.1 | Infographic Demonstrating the Task Analysis App in use.



The main features of the Task Analysis App include: (1) real-time monitoring capabilities for continuous data collection on work aspects like irregular breaks, continuous work periods, and scheduled breaks; (2) classification and categorization of work tasks based on factors like work environment and metabolic rate; (3) the ability to monitor multiple workers simultaneously (Figure 1.6.2).

Figure 1.6.2 | Task Analysis App.

Snapshot of the Task Analysis App displays the app's easy-to-use interface. The second screen shows the pre-setting options for each worker, the third screen presents the 14 task categories, and the last screen provides the labor definitions according to ISO 8996.



In summary, the app tracks 14 unique tasks, including monitoring various types of breaks and work duration. Breaks are categorized as planned (scheduled by management) or unplanned (irregular), with unplanned breaks further divided into those taken in the shade or under the sun. Work tasks are grouped into nine categories based on environmental factors, such as outdoor, indoor, or mixed settings, and metabolic rate, which includes low, moderate, or high levels as defined by ISO 8996⁴³.

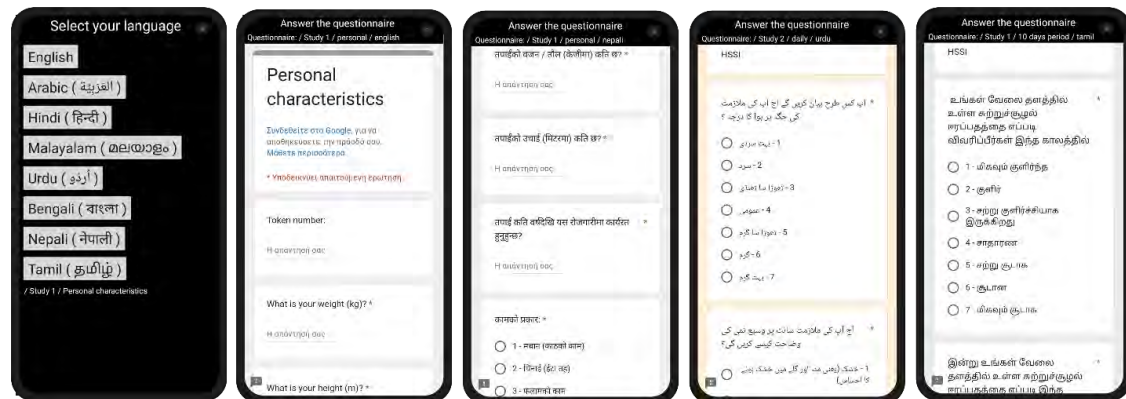
The Task Analysis App was put into action in the "Assessment of Occupational Heat Strain and Mitigation in Qatar" project⁴⁴ by researchers from the FAME Lab. This project, funded by the International Labour Organization, employed the app as an essential productivity assessment tool. It was used in analyzing work tasks and worker productivity across various worksites and environments, demonstrating its practical utility in real-world scenarios.

7. Questionnaire App

The Questionnaire App (Figure 1.7) is a mobile data collection tool developed using the AppyBuilder online platform (App Inventor, Massachusetts Institute of Technology, Cambridge, Massachusetts, USA) and Google Forms (Google Inc, Mountain View, California, U.S.). The app incorporates the Heat Strain Score Index (HSSI) in its questionnaires, allowing users to assess the impact of thermal stress on worker performance and well-being. Designed to gather information on individual workers across various industries, it supports eight languages, including English, Arabic, Hindi, Malayalam, Urdu, Bengali, Nepali, and Tamil. Additionally, it is compatible with both smartphones and tablets.

Figure 1.7 | Questionnaire App

Snapshot of the Questionnaire App displays the app's interface. The first image, starting from the left, illustrates the screen for language selection. The images that follow display the questionnaire in various languages: the second image reveals the questionnaire in English, the third image shows it in Nepali, the fourth image displays it in Urdu, and the last image demonstrates the questionnaire in Tamil.



The Questionnaire App was employed in the "Assessment of Occupational Heat Strain and Mitigation in Qatar" project ⁴⁴ by researchers from the FAME Lab. This project, funded by the International Labour Organization. During this project, the Questionnaire App was used as a key tool for collecting data, particularly on worker performance under thermal stress, further demonstrating its practical utility in various work environments.

8. FL-WebPHS

FL-WebPHS is a browser-based tool, developed using HTML, CSS, and JavaScript, and available free at <https://bit.ly/PHSwebtool>. It's equipped with two main components: first component (Figure 1.8) based on a modified version of the ISO 7933:2018 standard, known as the PHS_{FL}⁸, and the second (Figure A.1) following the original ISO 7933:2018 standard⁴⁵. FL-WebPHS is compatible with various operating systems, including Windows, Unix, MacOS, IOS, and Android, and can be accessed on devices like laptops, desktop computers, and smartphones.

Figure 1.8 | FL-WebPHS.

This figure provides a comprehensive screenshot of the main screen of FL-WebPHS, illustrating the first component based on the modified version of the ISO 7933:2018 standard, also known as PHS_{FL}.

The screenshot shows the 'FAME Lab Predicted Heat Strain' interface. At the top, it displays 'ISO 7933' and 'FAME LAB PHS'. The main area is divided into several sections for parameter input:

- Personal Data:** Height (input field, unit: cm), Weight (input field, unit: kg), and Acclimatization (dropdown menu, currently set to 'Acclimatized').
- Time of period:** '1 of 1' with 'Previous', 'Next', 'Delete period', and 'Add' buttons.
- Environmental Conditions:** Air temperature (input field, unit: °C), Globe temperature (input field, unit: °C), Humidity (input field, unit: %), and Air velocity (input field, unit: m/sec).
- Activity and Mechanical Data:** Activity type (Select or Insert buttons), Mechanical efficiency (input field, unit: W/m²), and Posture (dropdown menu, currently set to 'Standing').
- Clothing and Surface Area:** Clothing (Select or Insert buttons), Reflection coefficient (Select or Insert buttons), and Covered Body Surface Area (Select or Insert buttons).
- Movement:** Moving speed (input field, unit: km/h) and THETA angle (input field, unit: Degrees).

At the bottom, there are 'Clear All', 'Save', and 'Run simulation' buttons.

The main software interface, detailed in Appendix A, incorporates several additional functionalities. These include the capability to calculate the covered body surface area (Figure A.2), an option to choose from a list of reflection coefficients for

different clothing materials (Figure A.3), and a feature to compute total clothing insulation by selecting from a variety of clothing styles based on the American Society of Heating, Refrigerating and Air-Conditioning Engineers (ASHRAE) list⁴⁶ (Figure A.4). It also integrates an activity level selection feature that is based on the Compendium of Physical Activities⁴⁷ (Figure A.5).

The results obtained from the modified PHS_{FL} algorithm are presented through four charts (Figure A.6), providing predictions for rectal temperature, core temperature, skin temperature, and total sweat rate, with initial and final values and can be saved as .png files. For a detailed examination, the data is presented in a minute-by-minute format in a table (Figure A.7), which can be exported as a .csv file. The second component, using the ISO 7933:2018 standard algorithm, provides less detailed but equally valuable results, presenting only initial and final predicted values (Figure A.8).

Chapter 2

Effects of weather parameters on endurance running performance: discipline specific analysis of 1258 races

This work was conducted by Konstantinos Mantzios, Leonidas G. Ioannou, Zoe Panagiotaki, Styliani Ziaka, Julien D. Périard, Sébastien Racinais, Lars Nybo and Andreas D. Flouris. We all participated in the conception and design of the study. I contributed to the data collection, statistical and machine learning analyses, data interpretation, and drafted and revised the manuscript critically for important intellectual content. I had full access to all of the data in the study and take responsibility for the integrity of the data and the accuracy of the data analysis.

As of July 2021, this paper ¹ has been published online by MEDICINE & SCIENCE IN SPORTS & EXERCISE as follows: *Mantzios K., Ioannou L.G., Panagiotaki Z, et al. Effects of weather parameters on endurance running performance: discipline specific analysis of 1258 races. MSSE; [10.1249/MSS.0000000000002769](https://doi.org/10.1249/MSS.0000000000002769)*

Abstract

Introduction: This study evaluated how single or combinations of weather parameters (temperature, humidity, wind speed, solar load) affect peak performance during endurance running events and identify which events are most vulnerable to varying weather conditions. **Methods:** Results for the marathon, 50km race-walk, 20km race-walk, 10,000m, 5,000m and 3,000m-steeplechase were obtained from the official websites of large competitions. We identified meteorological data from nearby (8.9 ± 9.3 km) weather stations for 1258 races held between 1936 and 2019 across 42 countries, enabling analysis of 7867 athletes. **Results:** The Wet-Bulb Globe Temperature (WBGT) across races ranged from -7 to 33°C , with 27% of races taking place in cold/cool, 47% in neutral, 18% in moderate heat, 7% in high heat, and 1% in extreme heat conditions, according to the World Athletics classification. Machine learning decision trees (R^2 values: 0.21-0.58) showed that air temperature (importance score: 40%) was the most important weather parameter. But, when used alone, air temperature had lower predictive power (R^2 values: 0.04-0.34) than WBGT (R^2 values: 0.11-0.47). Conditions of 7.5 - 15°C WBGT (or 10 - 17.5°C air temperature) increase the likelihood for peak performance. For every degree WBGT outside these optimum conditions, performance declined by 0.3-0.4%. **Conclusion:** More than one-quarter of endurance running events were held in moderate, high, or extreme heat and this number reaches one-half for events other than the marathon. All four weather parameters must be evaluated to mitigate the health and performance implications of exercising at maximal intensities in a hot environment with athletes adopting heat mitigation strategies when possible.

Introduction

The implications of weather conditions on athletic performance have raised considerable attention, owing to the escalating climate change⁴⁸⁻⁵⁰, the desire to go beyond existing levels of human performance^{51,52}, and the safe globalization of sports across all continents and climates (e.g. first Youth Summer Olympics in Africa in 2026). The effect of weather parameters such as temperature (i.e. heat or cold), relative humidity (i.e. dry or humid), wind speed and solar radiation can undermine both athletic performance and event organization^{49-51,53}. It is clear that heat stress affects several parameters of importance for exercise endurance with associated performance impairment in both middle distance and marathon races, however with large variation in the average reported impact from ~ 3 to 14%^{54,55}. Translating this to Eliud Kipchoge's 2018 World Record at the Berlin Marathon in temperate conditions (17°C Wet-Bulb Globe Temperature [WBGT]) means an additional 3 min and 16 sec, which would make his race only the 7th fastest in the world at that time, had he ran in warmer conditions (i.e. 25°C WBGT – calculation based on a 2.7% performance decrement as suggested by Ely et al.⁵⁵).

To date, the handful of studies on the topic have clearly shown a strong link between weather parameters and endurance running performance, but this is mainly derived from studies on marathon running and its application in other endurance events is unclear⁵⁴⁻⁵⁹. Also, the focus has been primarily on the effects of high temperatures, although low temperatures^{60,61}, as well as high relative humidity⁵⁷, wind speed⁶², and solar radiation⁶³ can also affect race finishing times. Understanding the impacts of the different weather parameters can be critical for athletes and coaches aiming to optimize running performance as well as for event organizers and officials wishing to mitigate the risk of heat illness to competitors. Additionally, this knowledge will improve sports science education and create opportunities for companies that develop wearables and sports-related technologies and applications. In this

retrospective study, we analyzed the endurance running events included in the list of Olympic sports: the marathon, 50km race-walk, 20km race-walk, 10,000m, 5,000m, and 3,000m-steeplechase. We aimed to determine 1) the weather conditions observed in previously-held endurance events 2), the weather parameters associated with peak performance, and 3) the events most vulnerable to varying weather conditions.

Methods

Performance data

Results for the marathon, 50 km race-walk, 20 km race-walk, 10,000 m, 5,000 m and 3,000 m-steeplechase were obtained from the official websites of the largest competitions in the world (Table B1): Commonwealth Games, Diamond Leagues, World Athletics Continental Cup, World Athletics Gold Label Races, Olympic Games, World Athletics Race Walking Team Championships, and World Championships. Finish times for all races were collected from the first year of each competition for which data were available online until the end of 2019. The collection of these data was completed between February 2016 and September 2020. For each one of the World Athletics Gold Label Races (marathons), we screened out the earlier one-third (the initial 12 ± 5 years of each race) which were typically not established within the running community⁶⁴ and showed large performance fluctuations year on year that were unrelated to weather conditions. In the remaining two-thirds of the races, we followed previous methodology⁵⁵ and retrieved data for the top-three (reflecting elite athletes) as well as the 25th, 50th, 100th, and 300th place finishers (reflecting well-trained runners). In all other competitions, we retrieved data for all athletes competing in the finals.

For each race, we defined performance as the percent difference between an athlete's finish time and the competition's standing record at that time⁵⁵. For instance, Hicham El Guerrouj won the Olympic 5,000m event in 2004 in a time of 13:14.39, while

the standing Olympic record was 13:05.59, resulting in a 1.12% decrement in performance. Likewise, Eliud Kipchoge won the 2018 Berlin Marathon in 2:01:39, while the standing Berlin Marathon record was 2:02:57, resulting in a 1.05% improvement in performance. Expressing performance against the standing event record considers important race-specific factors, particularly in events held outside the track and field stadium. To gauge our results against the best possible finishing time, we repeated all our analyses by expressing performance as a percent difference between an athlete's finish time and the standing world record at that time (i.e., the standing world record in 2018 for the above example). We present these results in the Online Supplement (Figures B1 and B2), since they were similar to those seen for the standing event record.

Weather data

Our weather analysis builds on recently-introduced methods to assess environmental conditions during sporting events at a large and global scale ⁶⁵. During September 2020, we obtained the date, time, and location for each race from its official website (detailed list provided in Table B1), while the relevant longitude and latitude were obtained from www.locationiq.com. Weather data (air temperature, dew point, wind speed, and cloud coverage) corresponding to the time at half-way of the first finisher in each race were obtained from the closest meteorological station using the official dataset of the National Oceanic and Atmospheric Administration (www.ncei.noaa.gov/data/global-hourly). In cases where these data were not available (232 out of 1258 races), we retrieved the information from widely-used meteorology websites (www.wunderground.com and www.weatherspark.com). Wind speed was adjusted for height above the ground and air friction coefficient (i.e., large city with tall buildings) using previous methodology ^{66,67}. Dew point data were converted to relative humidity ⁶⁸. For cases where cloud coverage was not available in the National Oceanic and Atmospheric Administration datasets, the cloud coverage (in okta) was computed

using relative humidity data based on previous methodology and applying coefficients of 0.25 for low and high as well as 0.5 for middle clouds, as previously suggested ⁶⁹. Solar radiation was calculated using the date, time, and coordinates of each race ⁷⁰, while accounting for cloud coverage ⁷¹. Thereafter, the Heat Index (www.wpc.ncep.noaa.gov/html/heatindex.shtml), Simplified WBGT ⁷² and WBGT ⁷³, were calculated using previous methodology. To validate our approach for assessing weather conditions during the races, we compared our meteorological data against those reported by the race organizers on the official webpage of each race, for a total of 140 races (11% of total races; 2% of marathons, 33% of 50km race-walks, 39% of 20km race-walks, 21% of 10,000m, 20% of 5,000m and 30% of 3,000m-steeplechase races).

Data management and statistical analysis

For the cross-validity assessment of our weather data, we used Spearman's correlation coefficient, Wilcoxon signed-rank test and root mean square error to compare the weather data from the closest meteorological station against those reported by the race organizers. In the remaining analyses, data for each of the studied events (marathon, 50km race-walk, 20km race-walk, 10,000m, 5,000m and 3,000m-steeplechase) were analyzed separately. To address our first objective in terms of identifying the weather conditions in which previous endurance events were held, we categorized the WBGT of each race based on the World Athletics competition medical guidelines: $\leq 10.0^{\circ}\text{C}$ = cold/cool; $10.1\text{-}18.0^{\circ}\text{C}$ = neutral; $18.1\text{-}23^{\circ}\text{C}$ = moderate heat; $23.1\text{-}28.0^{\circ}\text{C}$ = high heat; $>28.0^{\circ}\text{C}$ = extreme heat ⁷⁴. These criteria may seem rather conservative for the general population, but are suited for well-trained and elite athletes who exercise at a high intensity (i.e., elevated rate of metabolic heat production) for a prolonged period of time.

To address our second objective of identifying the weather parameters associated with peak performance in each event, we used the decision tree regressor

algorithm⁷⁵ to develop classification rules linking weather parameters (i.e., air temperature, relative humidity, wind speed and solar radiation) and performance. The decision tree regressor is a machine learning method creating a decision tree that divides data points based on the feature that caused the highest disparity in the output⁷⁵. Hyperparameter selection was implemented to optimize the performance of the decision trees for each of the running events. Each decision tree was optimized with respect to several pre-selected hyperparameters described in Table S2. More specifically, we tested the criterion: ["mse", "mae"], max_depth: [sample-size*0.01, sample-size*0.02, sample-size*0.05, sample-size*0.1], max_leaf_nodes:[2, 4, 6, 8, 10, 15, 20], min_samples_leaf: [10, 20, 30, 40, 50, 60, 70, 80, 100], and min_samples_split: [5, 10, 20, 30, 50, 70, 100, 150, 200]. We separated the dataset for each event using 70-30% random data split to generate the training and testing subsets, respectively. The "learning" component of the decision tree regressor model was performed on training sets (70%) and the final R-square (R^2) and the root mean square error were estimated on the testing sets (30%). The feature importance score was used as an indicator of the usefulness of each weather parameter at predicting peak performance in each event. In addition to the machine learning approach, we used linear and non-linear regression analyses⁷⁶ (least-squares method; Origin Lab 2019, Origin Lab Corporation, Northampton, USA) with accompanying ANOVA tests to calculate the change in performance for every degree Celsius in air temperature, WBGT, Heat Index, and Simplified WBGT.

The above-mentioned least-squares regression models were also used to address our third objective of identifying the events most vulnerable to varying weather conditions by estimating the performance decline for every degree Celsius in air temperature, Heat Index, Simplified WBGT, and WBGT. To confirm that our regression models were not affected by the number of races held in different weather conditions, we repeated the analysis using multiple non-linear regression with the number of races

for each degree WBGT and air temperature inserted in each model as a covariate. For all regression analyses, we deemed as acceptable those models achieving a least-squares fit criterion of $p < 0.005$. Results across all analyses are shown as mean \pm SD, unless otherwise stated.

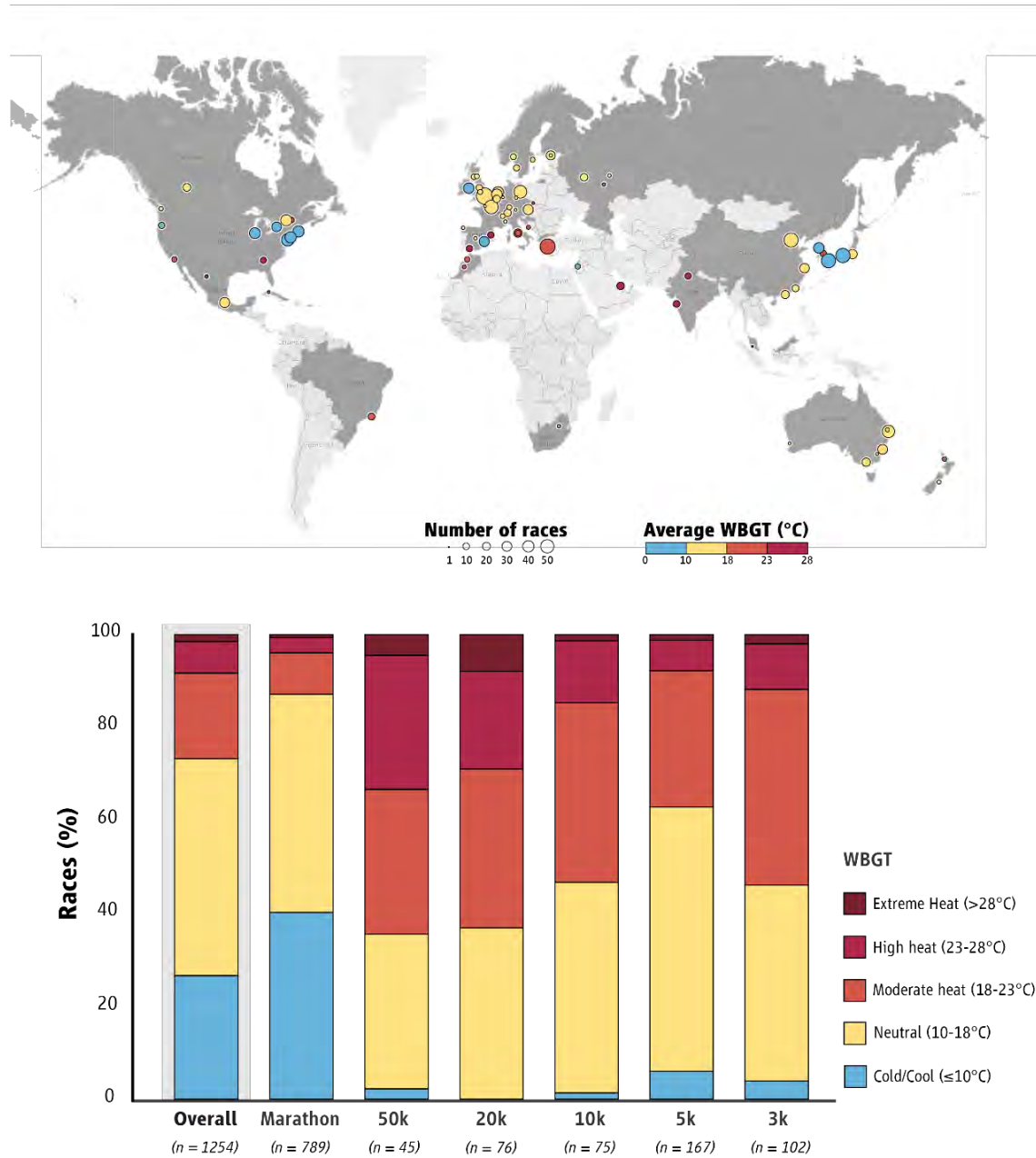
Results

Weather data and cross-validity

We found date and location information for 1316 races. Of these, we were able to identify meteorological data for 1258 races held between 1936 and 2019 across 84 locations and 42 countries (Figure 2.1). The majority (69 %) of these races were held in the period between 2000 and 2019, 19 % were held during the 1990's, and the remaining 12 % in the period between 1936 and 1989 (Figure B3). These data were collected from meteorological stations located in proximity (8.9 ± 9.3 km) to the race location (note: this figure is based on the 1026 events where NOAA data were used). The air temperature ($\rho: 0.82, p < 0.001$), simplified WBGT ($\rho: 0.92, p < 0.001$) and Heat Index ($\rho: 0.85, p < 0.001$) from the meteorological stations were strongly associated with the values reported by the organizers during the events. The values reported by the organizers were on average 0.7 to 1.5 °C higher (depending on the heat index) than those collected from the meteorological stations ($p < 0.05$), with a root mean square error ranging between 1.6 to 2.8 °C, while *Cohen's d* demonstrated no effect size of the differences ($d < 0.2$) between the two sets of data (Table B3).

Figure 2.1 | Endurance Events and Heat Stress.

Distribution of the 1258 races and location-average wet-bulb globe temperature (WBGT) across the 84 locations that hosted endurance events between 1936 and 2019, for which complete race and weather data is available (top), as well as the heat stress level across events based on the World Athletics competition medical guidelines (bottom).



Weather conditions in endurance events

The races were held in a wide range of weather conditions: air temperature from -5 to 35 °C (very cold to very hot), relative humidity from 14 to 100 % (dry to extremely humid), wind speed from 0 and 25 km/h (none to strong wind), and solar radiation from 0 to 1234 W/m² (dark/night to extreme sun). Mean \pm SD values for different competitions and events are provided in Table B4. The WBGT across races ranged from -7 to 33 °C, with 27% of all races taking place in cold/cool, 47% in neutral, 18% in moderate heat, 7% in high heat, and 1% in extreme heat conditions according WBGT classifications of World Athletics competition medical guidelines (Figure 2.1).

The 1258 races enabled a performance analysis of 7867 athletes (6567 elite endurance athletes and 1300 well-trained marathon runners). The mean performance decrement from the standing record was 3.1 ± 3.1 % for the elite endurance athletes (finalist athletes in each race) across all events. The well-trained marathon runners (25th, 50th, 100th, and 300th place finishers; see Methods) showed a mean performance decrement of 24.2 ± 11.1 % in relation to the standing record and a range of finishing times between 2:14 and 3:40 (h:min). All these data have been placed in an online data repository and are made freely available (<https://doi.org/10.6084/m9.figshare.14753565.v1>). The number of athletes as well as the air temperature, WBGT, and performance (mean \pm SD [min-max]) across each competition and event are provided in Tables B4 and B5.

Performance impacts of weather parameters

Decision trees linking weather conditions and performance for the marathon (Figure 2.2), 50km race-walk, 20km race-walk, 10,000m, 5,000m, 3,000m-steeplechase (Figures B4-B8), considering the best hyperparameters in each model (Table B2), indicated R² values between 0.21 and 0.58. When all endurance events were considered together, the R² was 0.33 and the feature with the highest importance was

air temperature (feature importance score = 40 %) followed by relative humidity (feature importance score = 26 %), solar radiation (feature importance score = 18 %) and wind speed (feature importance score = 16 %; Figure 2.3). This shows that air temperature is the most important weather parameter influencing endurance performance in elite athletes. However, decision trees predicting the impact on performance based only on air temperature showed R^2 values between 0.04 and 0.34, while similar decision trees based only on WBGT showed R^2 values between 0.11 and 0.47 (Table B6).

Figure 2.2 | Decision tree classification.

Decision tree linking weather parameters and performance in the marathon. The algorithm is organized in a binary tree: each node asks questions about a weather parameter and ultimately providing, an estimate of the performance decrement (since, on average, the percent difference from the standing record was negative, indicating impaired average performance). The values are rounded on the nearest integer and the decision tree is presented at a maximum depth of four.

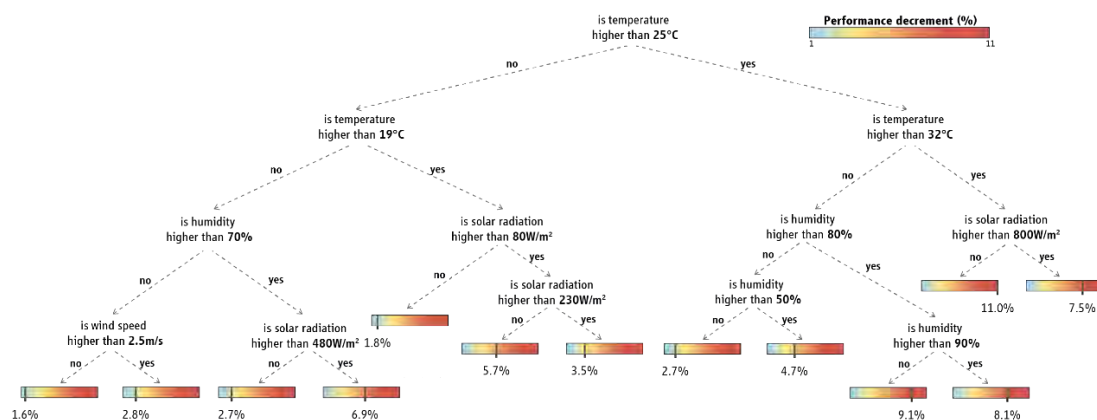
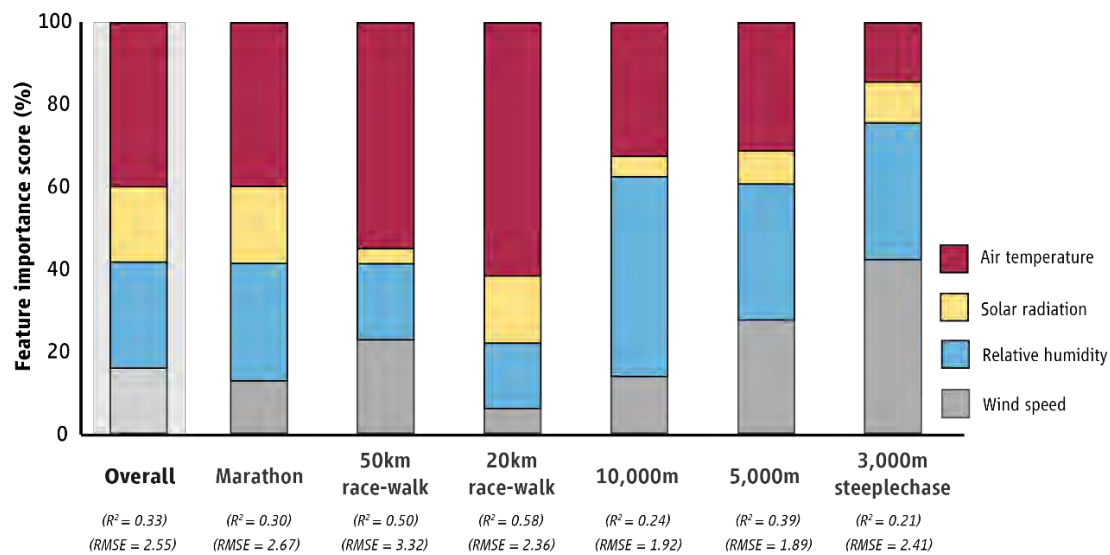


Figure 2.3 | Feature importance scores.

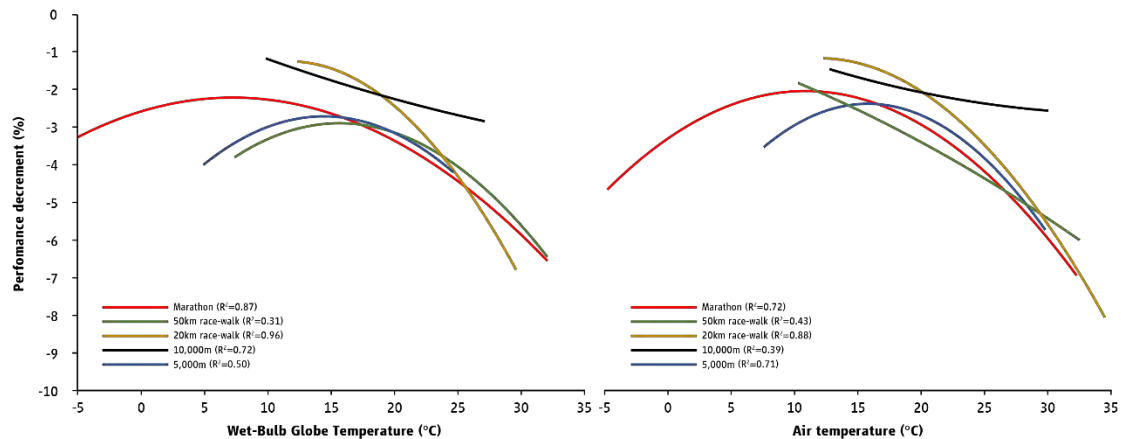
Feature importance scores of the input weather variables and R-square (R^2) and root mean square error (RMSE) of the testing datasets.



Across all studied events, we found that races with a WBGT >15 °C (or air temperature >17.5 °C) and <7.5 °C (or air temperature <10 °C) were associated with impaired performance (Figure 2.4 and Figure B1-B2). Regression analyses statistically confirmed this association for the marathon, the 50km race-walk, the 20km race-walk, the 10,000m race and the 5,000m (R^2 : 0.23-0.96, $p < 0.05$, least-squares fit criterion satisfied at $p < 0.005$; Figures B1-B2 and Table B7). For some of the weather parameters, the regression models showed R^2 ranging between 0.23 and 0.51 as well as non-significant ANOVA tests ($p > 0.05$). These models were deemed acceptable because they satisfied the least squares fit criterion of $p < 0.005$. This criterion was not satisfied for the models linking weather parameters and performance in the 3,000m-steeplechase ($p > 0.005$), therefore no modelling results are available for this event. For all other events, the regression equation and the indicators of each model are provided in Table B7.

Figure 2.4 | WBGT Performance decrement.

Performance decrement (percent difference between an athlete's finish time and the event's standing record) for every degree Wet-Bulb Globe Temperature (WBGT; left) and air temperature (right) across the studied events based on linear and non-linear regression analyses using the least squares method. Performance is always negative (indicating impaired average performance) because, on average, the percent difference from the standing record was negative. The models for marathon do not include well-trained athletes. No curves are shown for the 3,000m-steeplechase as the associated models did not satisfy the least squares fit criterion of $p < 0.005$.

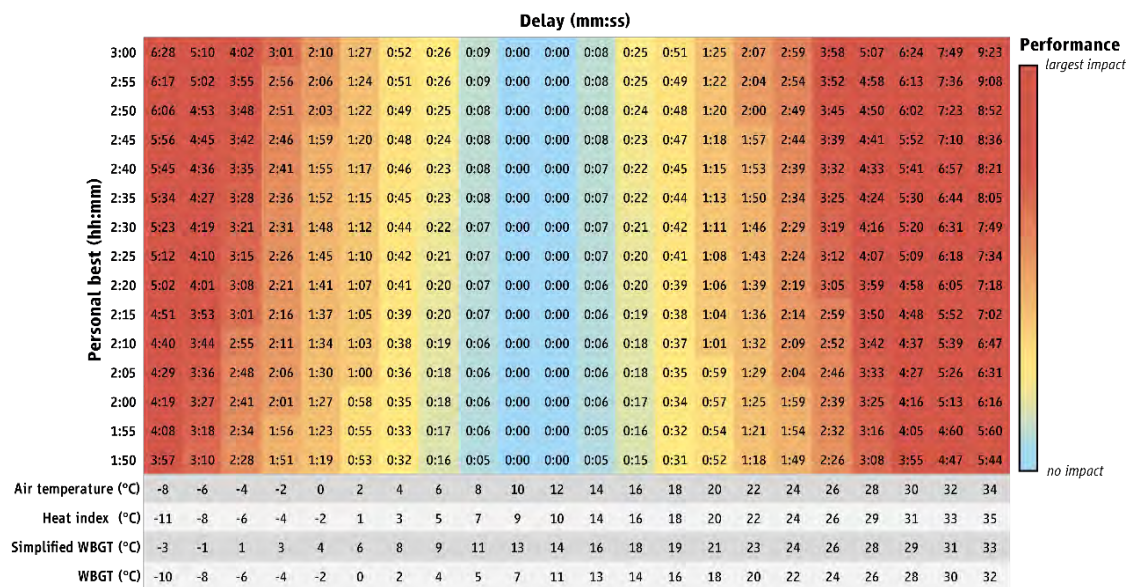


The anticipated impact of air temperature, Heat Index, Simplified WBGT and WBGT on the performance against the standing record of each event is illustrated in Figure 2.5 and Figures B9-B12 across a wide range of finishing times. We observed the highest performance at 7.5 °C WBGT for the marathon (Figure 2.5), at 15 °C WBGT for the 50km race-walk (Figure B9), at 12.5 °C WBGT for the 20km race-walk (Figure B10), as well as at 10 °C WBGT for the 10,000m (Figure B11) and 15 °C WBGT for the 5,000m (Figure B12). Outside these optimum conditions, performance across all events declined by 0.3 ± 0.2 % per 1°C WBGT decrease, and by 0.4 ± 0.4 % per 1°C WBGT increase (Figure 2.4, Table B7): marathon (heat: 0.2%; cold: 0.1%), 50km race-walk (heat: 1.1%; cold: 0.5%), 20km race-walk (heat: 0.4%), 10,000m (heat: 0.04%), 5,000m (heat: 0.3%; cold: 0.2%). Based on these results, the 50km and 20km race-walk events appear to be the most vulnerable endurance events to heat stress, followed by the marathon, the 5,000m, and the 10,000m races. At sub-optimal colder

conditions, the performance decline is the steepest in the 50km race-walk, followed by the 5,000m and the marathon. Multiple non-linear regression analyses confirmed that these results were not affected by the number of races held at different weather conditions. Specifically, multivariate non-linear models with the number of races per 1°C WBGT inserted in each model as a covariate showed larger p values as well as higher Akaike information criterion and Bayesian information criterion, indicating lower predictive capacity (Table B7).

Figure 2.5 | Heat Stress and Marathon Performance.

The impact of heat stress on marathon performance, across a wide range of finishing times. Numbers indicate minutes:seconds of added time to performance based on the air temperature, heat index, simplified WBGT, and WBGT. Colours illustrate the level heat-induced impact on performance. Performance is either unaffected or impaired because, on average, the percent difference from the standing record was negative.



Discussion

This large-scale analysis of the impact of weather parameters on performance showed that 27% of races across endurance events included in the list of Olympic sports were held in moderate, high, or extreme heat. Importantly, a small proportion of marathons (13%) were held in such conditions but this was much higher (49%) for the other events studied. We found that the 50km and 20km race-walk events were the most vulnerable endurance events to heat stress, with the 50km race-walk and the 5,000m being the most vulnerable endurance events to cold stress. Our analysis demonstrated that WBGT between 7.5 – 15 °C (10 – 17.5°C air temperature) is associated with peak performance in well-trained and elite athletes across the endurance events studied.

A large body of literature has established that environmental heat stress can reduce performance and increase the risk for unfavorable health outcomes^{59,77-82}. For instance, a heat exhaustion incidence of 3.3 per 1000 registered athletes has been reported in the World Athletics Championships⁸³. Additionally, injury analyses during the Berlin 2009 and Daegu 2011 World Athletics Championships revealed that heat illness due to environmental or exercise factors was the 2nd and 3rd most common clinical condition⁸³⁻⁸⁵. Interestingly, most heat illnesses in World Athletics Championships have occurred during race-walk events⁸⁵, which supports our finding that race-walking is the most vulnerable endurance events to heat stress. Future work using a similar methodology could be used to uncover specific weather conditions that promote a higher risk for heat-related illness. Overall, our finding that 27% of endurance races have been held in moderate, high, or extreme heat emphasizing the importance of heat mitigation strategies and upper limits to heat stress when events should be cancelled. These are vital to protect the health and performance of the athletes, particularly when considering the globalization of sports amidst an escalating climate change⁴⁸⁻⁵⁰ as well as the desire to go beyond existing levels of human performance^{51,52}.

Previous studies focusing on marathon performance reported that the optimum WBGT for this event is between 5 and 10 °C^{53,55,86}. Our analysis comparing performance against the standing record of an event and the standing world record confirms this, demonstrating that the marathon performance is optimized at a WBGT 7.5 °C. Moreover, we extend knowledge in this field by demonstrating that the WBGT for optimum performance across a range of endurance events is between 7.5 and 15 °C (10 - 17.5°C air temperature). For every degree increase in WBGT beyond 15 °C, performance decreases by ~0.2% in the marathon, ~1.1% in the 50km race-walk, ~0.4% in the 20km race-walk, ~0.04% in the 10,000m, and ~0.3% in the 5,000m. A previous study analyzing marathon races reported similar performance decrements of ~0.1%, ~0.3% and ~0.6% for every degree increase in WBGT for elite men, elite women and well trained runners, respectively⁵⁵. It is worth noting, however, that most of the marathons analyzed in our study included information only for the top three finishers. While this is based on previous methodology⁵⁵, the reported performance decrements may have been higher if more sub-elite athletes were included.

The machine learning analysis that we employed to examine the association between weather parameters and performance in major competitions demonstrated that air temperature is the most important parameter influencing performance in elite athletes. However, our results show that coaches, athletes, and organizers should evaluate all four weather parameters, since decision trees based only on air temperature explained a relatively low percent of variability in performance. Through our analysis, we provide exercise scientists, coaches, athletes, and organizers with two tools to estimate the anticipated impact on performance during a future endurance event: 1) the percent decrement in performance using decision trees (Figure 2.2 and Figures B4-B8) based on weather data from all four parameters; 2) the added time to performance based on athlete's personal best using the heat maps (Figure 2.5 and Figures B9-B12) based on air temperature, Heat Index, Simplified WBGT or WBGT.

The overarching message is similar across these tools, yet their different designs, structures, and functions may be more relevant to specific audiences. For example, the decision trees are likely to be more relevant for event organizers, while the heat maps are probably more useful for exercise scientists, coaches, and athletes. It must be acknowledged that these two tools provide an estimation of performance decrement and that varying combinations of environmental parameters may influence performance differently based on fitness, hydration status, heat acclimation status, and the use of heat mitigation strategies^{55,87-91}. A recently-developed software to predict heat strain can be also used by exercise scientists, coaches, and athletes who wish to estimate more accurately the anticipated impact of weather parameters on physiology and performance⁸.

We found that the 50km and 20km race-walk events were the most vulnerable to heat stress. Compared to running, race-walking has substantially lower mechanical efficiency, which means that more of the energy utilized to produce work ends up being lost as heat⁸. This is because race-walking requires constant contact with the ground, producing a larger pelvis displacement than running⁹². As a consequence, racewalkers reach higher core temperatures for the same movement speed compared to runners^{93,94}, which may explain why most heat illnesses in World Athletics Championships have occurred during race-walk events⁸⁵.

Methodological considerations

In the analyses presented within the main paper, performance is expressed against the standing event record to reflect race-specific factors which are important to consider particularly in events held outside the track and field stadium. For instance, the course remains unchanged across time for most marathon races, but there is wide course variation among races. This approach also accounts for other environmental factors such as in events always taking place in cities at higher elevations where performance is bound to be affected as compared to the standing world record. Yet,

comparing against the standing record does not account for variability in performance for some cases where major course changes have been introduced (e.g., more uphill) or competitions took place in higher elevations (e.g., Olympic games in Mexico City in 1968), that would affect race performance. Also, this approach reduces the impact of weather factors as a given race is typically held in similar conditions every year. For example, the Mumbai marathon held on the third Sunday of January every year in similarly hot conditions ($26.8 \pm 1.6^\circ\text{C}$ air temperature) will have its standing record always set in the heat. Another limitation of this approach is that it assumes that the competition was equally strong each year. Our analysis was designed to address these limitations by including a large number of races held across a wide range of locations and weather conditions (Figure 2.1). While standing records were specific for each particular race, this effect was diluted when all data were merged together, reflecting the true weather conditions that increase the likelihood for peak performance. Moreover, to address any potential limitations of using the standing record, we expanded our analysis to evaluate performance against the standing world record. This process is presented in the annex and revealed similar results, confirming the validity of the main analysis.

It is important to note that the weather data for the evaluated endurance races were not measured at the racing grounds but at the closest meteorological station, on average 9 km away. Therefore, the true conditions during the races may have been different. Our cross-validity analysis performed in 11% of the races showed that the weather parameters from the meteorological stations were highly associated with the values reported by the organizers during the events with no effect size of the differences between the two datasets. These results are in line with a previous cross-validity study of this method⁶⁵, which showed that using WBGT values from the closest weather station (situated 33 km away in that study) generally reflected the WBGT values recorded at the racing grounds. This previous cross-validity exercise showed

that the meteorological station WBGT values were 1.2 ± 2.1 °C lower. This was also the case for the present analysis, which showed that the values reported by the organizers were on average 0.7 to 1.5 °C higher (depending on the heat index) than those collected from the meteorological stations. While a difference of about 1 °C is unlikely to have a strong physiological impact for the present study, it may suggest that a larger percent of races took place in hot conditions. It is logical to anticipate some degree of variability because meteorological stations are located in areas so as to be as unaffected by microclimate and the natural surroundings⁹⁵. A recent study in Brazil using meteorological station data to calculate WBGT using methods similar to those followed in our study showed no significant deviation for distances as large as 80 km⁹⁶. On the whole, our cross-validity analysis, the large number of competitions covered across 42 countries, and the limited distance between the meteorological stations and the racing grounds in most cases support the robustness of the approach used, suggesting that the findings reflect the true conditions.

Conclusion

This large-scale analysis of 1258 races held between 1936 and 2019 across 84 locations and 42 countries demonstrates that more than one-quarter of endurance running events held since the beginning of sports record-keeping and weather data recording were held in moderate, high, or extreme heat and this number reaches one-half for events other than the marathon (i.e., 50km race-walk, 20km race-walk, 10,000m, 5,000m, and 3,000m-steeplechase). The high number of races held in moderate, high, or extreme heat confirms previous suggestions that athletes, coaches, organizers, and officials must be very aware of the health and performance implications of exercising at maximal intensities in a hot environment^{48,49,53,79,80}. Organizers of endurance running events included in the list of Olympic sports must evaluate all four weather parameters and adopt measures that mitigate risks to the health and performance of athletes. At the same time, athletes, coaches, and officials

must be educated about these risks and prepare for the heat by employing heat mitigation strategies where possible.

Acknowledgments

The authors declare that the results of the study are presented clearly, honestly, and without fabrication, falsification, or inappropriate data manipulation, and the results of the present study do not constitute endorsement by the American College of Sports Medicine. The authors declare no conflict of interest.

Chapter 3

Risk assessment for heat stress during work and leisure

This work was conducted by Leonidas G. Ioannou, Giorgos Gkikas, Konstantinos Mantzios, Lydia Tsoutsoubi, and Andreas D. Flouris. We all participated in the conception and design of the study. I contributed to the data collection, performed statistical and machine learning analyses, interpreted the data, and participated in manuscript revisions. I had full access to all the data in the study and take responsibility for the integrity of the data and the accuracy of the data analysis.

As of August 2021, this study ² has been published online by Academic Press as book chapter in Toxicological Risk Assessment and Multi-System Health Impacts from Exposure as follows: *Ioannou L.G., Gkigas G., Mantzios K., et al. Chapter 32 - Risk assessment for heat stress during work and leisure. [10.1016/B978-0-323-85215-9.00004-0](https://doi.org/10.1016/B978-0-323-85215-9.00004-0)*

The inclusion of this study in my thesis is justified as it closely aligns with the central theme of my PhD research. The study's focus on environmental impacts on human health and the use of machine learning analyses to identify factors influencing the risk of heat stress provides significant context for my thesis. My active role in data collection, development of applications for assessing and collecting data on workers' health and productivity (Chapter 1.6 and 1.7), and the application of machine learning methods for data analysis provided me with distinct understandings, particularly regarding how occupational heat strain can potentially affect health and productivity.

All the authors have approved the inclusion of this study in my PhD thesis and hereby affirm that I have made significant contributions to the experimental work conducted, as well as the review process of the manuscript, for the study to be completed (Annex B).

Abstract

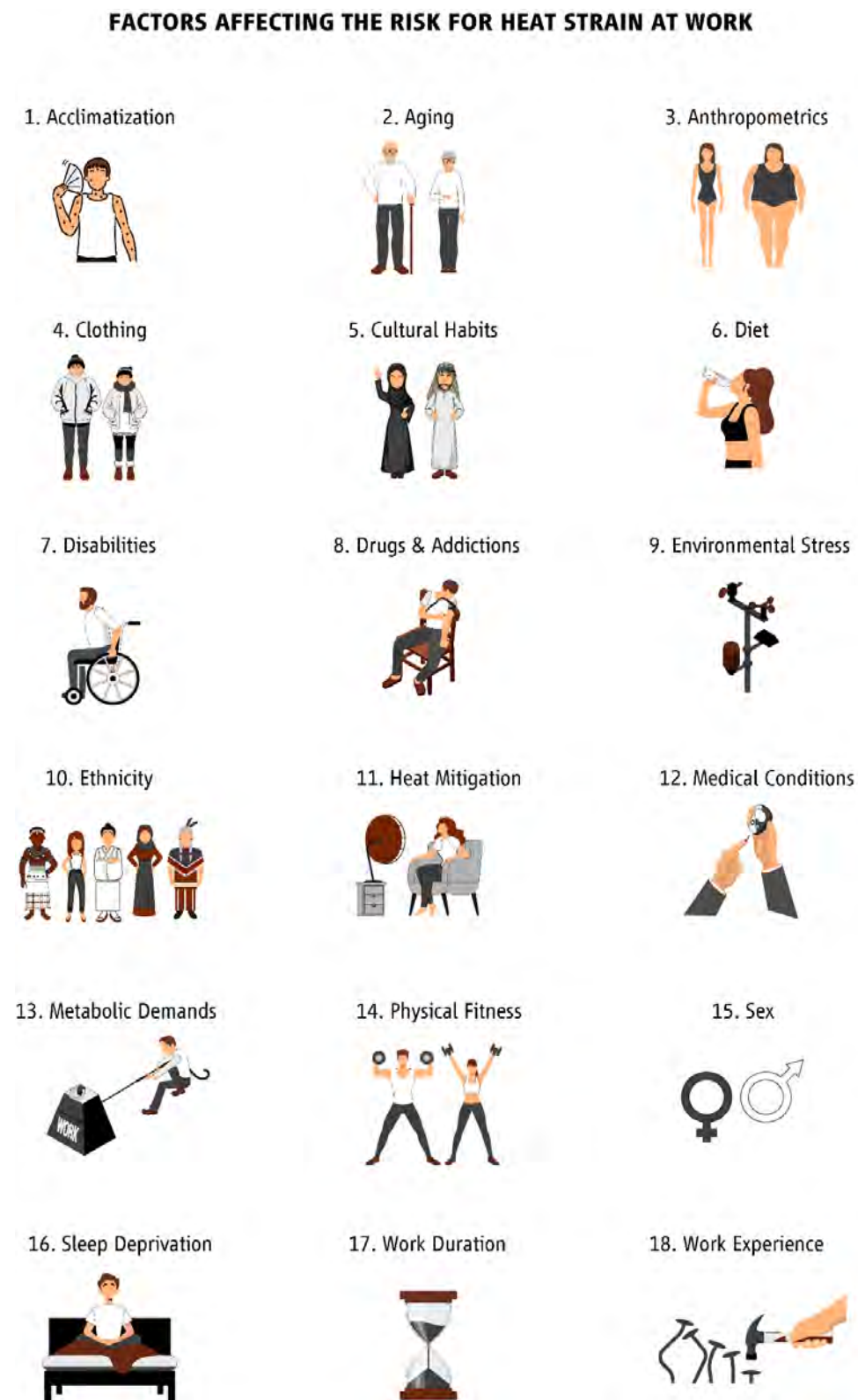
Rising environmental temperatures have become a growing challenge for societies across the globe. At the same time, occupational heat strain undermines the health and productivity of individuals working in key industries. In this Chapter, we combine a narrative review with observational studies to outline the 18 factors affecting the risk for experiencing heat strain during work and leisure, which are: acclimatization, aging, anthropometrics, clothing, cultural habits, diet, disabilities, drugs and addictions, environmental stress, ethnicity, heat mitigation, medical conditions, metabolic demands, physical fitness, sex, sleep deprivation, work duration, and work experience. Addressing these risk factors will generate significant savings to healthcare systems from the occupational heat illness, absenteeism, and mortality associated with heat strain. Increased efforts should be made to educate individuals and organizations about the health, performance, and productivity risks related to heat strain and appropriate screening protocols should be incorporated within health and safety legislation.

Introduction

Rising environmental temperatures have become a growing challenge for societies across the globe⁹⁷⁻⁹⁹, and extreme heat events result in the highest short-term rise in morbidity and mortality when compared with all other natural weather hazards^{17,100}. A number of studies have reported that occupational heat strain may undermine the health and productivity of individuals working in key industries such as agriculture, construction, manufacturing, tourism, and transportation^{24,101,102}. Also, the quality of life in non-working populations has been greatly affected¹⁶. This growing issue has not been adequately addressed to date in relevant policies and programs, despite that nearly one million “work life years” (similar notion as DALYs) will be lost by 2030 due to occupational heat stroke fatalities, while the “work life years” lost due to reduced labour productivity may be 70 times greater^{103,104}. Moreover, while warning systems for extreme weather events have been recently piloted in some countries^{105,106}, they are designed for the general population whose needs and exposure to heat are vastly different from those of workers. For instance, the typical adaptation strategy in the afore-mentioned warning systems is to advise individuals to stay indoors throughout the day or to remain in “cooling shelters” at public buildings¹⁰⁷. However, such strategies are difficult to implement in industrial settings due to the need to maintain productivity regardless of the prevailing environmental conditions. This is a crucial issue since a recent questionnaire-based study in Australia reported that three-quarters of all employees are affected by occupational heat stress which reduces productivity and leads to an annual cost of 655 USD per worker¹⁰⁸. In agriculture, the prevalence of occupational heat stress is high and causes labour productivity to drop by up to 30%^{24,102}. Also, a recent systematic review and meta-analysis of 111 studies, including more than 447 million workers from over 40 different occupations, estimated that 35% of individuals who frequently work in heat stress conditions experience negative effects of occupational heat strain²⁶. In the following sub-sections we

combine a narrative review with observational studies to outline the factors affecting the risk for experiencing heat strain, which are illustrated in Figure 3.1.

Figure 3.1 | Graphical illustration of the factors affecting the risk for experiencing heat strain.



Factors affecting the risk for heat strain

1. Acclimatization

Humans are tropical animals capable to adapt and survive in adverse climatic conditions. This tremendously valuable ability for acclimatization to harsh and extreme environments exemplifies the most important evolutionary advantage which let humans expand their range of habitats all around the globe. Acclimatization to the heat is a temporary physiological adaptation which follows prolonged heat exposure and improves gradually, through repeated exposure until it reaches its full benefits after approximately two weeks ^{109,110}. Its importance is best understood when acclimatized individuals are able to complete tasks while experiencing much lower physiological strain compared to before acclimatization ^{109,111}. It is also considered a key determining factor which is able to enhance physical ¹¹² and cognitive ¹¹³ performance in hot conditions, as well as to mitigate the physiological strain experienced by humans who perform in the heat ¹⁰⁹. Considering all the above, it is a fair to say that heat acclimatization plays a crucial catalytic role in the heat strain experienced by workers and therefore it should be considered when a new worker is hired or when someone returns from vacation and he/she is expected to work in a hot workplace. In this light, reputable organizations ^{19,44} and international standards ¹¹⁴ recommend different approaches for acclimatized and non-acclimatized workers.

2. Aging

Aging is typically related with an inescapable decline of human psychophysical abilities and thus reduced capacity for heat dissipation. A series of experiments conducted using gold-standard direct calorimetry revealed that chronological age plays a crucial role in the heat-strain experienced by someone ¹¹⁵, identifying that males and females older than 53 and 55.8 years old, respectively, are more susceptible to heat stress in comparison to their younger counterparts. This is because the process of aging in

humans implies a gradual deterioration of several physiological mechanisms that make significant contribution to human capacity for heat dissipation, including sweating and cardiovascular responses ¹¹⁶⁻¹¹⁸. Generally speaking, after the 20th year of age, whole-body heat dissipation is progressively reduced by about 12 W every decade of aging (calculated from data presented in Figure 3 in ¹¹⁹). Considering this information as well as the fact that heat balance is a function of metabolic heat production and whole-body heat loss, it is clear that older workers experience increased heat strain in comparison to their younger co-workers. For instance, in case where a typical (body surface area: 1.8 m²) 55-year-old individual performs moderate intensity work (295 W), he/she is predicted to experience a 14.2 % increase in the amount of heat stored in his/her body, in comparison to an average 20-year-old worker. That is to say, from a heat strain perspective, a typical occupational activity included in the ISO 7933 ¹²⁰ such as “walking on the level without load at 4 km/h” leads to a level of heat strain for a 20-year-old person that corresponds to a lower-intensity activity (i.e., walking on the level without load at 3 km/h) for a 55-year-old worker ⁸, assuming they work in the same environmental conditions and wearing the same clothing.

3. Anthropometrics

A series of experiments conducted using gold-standard direct calorimetry revealed that body mass index, body fat percentage, and body surface area play a crucial role in the heat strain experienced by someone ¹¹⁵. Specifically, males and females with a body mass index higher than 29.5 and 25.7 kg/m², respectively, were found to be more susceptible to heat stress compared to individuals characterized by a lower body mass index. However, although body mass index seems to be able to guide experts on how to protect individuals who are physically active in the heat, it remains a simplified indicator and, thus, may not apply in some cases (e.g., for highly trained individuals). For this reason, the same study provided recommendations on the use of body composition as a guiding principle to classify people based on their susceptibility to

heat stress, showing that males and females with a body fat percentage higher than 28.8 and 34.9 %, respectively, should be considered more vulnerable to heat stress. This could be explained through two main avenues: (i) adipose tissue is a poor heat conductor and therefore it serves as an external insulative barrier to heat loss from the human body to the surrounding environment, and (ii) it does not have ergogenic aids, which means that obese individuals work more intense (i.e., higher metabolic heat production) to carry out a certain physical task, simply because in addition to the task performed, they must also carry their own overweight body.

In contrast to body mass index and body fat percentage which show a direct relationship with susceptibility to heat stress, body surface area acts in the opposite manner, meaning that the higher the surface area of someone's body the greater the heat loss from his/her body to the surrounding environment. This is the same principle as a school-type experiment where water in a flat shallow dish evaporates quicker compared to the same volume of water placed in a narrow skinny glass. For risk assessment, therefore, it is important to know that males and females having a body surface area higher than 2.0 and 1.7 m², respectively, are less vulnerable to heat stress

115.

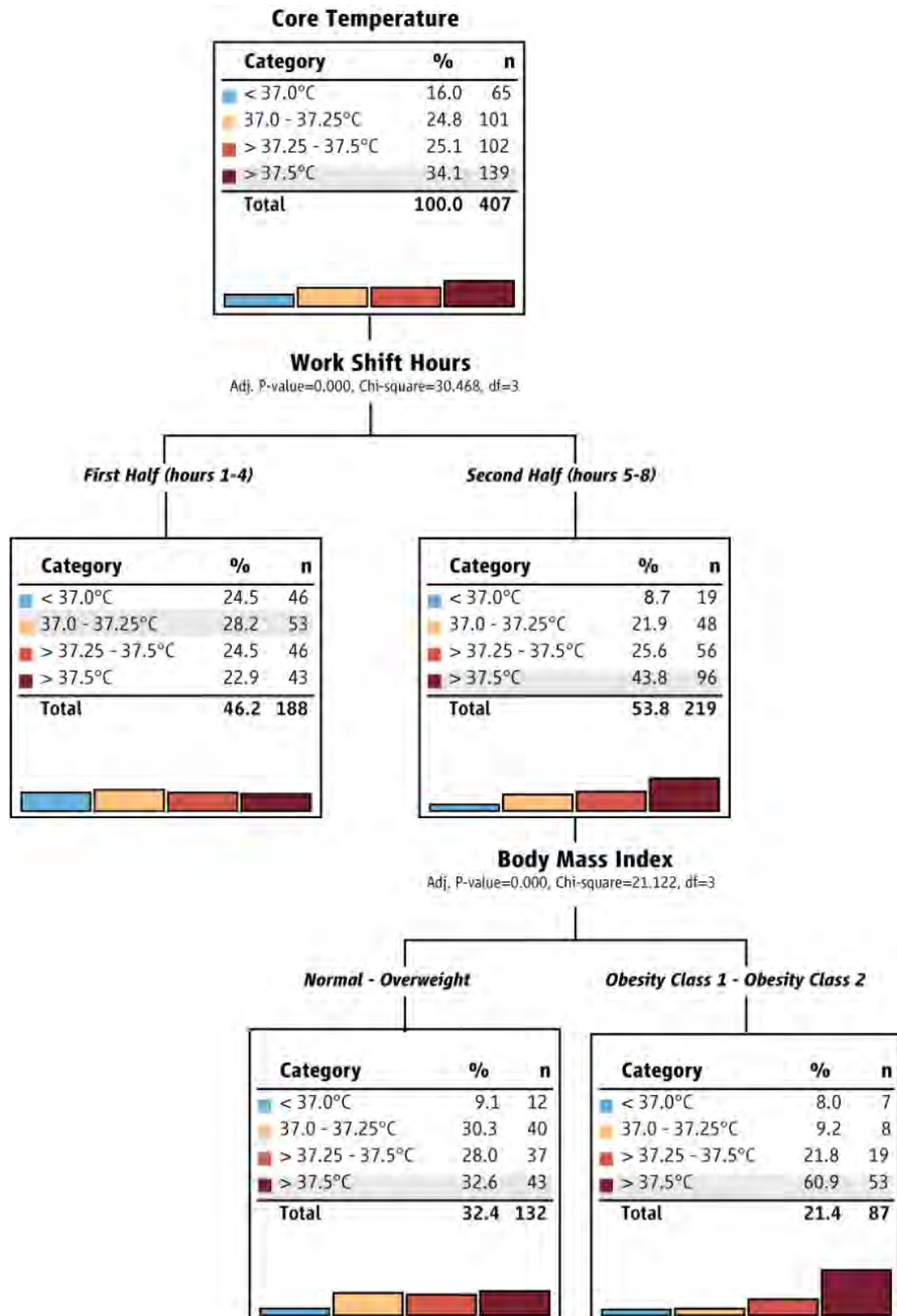
Based on the information presented in this section, risk assessment for heat stress during work and leisure could use anthropometric characteristics as a first screening approach that can mitigate the risk for developing life-threatening heat illnesses. For this reason, simple to calculate indicators that workers are likely to be familiar with could serve as a screening tools to mitigate the risk for heat-related illnesses, even in cases where their efficacy may be somewhat reduced.

To further investigate the effect of body mass index, which is the simplest indicator to calculate, on the heat strain experienced by workers, we conducted a series of field experiments. The experimental protocol (ClinicalTrials.gov ID:

NCT04160728) was approved by the National Bioethical Review Board of Cyprus and the School of Exercise Science of the University of Thessaly in accordance with the Declaration of Helsinki. The study involved monitoring 60 experienced and acclimatized manual labor workers from Cyprus, Greece, and Spain. Specifically, 46 male (body mass: 86.7 ± 11.7 kg; body stature: 173.7 ± 161.6 cm; age: 40.0 ± 11.2 years) and 16 female (body mass: 61.7 ± 12.3 kg; body stature: 161.6 ± 6.8 cm; age: 40.1 ± 9.6 years) agriculture and construction workers were recruited after detailed explanation of all the procedures involved. Prior to their participation in the study, written informed consent was obtained from all volunteers. Anthropometric characteristics were measured prior to the work shift and participants were categorized based on their body mass index as follows: normal (18.5 to 25.9 kg/m²), overweight (25 to 29.9 kg/m²), obesity class 1 (30.0 to 34.9 kg/m²), and obesity class 2 (35.0 to 39.9 kg/m²). The core body temperature of all participants was measured throughout the work shift using ingestible telemetric thermistors (BodyCap, Caen, France). A decision tree analysis was conducted using the dichotomous variables of work shift duration (a: first four hours; and b: last four hours of the work-shift), body mass index (a: normal-overweight; and b: obesity class 1/2), sex (a: male; and b: female), and the continuous variables of age and ambient temperature. The analysis identified that work duration and body mass index play a significant role in susceptibility to heat stress, demonstrating that obese workers have 87% increased risk (95% CI: 1.39 – 2.52) for experiencing elevated core body temperature (> 37.5 °C) during the second half of the work-shift in comparison to non-obese individuals (Figure 3.2). This finding confirms that body mass index could be utilized as a first screening approach to classify workers based on their anthropometric characteristics and thus protect them against the harmful workplace heat stress.

Figure 3.2 | Decision tree classifying.

Decision tree classifying the risk for having increased core body temperature based on work shift hours (first half vs. second half of the work-shift) and body mass index (non-obese vs. obese workers).



4. Clothing

Humans are tropical animals and therefore our anatomy and physiology were evolved through natural selection to optimize life in warm and hot conditions. In such climates, humans are capable of maintaining a relatively stable core body temperature within a narrow range without the need of any artificial means ¹²¹. On the other hand, clothing was found to be an essential protective mean which reduces the heat loss from our body to the surrounding environment and thus played a crucial role for civilizations living far away from the equator. Cultural differences in clothing evolved throughout the years and are still obvious today. This is especially true when comparing the clothing of indigenous people from two diametrically opposed regions such as the sub-Saharan Africa and the eastern Siberia/Alaska. Similarly, technology contributed to the development of work coveralls and other clothing ensembles that protect workers who perform in adverse environmental conditions. However, although protective clothing is a vital component of firefighters ¹²² and armed forces ¹²³ daily routine, it might also make a significant contribution to increasing the heat strain experienced by someone. Of course, this is a well-known fact and thus the scientific community developed thermal stress indicators that are either coupled with clothing models ¹²⁴ or capable to calculate the optimum clothing insulation considering the ambient temperature ¹²⁵. Also, some thermal stress indicators such as the Wet-Bulb Globe Temperature provide adjustments for clothing insulation by adding from 0.5 to 11 °C to the measured value, depending on the clothing ensemble worn ¹²⁶. As a general prescription, there should be a change of 0.0436 clothing insulation units (clo) for every degree Celsius increase or decrease in ambient temperature ¹²⁵.

5. Cultural habits

Cultural habits refer to a patchwork of independent factors reflecting the ethnic and religious traditions that a group of people developed over the years. These include traditions in clothing ¹²⁷, tattoos ¹²⁸, and religious fasting ¹²⁹, which are directly or

indirectly linked with the risk of heat stress during work and leisure. For instance, thick clothing covering a large fraction of the body surface area, such as the traditional burqa worn by females in middle east, are known to reduce the heat loss from the body to the surrounding environment ^{121,130}. Skin tattooing which is a common practice in many countries ¹³¹ can affect sweat rate ¹²⁸ and thus the evaporative heat loss through this enormously important thermoregulatory mechanism. Similarly, religious fasting, such as that followed by Muslim people during the Ramadan, may promote dehydration ¹²⁹, reducing the body's capacity for evaporative heat loss. Therefore, it becomes clear that cultural habits such as the ones described above should be considered as an additional contributing factor when assessing the risk for experiencing increased heat strain in occupational or other settings.

6. Diet

The variety of the food consumed by a person varies based on national, cultural, seasonal, medical, preferential, and financial factors, with numerous combinations of food for people to consume in order to satisfy their daily food needs. This is an important component of risk assessment that should be considered, since meal and nutrient characteristics are known to significantly impact diet-induced thermogenesis ¹³². Specifically, 5 to 15 % of daily energy expenditure is devoted to diet-induced energy expenditure when a mixed diet is consumed at energy balance ¹³². Higher values are linked with a high protein and alcohol consumption and lower ones with a high fat consumption ¹³², indicating that meals low in protein and alcohol should be recommended during work in the heat. Another important diet-related component which makes an even larger contribution to human capacity for thermoregulation is water consumption ^{133,134}. This is especially true if we consider that two thirds of our body is consisted of water which is lost, in the form of sweat, often in higher quantities than the ones consumed ¹³⁴. When dehydrated, human capacity for evaporative heat loss, which is the most important component of thermoregulation during physical work,

is limited. This, in turn, increases the overall heat strain experienced by someone and should therefore be considered an important contributing factor when assessing the risk for experiencing increased heat strain during work in the heat.

7. Disabilities

People with disabilities represent a sizable fraction of the workforce due to their increasing labor force participation particularly over the last 30 years ¹³⁵. This indicates that it is becoming more and more frequent for people with disabilities to cooperate and coexist in the same environment with able-bodied individuals. Although from a psychosocial point of view this is a good practice that improves social behavior and communication as well as the acceptance of people with disabilities at work ¹³⁶, it may create challenges from a physiological and health perspective. This is because people with disabilities have impaired vasomotion and sweating mechanisms and, thus, reduced capacity for thermoregulation below the level of the lesion when exposed to thermally challenging environments ¹³⁷. It is not surprising, therefore, that thermal comfort of people with disabilities is known to have a much larger variability than that of able-bodied individuals ¹³⁸. That is to say that coexistence between disabled and able-bodied individuals in the same workplace may promote friction, for instance, when using air-conditioning which is one of the most common and efficient methods to mitigate workplace heat stress. Hence, disability should be considered as an important factor to keep in mind when assessing the risk for experiencing heat strain during work and leisure.

8. Drugs and addictions

Under elevated heat stress, the hypothalamus, which is the thermoregulatory center of human brain, activates appropriate behavioral and physiological responses to maintain a relatively stable core body temperature. However, pharmaceutical agents may impair a person's capacity for thermoregulation, therefore increasing core body temperature through five avenues: (i) altered thermoregulatory mechanisms, (ii) drug

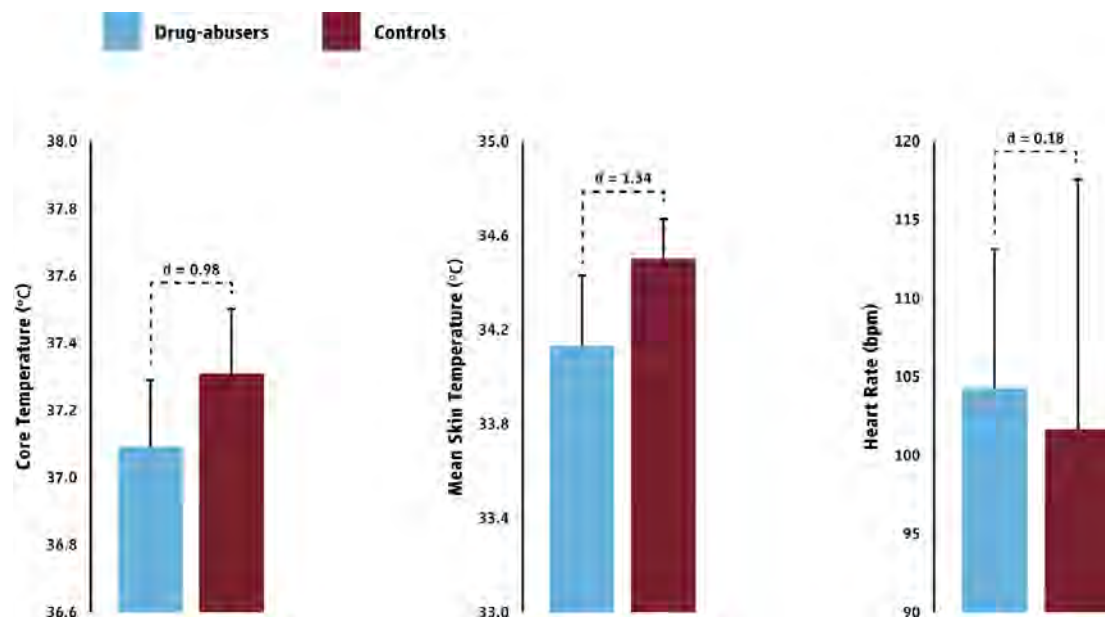
administration-related fever, (iii) fever from pharmacologic action of the drug, (iv) idiosyncratic reaction, and (v) hypersensitivity reactions¹³⁹. This becomes even worse when non-prescribed psychostimulants such as morphine, methamphetamine, and cocaine are abused, leading to the development of profound side-effects including brain dysfunction and death¹⁴⁰. Although the loss of, predominantly, young lives is a huge burden on our society, the underlying mechanisms of drug-abuse mortality are still not well understood. It has been previously stated that it might be associated with the well-known drug abuse-induced hyperthermia during exposure to high ambient temperatures¹⁴⁰⁻¹⁴². Therefore, the use of prescribed medications and the abuse of recreational psychostimulants should be considered as a determinant factor which increases the overall risk for experiencing increased heat strain.

To investigate deeper the risk for experiencing heat strain in occupational settings, we examined the impacts of occupational heat stress on former drug abusers participating in an occupational rehabilitation program. The experimental protocol was approved by the National Bioethical Review Board of Cyprus and the School of Exercise Science of the University of Thessaly in accordance with the Declaration of Helsinki. The study involved monitoring eight males consisting of four drug abusers and four matched-controlled individuals (all normoweight and aged between 28-35 years old). It is important to note that all former drug abusers underwent a methadone-assisted rehabilitation treatment at the time of data collection. Prior to their participation in the study, written informed consent was obtained from all volunteers after detailed explanation of all the procedures involved. The two groups of participants (controls and drug abusers) were picking vegetables from 09:00 to 13:00 in environmental conditions of similar magnitude (26.4 vs. 26.9 °C Wet-Bulb Globe Temperature). We found that former drug abusers experience reduced heat strain compared to their control co-workers (Figure 3.3). This may be explained by the fact that methadone induces

peripheral vasodilation¹⁴³ and excessive sweating¹⁴⁴, two mechanisms with well-determined heat-dissipative potential.

Figure 3.3 | Differences in the physiological.

Differences in the physiological strain experienced by former drug-abusers during occupational rehabilitation (blue bars) and controls during work of similar dynamic and kinematic characteristics (red bars).



9. Environmental stress

Heat balance between the body and the external environment is a function of metabolic heat production and the heat loss through the four fundamental heat exchange mechanisms: conduction, convection, evaporation, and radiation. These mechanisms are directly affected by factors of the surrounding environment: ambient temperature, humidity, wind, and thermal/solar radiation. From these four factors, ambient temperature and thermal radiation always make an incremental contribution to the heat strain experienced by someone, meaning that the higher their values the larger the risk for experiencing increased heat strain. On the other hand, humidity and wind speed are bidirectional factors, meaning that their contribution to the heat loss from the human body to the surrounding environment might be positive or negative, depending on the ambient temperature and thermal radiation, as well as on other non-

environmental parameters. It is beyond any doubt that all four environmental factors play their own unique role in the heat strain experienced by someone, and thus they should all be considered when assessing the risk for environmental heat stress. For this reason, from the dawn of scientific research, more than 300 thermal stress indicators were developed aiming assess the interaction between these environmental factors and provide physicians and other health professionals with a single value describing the overall thermal stress experienced by someone. For instance, Wet-Bulb Globe Temperature ¹⁴⁵ is a widely accepted thermal stress indicator and it is recommended for use in occupational settings by reputable organizations ^{19,44,126} and international standards ¹¹⁴. It is important to note that, although the risk for experiencing increased heat strain is mostly affected by the thermal components of the surrounding environment, additional non-thermal environmental factors such as the oxygen level ¹⁴⁶ and gravitational force ¹⁴⁷ were found to make a significant contribution as well. Therefore, it is important to have a holistic view on thermal and non-thermal factors before assessing the risk for experiencing increased heat strain.

10. Ethnicity

Tens of thousands of years after humans left Africa, natives in cold regions have been evolved to survive and perform under their local climatic conditions by developing behavioral and physiological adaptations to the cold ¹⁴⁸. Population studies identified that Caucasian and Inuit people have improved responses to cold stimuli, including shivering thermogenesis and cold induced vasodilation, in comparison to Indigenous black Africans ¹⁴⁸. Additionally, a study incorporating data from 45 distinct global populations showed that the genes ADRA2A and ADRA2C, that may have cold-induced vasoconstrictive potentials, were more prevalent in people who live in colder regions ¹⁴⁹. However, other sources of evidence suggests that migration to colder regions may have reduced the capacity of humans for thermoregulation in the heat ¹⁴⁸. This is because, black indigenous Africans in hot regions have been found to have

significantly more mixed apocrine-ecrine sweat glands in comparison to Caucasians¹⁵⁰. These evolutionary adaptations may explain the fact that people with different ethnic backgrounds have been consistently found to have different thermal preference temperatures¹⁵¹. Therefore, ethnicity should also be considered as an important contributor to the risk for experiencing increased heat strain, and probably different heat mitigation approaches should be adopted in multicultural workplaces where individuals with different ethnicities coexist and work.

11. Heat mitigation

Human abilities for building dwellings and processing animal fur to create garments could be considered the first mitigation strategies that our species advanced to counterbalance the heat loss/gain to/from the external environment. From an evolutionary perspective, these early mitigation strategies together with our capacity for physiological adaptations in different climatic conditions might be the puzzle piece explaining how humans expanded their range all around the world. Undoubtedly, the above strategies are of great importance during leisure since they can protect humans who rest or sleep in unfavorable environmental conditions. During work, however, more advanced approaches are needed to safeguard worker's health and wellbeing. This is because the external work performed, particularly during manual labor tasks, requires high metabolic rates and thus a significant amount of energy is released as heat warming up the body. To counterbalance this endogenous metabolic heat production, several exogenous strategies were proposed and tested in literature. From all the solutions examined, the most effective ones are wearing cooling garments, heat acclimation, enhancing aerobic fitness, immersion to cold water, and ventilation¹⁵². Heat mitigation strategies are of paramount importance and therefore should always be considered when assessing the risk for experiencing increased heat strain.

12. Medical conditions

More than one-fifth of the world population has currently an underlying medical condition affecting its capacity for thermoregulation, including cardiovascular diseases¹⁵³ and diabetes¹⁵⁴. Therefore, it is logical to assume that an important fraction of global workforce is currently working with impaired thermoregulatory function, causing elevated thermal and cardiovascular strain and thus increasing the overall risk for heat-induced cardiovascular mortality^{155,156}. Both cardiovascular diseases¹⁵⁷ and diabetes¹⁵⁸ are known to affect peripheral blood flow adaptations, which is one of the most important mechanisms to dissipate body heat. Hence, it becomes more and more clear that underlying medical conditions should be an important classification tool which might allow managers to group their workforce into different clusters of work activities based on their thermal demands. This classification should always consider intra-individual and inter-individual factors, while taking into account both the metabolic and thermal components of the work required to be performed.

13. Metabolic demands

The first law of thermodynamics states that energy can only be transferred or changed from one form to another and this applies on everything, including humans. In this light, during labor most of the metabolic energy of the food consumed is converted to heat and only a small fraction of it is transformed to kinetic energy and thus mechanical work^{159,160}. This is because, “mechanical efficiency” or simpler the human capacity for converting metabolic energy to external mechanical work is inefficient and limited. At work of low intensity this inefficiency becomes even more apparent, approaching null values, while when work activities of higher metabolic demands are performed it follows an exponential growth, plateauing at a theoretical maximum of 20%¹⁶⁰. For instance, when walking at 3.2 km/h (116.3 W/m²) the external work produced is 3 W/m², which is lower than 4 %. However, when walking and at the same time carrying a box of 45 kg (494.3 W/m²) the work produced is 98 W/m², which is about 20 % of the

total energy metabolized⁸. It is important to note that, in both cases the remaining energy is released as heat warming up the body. Although humans developed behavioral mechanisms that work inconspicuously to regulate the metabolic heat production counterbalancing the heat gain from the surrounding environment^{26,161}, additional work-intensity-oriented measures should always be considered to safeguard worker's health and wellbeing.

14. Physical fitness

The ability of human body systems to work together efficiently and optimize our capacity to perform various daily activities is known as "physical fitness". This parameter is vital not only because it improves our daily life, but also because it contributes substantially to human capacity for thermoregulation. A series of experiments conducted using gold-standard direct calorimetry revealed that aerobic capacity plays a crucial role in thermoregulation, demonstrating that non-fit males (≤ 48.3 ml O₂/kg/min) and females (≤ 41.4 ml O₂/kg/min) are more susceptible to heat stress¹¹⁵. This is because aerobic fitness is associated with reduced core temperature threshold for skin vasodilation and sweating¹⁶², and thus triggering a faster response to counterbalance the heat gain from endogenous and exogenous factors. It is important to note that, increased physical fitness is also associated with reduced body mass index and body fat percentage, two anthropometric variables that make a significant contribution to human capacity for thermoregulation¹¹⁵. Therefore, reduced physical fitness is considered a critical factor affecting the overall risk for experiencing increased heat strain, and therefore it should be taken into account by the management when laborers are expected to work under heat stress.

15. Sex

"Gender-blindness" is a term used to describe the concept of ignoring that people of different sex are differently affected by a situation due to their distinct nature¹⁶³. In this light, a work schedule that fails to consider sexual differences in physiological

capabilities between men and women could be defined as gender-blinded, and it might promote inequalities on how workers of different sex perceive a job of equal kinematic and metabolic characteristics. This is especially true if we consider that females tend to have (i) a larger ratio of body surface to body mass, (ii) more subcutaneous fat, and (iii) reduced exercise capacity ¹⁶⁴. Moreover, sex hormones released during the menstrual cycle can modify women's capacity for thermoregulation during work under heat stress ¹⁶⁴. Hence, it now becomes more apparent that sex differences should be considered as an important contributing factor affecting the overall risk for experiencing heat strain and should be taken into account when work duties are assigned to laborers.

16. Sleep deprivation

Across the world, between 15 % and 30 % of adult workers are engaged in some type of night shift work (defined as >2 hours of work performed between 22:00 and 06:00) ¹⁶⁵. Also, night shifts represent a very common approach in large-scale manual labor workplaces such as construction ^{166,167}. In support of night shift work, specific elements of work such as commuting, work interference, idle-machinery times, and occupational heat stress exposure are improved ¹⁶⁸. However, the adverse effects of night shift on manual laborers on safety, productivity, and health have also been widely reported ¹⁶⁹. An individual working at night and sleeping during the day experiences a state of desynchrony similar to that of a traveler who flies rapidly across several time zones. Depriving sleep for one day can impair alertness and performance levels ¹⁷⁰. Sleep deprivation accumulating over consecutive days can lead to acute or chronic fatigue and sleepiness, particularly if adequate time is not allowed for recovery. Moreover, the risk for accidents at work can be increased by 50 to 100 % in workers performing consecutive night shifts ¹⁷¹, and can affect all tasks in which workers are required to operate ¹⁷², causing up to 53 % increase in absenteeism and up to 92 % increase in compensations for absenteeism ¹⁷³. One factor contributing to the increased accidents

due to sleep deprivation is that individuals are typically very poor judges of the true impact of sleep restriction on their alertness levels, reporting that they are much less affected than what's in fact true¹⁷⁴. A typical example is a driver who feels that he/she is fit to drive but, in fact, is not alert enough to operate the vehicle and is likely to cause an accident.

17. Work duration

There is no better way to avoid finding yourself in a harmful situation than avoiding the factors leading to it in the first place. In an ideal world, there would be no reason for writing this chapter as work absenteeism would be the panacea for safeguarding individuals who work under heat stress. However, in the real world, humans are expected to work for several hours every day in environments that are often harmful and can damage the health of those involved. In an attempt to find a middle ground, reputable organizations^{19,44,126} and international standards¹¹⁴ recommend work-rest cycles for work in the heat. This is because work duration is directly and strongly related with the thermal strain experienced by individuals who work under heat stress, and thus providing them with small regular breaks throughout the work-shift adds an additional protective layer in the fight against occupational heat strain. It is encouraging that more and more countries adopt similar work-rest cycles enacting legislation aiming to protect their workforce in the face of climate change. However, we are still far away from worldwide adoption of such guidelines, and thus work duration should be considered as an important contributor the risk for experiencing increased heat strain.

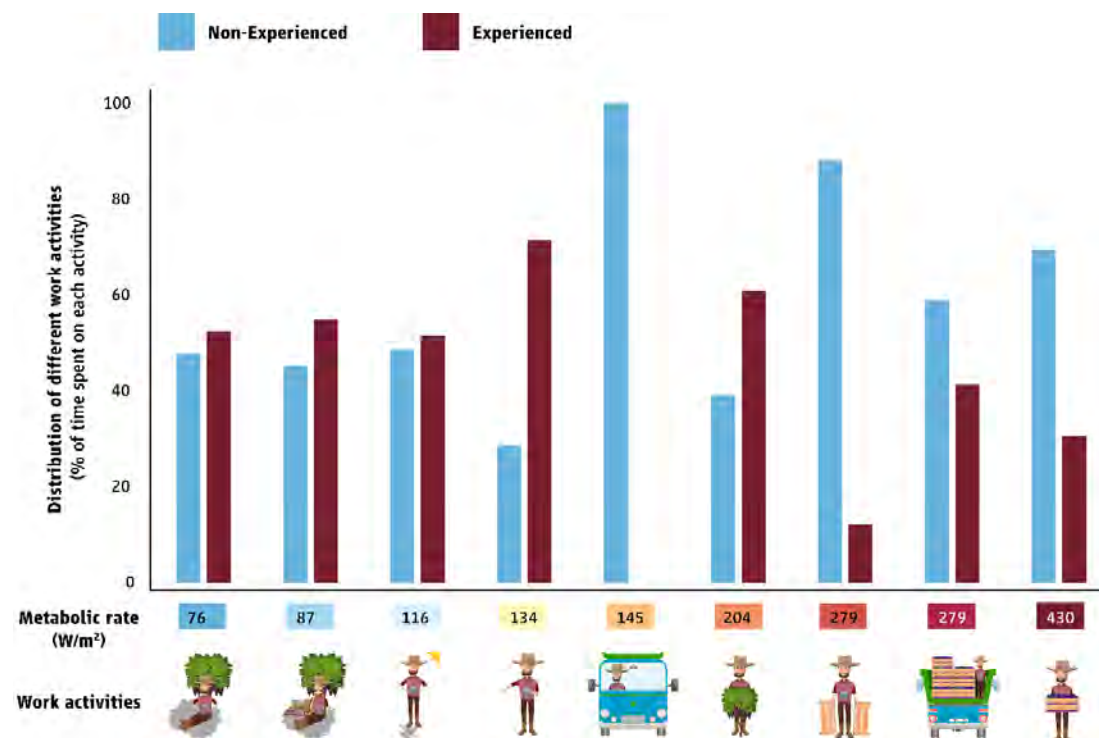
18. Work experience

Work experience is not among the classical factors considered when assessing the risk for experiencing heat strain during work. This is because there are no direct links between human thermoregulation and work experience. Also, there are no published studies that have examined the impact of work experience on the risk for experiencing heat strain. Therefore, we conducted a series of time-motion experiments¹⁶¹ to detect

potential differences in human behavioral thermoregulation between experienced and non-experienced workers. The experimental protocol (ClinicalTrials.gov ID: NCT04160728) was approved by the National Bioethical Review Board of Cyprus and the School of Exercise Science of the University of Thessaly in accordance with the Declaration of Helsinki. The study involved filming 20 full work-shifts performed by agriculture workers (body mass: 72.9 ± 15.7 kg; body stature: 171.5 ± 2.7 cm; age: 40.9 ± 10.0 years) in Cyprus. Workers were grouped as experienced (4 to 6 years) and non-experienced (1 to 3 years) based on their previous involvement with such work tasks. Our findings indicate that experienced workers (200.5 ± 20.6 W/m²) tend to select tasks of lower metabolic demands compared to non-experienced workers (228.3 ± 24.9 W/m²) (Figure 3.4). This metabolic reduction of 12.2 % may be linked with behavioral thermoregulation and it is associated with the years of work experience ($r = -0.48$, $p = 0.033$). Therefore, work experience should be considered as an important contributing factor affecting the overall risk for experiencing increased heat strain, and thus it should be taken into account during work under heat stress.

Figure 3.4 | Differences in work activities.

Differences in the time spent performing work activities of varying metabolic intensity, across experienced and non-experienced agriculture workers.



Concluding remarks

The present Chapter describes the factors that can modify an individual's risk for heat stress during work and leisure. Addressing these risk factors will, undoubtedly, generate significant savings to healthcare systems from the occupational heat illness¹⁷⁵, absenteeism¹⁰⁸, and mortality¹⁷⁶ associated with heat strain. This is of particular importance for industries relying on manual labor jobs performed outdoors and, often, in hot conditions. In these situations, appropriate strategies (work-rest ratios, hydration, clothing, shading, etc.) can mitigate, at least partly, the heat strain experienced by workers¹⁷⁷.

The risk for heat strain during work and leisure is increasing due to the occurring climate change and the anticipated rise in environmental heat stress¹⁷⁸. To reverse this situation, concerted international action encompassing different scientific,

health and safety, as well as labor-related disciplines is needed. At the same time, increased efforts should be made to educate individuals and organizations about the health, performance, and productivity risks related to heat strain and appropriate screening protocols should be incorporated within health and safety legislation.

Chapter 4

Towards Model-Based Online Monitoring of Cyclist's Head Thermal Comfort: Smart Helmet Concept and Prototype

This work was conducted by Ali Youssef, Jeroen Colon, Konstantinos Mantzios, Paraskevi Gkiata, Tiago S. Mayor, Andreas D. Flouris, Guido De Bruyne, and Jean-Marie Aerts. We all contributed to the conception and design of the study. I developed the prototype, conducted lab measurements, and collected data. I performed statistical analyses, interpreted the data, and drafted and revised the manuscript. I also maintain full access to all algorithms, codes, and data used in the study and assume responsibility for the integrity of the data and the accuracy of the data analysis.

As of August 2019, this study ³ has been published online by Applied Sciences MDPI as follows: Youssef A., Colon J., Mantzios K., et al *Towards Model-Based Online Monitoring of Cyclist's Head Thermal Comfort: Smart Helmet Concept and Prototype*. Applied Sciences MDPI; [10.3390/app9153170](https://doi.org/10.3390/app9153170)

The inclusion of this study in my thesis is justified as it closely aligns with the central theme of my PhD research. This study's emphasis on designing a smart helmet for monitoring the thermal comfort of cyclists to protect their health and optimize performance, provides a valuable context for my thesis. My active role in the development of prototype and application (Chapter 1.1), data collection, analysis, and manuscript drafting has resulted in vital insights, particularly the understanding of how technology can help in monitoring thermal comfort in athletes.

All the authors have approved the inclusion of this study in my PhD thesis and hereby affirm that I have made significant contributions to the experimental work conducted, as well as the review process of the manuscript, for the study to be completed (Annex B).

Abstract

Bicyclists can be subjected to crashes, which can cause injuries over the whole body, especially the head. Head injuries can be prevented by wearing bicycle helmets; however, bicycle helmets are frequently not worn due to a variety of reasons. One of the most common complaints about wearing bicycle helmets relates to thermal discomfort. So far, insufficient attention has been given to the thermal performance of helmets. This paper aimed to introduce and develop an adaptive model for the online monitoring of head thermal comfort based on easily measured variables, which can be measured continuously using impeded sensors in the helmet. During the course of this work, 22 participants in total were subjected to different levels of environmental conditions (air temperature, air velocity, mechanical work and helmet thermal resistance) to develop a general model to predict head thermal comfort. A reduced-order general linear regression model with three input variables, namely, temperature difference between ambient temperature and average under-helmet temperature, cyclist's heart rate and the interaction between ambient temperature and helmet thermal resistance, was the most suitable to predict the cyclist's head thermal comfort and showed maximum mean absolute percentage error (MAPE) of 8.4%. Based on the selected model variables, a smart helmet prototype (SmartHelmet) was developed using impeded sensing technology, which was used to validate the developed general model. Finally, we introduced a framework of calculation for an adaptive personalised model to predict head thermal comfort based on streaming data from the SmartHelmet prototype.

Introduction

Bicycling, for recreational, transport and sport purposes, provides health benefits for the individual as well society ¹⁷⁹. However, due to different reasons, bicyclists can be subjected to crashes, which can cause injuries over the whole body. Of these, head injuries can lead to serious brain damage and, in extreme cases, death ¹⁸⁰.

Head injuries can be prevented by wearing bicycle helmets, thereby increasing cycling safety ¹⁸¹. However, while it is well known that bicycle helmets can be lifesaving in case of an accident, they are not worn frequently. A variety of barriers of social, psychological, cultural and biological origin have been reported ¹⁸².

One of the most common complaints associated with wearing bicycle helmets appears to be thermal comfort ¹⁸³. In a survey study by Finnoff et al. ¹⁸³, it appeared that “uncomfortable” and “it’s hot” were two of the most important barriers for wearing a bicycle helmet in all three age categories (children (7–10), adolescents (11–19) and adults (>19)). Furthermore, Bogerd et al. ¹⁸⁴ concluded in their review study, which investigated the ergonomics of headgear, that unfavourable thermal sensation or thermal discomfort is frequently used as an argument for not wearing headgear. Wearing a bicycle helmet alters the local skin temperature and sweat rate, which can lead to thermal discomfort ¹⁸⁴. Moreover, under exertion, the human body dissipates a significant fraction of its excess heat through the head, which, during cycling, is placed in a strong air current. The helmet insulates the head, limiting the transfer of heat to the air and the evaporation of sweat ¹⁸⁵. Therefore, it is of utmost importance for bicycle helmets to be designed in a way that favours thermal comfort whilst meeting mechanical protection requirements. This dual goal of protection and comfort poses a great challenge because of the often-contradictory requirements of thermal comfort and impact protection ¹⁸⁶.

Sensations concerning thermal comfort are the result of a cognitive process described by the American Society of Heating, Refrigerating and Air-Conditioning Engineers (ASHRAE) standard 55¹⁸⁷ as “that condition of mind, which expresses satisfaction with the thermal environment” (ASHRAE standard 55–66). Comfort is a recognisable state of feeling which is the result of the entire environment, including psychological and physiological variables. It is usually associated with conditions that are pleasant and compatible with health and happiness, whereas discomfort is associated with pain, which is unpleasant¹⁸⁸.

Skin temperature and sweat rate are examples of the body's mechanisms to keep body temperature quasi-constant. These mechanisms are controlled by a region in the brain called the hypothalamus. This regulation centre monitors body temperature and controls it directly by physiological processes and/or indirectly by behaviour (i.e., behavioural thermoregulation). Although a person's reported state of thermal comfort is purely perceptive, the body's thermoregulatory actions influence thermal comfort by its outcomes (e.g., sweat rate, skin temperature, etc.)¹⁸⁸⁻¹⁹⁰.

An often-used method to accurately assess thermal sensation (TS) and comfort (TC) is to ask individuals directly about their thermal sensation perception^{189,191}. Individuals express their opinion to rate their thermal sensation/comfort when they are exposed to given thermal conditions by using a scale from cold to hot that has a predefined number of points. Mathematical models of thermal sensation and comfort have been developed to overcome the difficulties of direct enquiry of subjects. The development of such models has mostly depended on statistical approaches that correlate experimental condition data (i.e., environmental and personal variables) with thermal sensation votes obtained from human subjects^{189,192}. Thermal comfort models, such as predicted mean vote (PMV), predict the state of thermal comfort from thermoregulatory actions such as skin temperature and sweat secretion. These two types of models are therefore often combined to predict the thermal comfort of an

average person under different environmental conditions ^{191,193}. Many advanced mechanistic thermoregulation models, such as the “Fiala thermal Physiology and Comfort” (FPC) model, were developed to predict the thermal comfort status of humans ¹⁹⁴. By implementing thermoregulation models in wearable devices connected to the body, thermal comfort can be monitored and, in a further stage, even controlled. However, for real-time applications, such models are too complex and have a high computational cost, thus making them less suitable for monitoring and control applications. Data-based models, on the other hand, are less complex and thus more adequate for real-time monitoring and control purposes. Youssef et. al. ¹⁹⁵ demonstrated that such compact data-based mechanistic models are promising for modelling body temperature response using metabolic activity alone or metabolic activity and skin temperature as inputs by means of, respectively, a single-input single-output (SISO) or a multiple-input single-output (MISO) discrete-time transfer function model.

Recent developments in compact wireless sensors allow the implementation of sensors in wearable devices such as bicycle helmets. Considering this, bicycle helmet design should be optimised for thermal comfort, so that bicycle helmets not only allow monitoring an individual's thermal comfort but also support its active control.

In this reported research, we aimed at

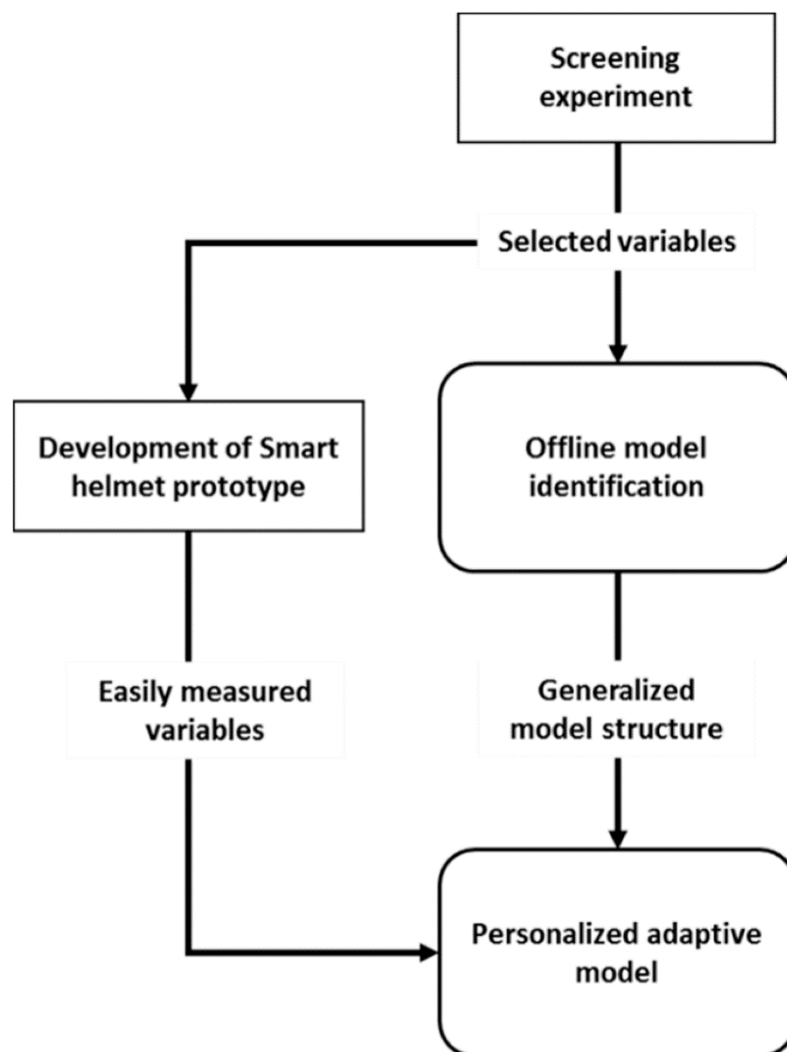
- i) identifying a general model to estimate thermal comfort based on a few variables, the measurements of which can be integrated in helmets;
- ii) developing and testing a prototype of a smart helmet based on the identified general thermal comfort model; and
- iii) introducing the framework of calculation for an adaptive personalised reduced-order model to predict a cyclist's under-helmet thermal comfort using nonintrusive, easily measured variables.

Materials and Methods

The main goal of this paper is to introduce a framework for developing a personalised adaptive model for predicting a cyclist's head thermal comfort by utilising the smart helmet concept. Figure 4.1 presents the general framework introduced in the present paper.

Figure 4.1 | Schematic diagram of the smart helmet prototype.

Schematic diagram showing the general framework of the development of a personalised adaptive model for the smart helmet prototype.



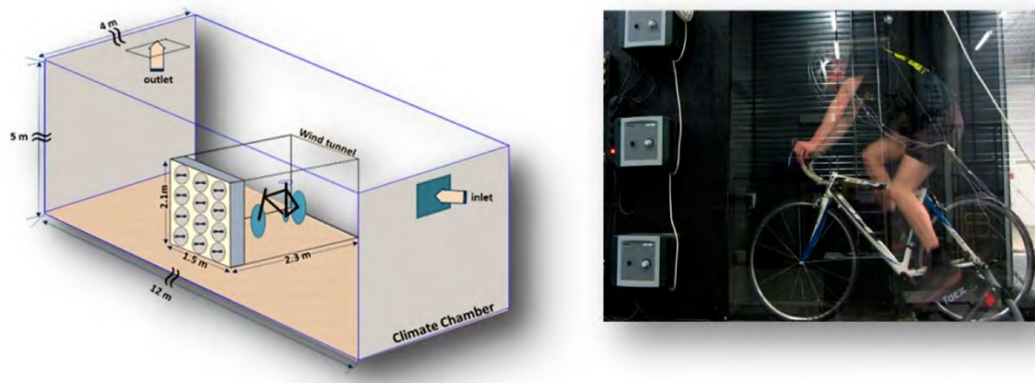
Development of General Thermal Comfort Predictive Model

Experimental Setup and Test Subjects

During the course of these experiments, 15 male test subjects with an average age ($\bar{\mu}$ age) of 22 (± 1) years and an average weight ($\bar{\mu}$ mass) of 74.3 (± 9.2) kg were used in this study. The experimental protocol was approved by the Social and Societal Ethics Committee (SMEC) of KU Leuven. The experiments were conducted using a professional bicycle trainer (Tacx Ironman Smart) with a fastened racing bicycle (BH L52C8 Speedrom) controlling the power delivery of the subject with a power brake. The power brake itself was wirelessly controlled via the Tacx Trainer software. The bicycle trainer was placed in a customised wind tunnel to simulate the wind effect on the test subjects during the course of the experiment (Figure 4.2). The wind tunnel was 2.1 m high, 2.3 m long and 1.5 m wide. Four rows with three fans each (Fanco type 1435/L7-588 fans) were used as the actuators for wind speed. Each fan produced a maximum ventilation rate of 3000 m³·h⁻¹. A 50 cm long honeycomb gauze structure, placed 25 cm from the fans, was used to obtain a quasi-laminar flow within the open-loop wind tunnel (for more information about the wind tunnel, see ¹⁹⁶). The air speed near the test subject's head was set to 2.5 m·s⁻¹ to simulate recreational cycling for adults and children. The wind tunnel was placed inside a climate-controlled chamber (Figure 4.2), the inner dimensions of which were 4 × 11 × 5 m (w × l × h). The air temperature within the climate chamber was controllable within the range of 15–35 °C. Additionally, the ventilation rate within the climate chamber was controllable within the range of 0–2700 m³·h⁻¹ (i.e., 0–11.25 volume refreshments per hour).

Figure 4.2 | Representation of customized wind tunnel.

Schematic representation showing the used bicycle fixed inside a customized wind tunnel and placed within a climate chamber (left) and a photograph of a test subject riding the bike within the wind tunnel (right).



Pretest Experiments

The pretest was a modification of the widely used physiological test protocols described by the Australian Institute of Sport ¹⁹⁷. The aim of the pretest was to obtain a power (P) value that could be maintained by each of the 15 test subjects for a period of at least 20 min. The maximal lactate steady state (MLSS) and the corresponding workload steady state (WLSS) are presumed to be the maximum workload that can be maintained for endurance sports ^{198,199}. This lactate threshold is defined as the highest oxygen consumption rate that can be achieved during exercise without a systematic increase in blood lactate concentration ²⁰⁰. A respiratory exchange ratio (RER) > 1.0 is an indication of the growing contribution of anaerobic metabolism, which causes muscle acidification and leads to muscle fatigue ²⁰¹.

A bicycle incremental step test was designed in such way that the power increased 30 W every 5 min starting from 100 W. During the test, the subject's RER was measured with a spirometer (Metamax 3B) and the test was terminated when he exceeded an RER value of 1 for more than 20 s (the corresponding power, PRER = 1, was used further in the thermal comfort experiment). The tests were conducted at

normal indoor climate conditions with 47% ($\pm 4\%$) relative humidity and an ambient temperature of 20 (± 1) °C.

Thermal Comfort and Variable Screening Experimental Protocol

The main objective of this stage was to screen the most suitable variables to predict the cyclist's under-helmet thermal comfort which can also be easily measured so as to be combatable for smart helmet application. During the course of these experiments, each experimental trial lasted 80 min and was divided into four consecutive timeslots of 20 min each. At each timeslot, a combination of changes in the environmental variables, namely, relative air velocity imposed by the fan (v), ambient air temperature (T_a), thermal resistance of the scalp (R_h) and the delivered cycling power (P), was applied. The quantification of the scalp thermal resistance (R_h) was developed based on computational fluid dynamic (CFD) simulation for a bare head²⁰². The thermal resistance was quantified (see Table 4.1) for the following cases: no-helmet wearing, where R_h was 0; wearing helmet; and wearing helmet with helmet fast (aeroshell). The applied combinations of the different variables with their different levels (low, mid and high) are shown in Table 4.1.

Table 4.1 | The applied values for each variable.

	T_a [°C]	v [m.s ⁻¹]	P [W]	R_h [m ² °C.W ⁻¹]
Low-level	20	0	50% ($P_{RER=1}$)	0 (no helmet)
Mid-level	/	/	/	0.045 (with helmet)
High-level	30	4	90% ($P_{RER=1}$)	0.060 (helmet + aeroshell)

During the course of each trial, the heart rate (HR), in bpm, of the test subject was measured and logged with a validated heart rate belt sensor (Zephyr™ bioharness Bt) in combination with a built-in optical heart rate sensor (PPG, Lifebeam) in the bicycle helmet (Lazer Z1 and Lazer Z1 fast = Lazer Z1 + aeroshell). The temperatures of the subject's forehead, neck, inside of the ear and the air under the

bicycle helmet (at front, back, right and left) were continuously measured using calibrated thermocouples (type-T) with a sampling frequency of 1 Hz.

During the experiment, all test subjects were verbally asked about their thermal comfort every 5 min from the start (minute 0) until the end (minute 80) based on the thermal comfort scale introduced by Gagge et al. ¹⁸⁸. For convenience, the cold thermal sensation votes were excluded, as shown in Table 4.2, as the present work only focused on discomfort perception due to high temperatures.

Table 4.2 | Thermal comfort scale introduced by Gagge et al. ¹⁸⁸, excluding the cold sensation votes.

Scale	Thermal Comfort Perception
1	Comfortable
2	Slightly uncomfortable
3	Uncomfortable
4	Very uncomfortable

The experimental design was done using JMP Pro software. A preliminary screening experiment was set up to investigate the contribution of the different variables that, potentially, have an effect on the thermal sensation and thermal comfort under the bicycle helmet. Therefore, each subject was subjected to a combination of different levels of environmental conditions during the experiment.

The experiment was designed to investigate the main effects of the defined environmental input variables, the two-variable interactions between these variables and, due to the particular interest in the effect of a bicycle helmet, the quadratic effect of R_h , which can be mathematically expressed as follows:

(1)

$$T_C = \beta_{T_a} T_a + \beta_{R_h} R_h + \beta_P P + \beta_v v + \beta_{Pv} Pv + \beta_{PT_a} PT_a + \beta_{PR_h} PR_h + \beta_{R_h T_a} R_h T_a + \beta_{R_h^2} R_h^2,$$

where T_C is the thermal comfort and β_i is the weighting factor for each variable or variable combination (i).

The inclusion of the quadratic effect was anyhow necessary to generate an experiment that has multiple levels of R_h so that analysis of a dynamic response due to the bicycle helmet was possible. With the help of the JMP Pro® software, different combinations (referred to as a *run*) of the input variables were generated. In general, each test subject was subjected to four runs (combinations) of the generated ones. In general, each participant (test subject) was subjected to four runs (combinations) of the generated ones. Table 4.3 shows the experimental design for test subjects (j) 1 and 8 as an example, where each time slot corresponds to one run (a combination of the four input variables).

Table 4.3 | Experimental design

For test subjects 1 and 8, showing the four runs (combinations) of input variables with three different levels, namely, high (↑), mid (–) and low (↓).

Subjects (no.j)	Variables	Timeslot [1]	Timeslot [2]	Timeslot [3]	Timeslot [4]
<i>j</i> = 1	T_a (°C)	↓	↓	↓	↓
	v (m.s ⁻¹)	↑	↓	↑	↓
	P (% $P_{PER=1}$)	↓	↓	↑	↑
	R_h (m ^{2o} CW ⁻¹)	–	↑	–	↓
<i>j</i> = 8	T_a (°C)	↑	↑	↑	↑
	v (m.s ⁻¹)	↑	↑	↓	↓
	P (% $P_{PER=1}$)	↑	↓	↑	↑
	R_h (m ^{2o} CW ⁻¹)	–	–	↓	↑

General Linear Regression (LR) Model Identification and Offline Parameter Estimation

The main objective of this stage was to identify a general reduced-order and the most parametrically efficient (parsimonious) model structure with the minimum number of easily measured variables (based on the results of the previous stage) to predict the cyclist's under-helmet thermal comfort. For the sake of the main objective of the present work, the selected predictive model had to be suitable, concerning the computational cost, for wearable sensing technology. Due to the subjective nature of the thermal comfort data, it could not be performed

in a continuous pattern, unlike the other input variables, which was a challenge for identifying the predictive model. Hence, in the present paper, we used a simple multivariate regression model with the following general form ²⁰³:

$$T_{ci} = \alpha + \beta_1 u_{i1} + \beta_2 u_{i2} + \dots + \beta_m u_{im} + \epsilon_i, \text{ for } i \in \{1, \dots, n\},$$

where $T_{ci} \in \mathbb{R}$ is the response (thermal comfort) for the i^{th} observation, $\alpha \in \mathbb{R}$ is the regression intercept, $\beta_j \in \mathbb{R}$ is the j^{th} predictor's slope, $u_{ij} \in \mathbb{R}$ is the j^{th} predictor for the i^{th} observation and $\epsilon_i \sim N(0, \sigma^2)$ is an independent and identically distributed Gaussian error term. This can be formulated in matrix form as follows:

$$T_C = X\beta + \epsilon, \text{ subjected to : } T_C \in \mathbb{R}^{n \times 1} \text{ and } X \in \mathbb{R}^{n \times m}$$

where n and m are the number of samples and number of predictors (input variables), respectively. In the present paper, we used the ordinary least-squares (OLR) approach to find the regression coefficients estimates ($\hat{\beta}$) that minimised the sum of the squared errors as follows:

$$\hat{\beta} = \arg \min_{\beta} (T_C - X\beta)^T (T_C - X\beta) = (X^T X)^{-1} X^T T_C.$$

Development of Smart Helmet Prototype

A standard cyclist helmet (312 g) was utilised for the development of the smart helmet prototype (Lazer Bullet 1.0, Lazer Sport, Antwerp, Belgium). The helmet was equipped with a Lifebeam heart rate sensor (Lazer Sport, Antwerp, Belgium; Figure 1.1.1) and a 3 × 3 mm digital humidity and temperature sensor (CJMCU-1080 HTC1080, Texas Instruments, Dallas, Texas; accuracy: ±2% for relative humidity and ±0.2 °C for temperature) to measure the surrounding air humidity and temperature. Additionally, four temperature sensors (Negative-Temperature-Coefficient “NTC” temperature sensors, 100 kΩ at 25 °C) were used at the front, back, right and left of the helmet inner body. The final weight of the equipped helmet was 358 g. All sensors were connected directly to a microcontroller (Adafruit Feather 32u4 Bluefruit, Adafruit

Industries, New York, NY, USA) that transmitted all data from the helmet to a smartphone via Bluetooth. The Adafruit Bluefruit was chosen as it is the smallest “all-in-one” Arduino-compatible and Bluetooth Low Energy microcontroller with built-in USB and battery charging. The developed system was compatible with a 3.7 V Li-polymer rechargeable battery (LP-523450-1S-3) with the ability to power the system for up to 10 h. A circuit diagram of the used electronics and sensors is shown in Figure 1.1.2. The impeded electronics and sensor technology in the smart helmet increased the final original weight of the helmet (312 g) by only 14.7% and did not alter the geometric and aerodynamic characteristics of the original standard helmet. As such, the developed smart helmet is comparable to the original standard helmet (Lazer Bullet 1.0, Lazer Sport, Antwerp, Belgium).

An android-based application “SmartHelmet App” (Figure 1.1.4) was developed to simultaneously communicate with both the Adafruit Feather microcontroller and the Lifebeam heart rate monitor via a Bluetooth communication protocol. The SmartHelmet App was developed using the AppyBuilder online platform (App Inventor, Massachusetts Institute of Technology, Cambridge, Massachusetts, USA). The application was designed to receive, display in real-time and store all the data from the SmartHelmet at a 0.2 Hz sampling rate.

Testing the Developed Smart Helmet Prototype

Test Subjects

In total, seven well-trained male cyclists were recruited for the course of this experiment. Their average physical characteristics were as follows: age—34.5 (± 5) years; body mass—74.5 (± 7.3) kg; body height—177.6 (± 5.4) cm; body mass index (BMI)—23.6 (± 1.8) $\text{kg}\cdot\text{m}^{-2}$; and body surface area—1.9 (± 0.1) m^2 . Prior to the trial, a signed written consent form was obtained from all participants after a detailed description of the protocol, discomforts and benefits. The experimental protocol was

approved by the ethical review board at the University of Thessaly, School of Exercise Science in accordance with the recommendations of the Declaration of Helsinki.

Experimental Design and Protocol

Participants were exposed to a hot (34 °C and 56% relative humidity) environment and completed a 30 km cycling time-trial (TT) inside an environmental chamber. In addition, exposure to 800 W of solar radiation was simulated using compact source iodide (CSI) lamps, while a constant wind speed of 5.1 m·s⁻¹ was provided with a large 80 cm diameter industrial fan positioned in front of the participant at a distance of 140 cm from the bicycle saddle. All participants were instructed to abstain from vigorous physical activity 24 h prior the experimental trial and consume at least 500 mL of water and a light meal 2 h before arrival at the laboratory.

Upon arrival at the laboratory, participants changed into their standardised cycling apparel and underwent basic anthropometric measurements. Body height was measured using a stadiometer (Seca 213; Seca GmbH & Co. KG; Hamburg, Germany), while body mass was determined with a digital weighing scale (Version 5.3 KERN & Sohn GmbH). BMI and body surface area were calculated from the measurements of body height and mass. After instrumentation, participants wore the SmartHelmet, entered the controlled environmental chamber and sat on the cycle for 10 min for a baseline period. Thereafter, they performed a 15 min warm-up followed by the 30 km TT. Participants were allowed to drink water ad libitum throughout the TT. No verbal encouragement was provided during the TT.

Cyclists performed the TT on an adjustable friction-braked cycle ergometer (CycleOps 400 Pro Serie Indoor Cycle, Fitchburg, MA, USA), which was combined with the commercially available software Rouvy (VirtualTraining, Vimperk, Czech Republic), allowing simulation of a route on a computer screen. During the 30 km TT, all cyclists were instructed to complete the race as fast as possible with free access to

controlling power (W) and cadence (rpm). To simulate real cycling, participants could see their power, cadence and covered distance throughout the TT.

Ratings of perceived exertion (RPE) were reported with the 6–20 point Borg scale²⁰⁴ before the baseline period, at the beginning of the warm-up period as well as at the start and end times of the TT. Thermal comfort (TC) and thermal sensation (TS) were measured at the same time points using 7- and 9-point scales, respectively¹⁸⁸.

The average power output, pedalling cadence and 30 km TT duration of all the participants (test subjects) are shown in Table 4.4.

Table 4.4 | The mean average power output, pedalling cadence and 30 km time-trial (TT) obtained from all test subjects.

Variable	Average (\pm Standard Deviation)
Power output (W)	176.5 (\pm 24.2)
Cadence (rpm)	93.7 (\pm 14.2)
30 km TT duration (min)	56.9 (\pm 7.9)

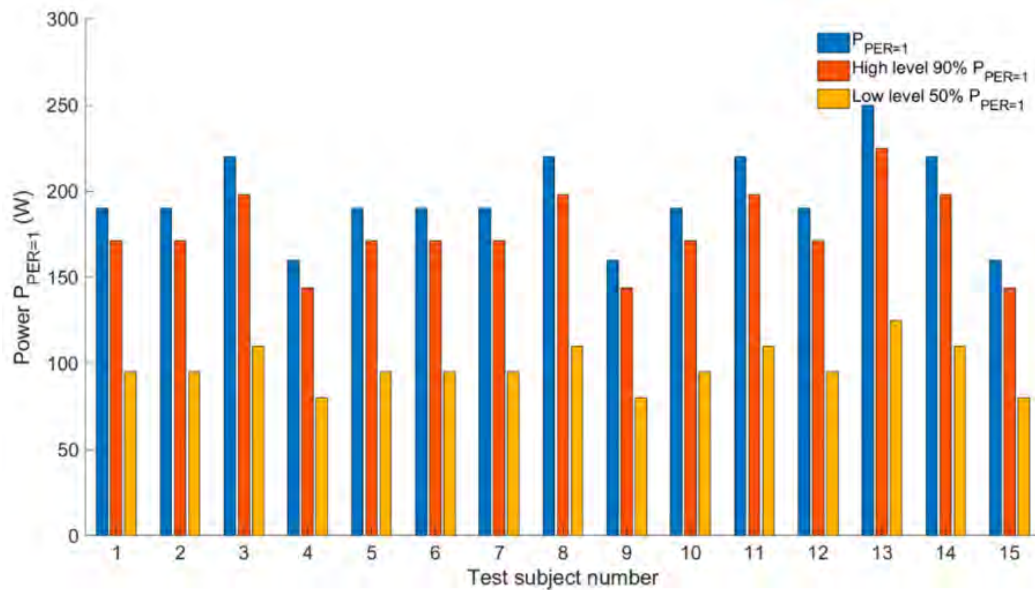
Results

Pretest Experiments

Figure 3 shows the resulting $P_{\text{RER}} = 1$ value for each test subject and the corresponding low and high levels of power. The corresponding low ($P = 50\%$ of $P_{\text{RER}} = 1$) and high ($P = 90\%$ of $P_{\text{RER}} = 1$) levels for each test subject were used in the screening experiments.

Figure 4.3 | Power values of pretest.

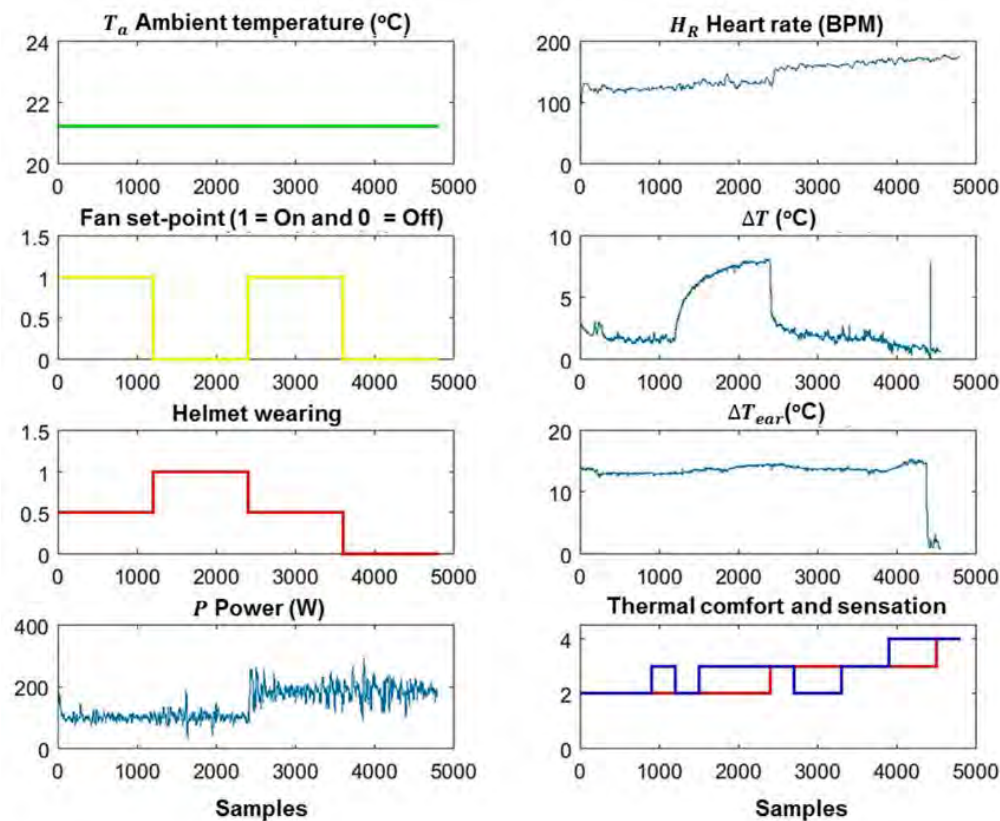
Obtained power values of the pretest. These power values correspond to the power value when they exceeded a respiratory exchange ratio (RER) of one.



Development of Offline (General) Thermal Comfort Model

Figure 4.4 shows the acquired measurements from test subject 1, including environment-related variables, namely, ambient temperature (T_a), air velocity (v), helmet thermal resistance and applied power level (R_h) and the applied mechanical work rate (P). Bioresponse-related variables, including heart rate (H_R), the temperature difference (ΔT) between the average temperature beneath the helmet and the ambient air temperature, the temperature difference (ΔT_{ear}) between the ear temperature and the ambient air temperature as well the thermal comfort (T_c), were considered.

Figure 4.4 | The recorded measurements of the different variables obtained from test subject 1.



The graphs show the environmental variables (left graphs), including the ambient air temperature (T_a , °C), fan set-points (v , $1 = 4 \text{ ms}^{-1}$), the helmet wearing level ($0 = \text{no helmet}$, $0.5 = \text{helmet}$ and $1 = \text{helmet} + \text{aeroshell}$) and the applied mechanical work rate (power) level (P , W). The measured variables related to the bioresponses of the test subject (right graphs) were heart rate (H_R , bpm), the temperature difference (ΔT , °C) between the average temperature beneath the helmet and the ambient air temperature, the temperature difference (ΔT_{ear} , °C) between the ear temperature and the ambient air temperature and the thermal comfort (red line) and sensation (blue line) scores.

To investigate the effect of the different inputs on thermal comfort, different linear regression models (general models) were identified to estimate and predict the perceived under-helmet thermal comfort TC (output) using continuously measured

variables (inputs), including the aforementioned environmental and bioresponse-related variables. The most suitable combination of input variables was selected by retaining only the input variables with a significant ($p < 0.05$) effect on thermal comfort. Additionally, the best model structure was selected based on two main selection criteria, namely, the goodness of fit (R^2) and Akaike information criterion (AIC). The results showed that the most suitable LR model structure, with the highest goodness of fit (average $R^2 = 0.87 \pm 0.05$) and lowest Akaike information criterion (average AIC = 138 ± 12), to predict the thermal comfort for all test subjects was as follows:

(2)

$$T_C = \alpha + \beta_1 T_a + \beta_2 v + \beta_3 P + \beta_4 [T_a R_h].$$

The average parameter estimates, t-ratio and p-value of $P > |t|$ for each selected input variable are given in Table 4.5. The results showed that the main effect of the thermal resistance R_h was not significant ($p > 0.05$); however, the variable interaction of R_h with T_a showed a significant ($p = 0.015$) effect on the prediction of the under-helmet thermal comfort.

Table 4.5 | Estimation results.

The estimation results of the selected linear regression model (3) to predict thermal comfort, showing the average model estimates for the 15 test subjects.

Term	Parameter	Estimate	Std. Error	t-Ratio	$P > t $
intercept	α	2.36	0.14	16.80	<0.0001 *
Ta	β_1	-0.40	0.11	-3.52	0.0025 *
v	β_2	-0.36	0.07	-4.85	<0.0001 *
P	β_3	0.41	0.07	5.45	<0.0001 *
[TaRh]	β_4	0.25	0.01	2.52	0.015

* significant ($p < 0.05$).

To understand the interaction effect of R_h and T_a on the prediction of thermal comfort, a prediction trace analysis of the model²⁰⁵ was employed using prediction the JMP® profiler tool²⁰⁶, as visualised in Figure 4.5. For convenience of this analysis, the values of each input variable were scaled (normalised) in such a way to lie in the closed

interval $[-1, +1]$, where -1 indicates the variable's low level and +1 indicates its high level (Figure 4.5). The scaling of each variable value $i(k)$ was done according to the following formula:

$$x_i(k) = \frac{i(k) - M_i}{\Delta_i}$$

where $x_i(k)$ is the scaled variable value at time instance k , M_i is the midpoint [$M_i = (L_i+U_i)/2$] and L_i and U_i are the particular lower and upper limits of input variable i , respectively. The term $\Delta_i [(L_i-U_i)/2]$ is half of the range of the interval.

Figure 4.5 | Model prediction traces.

Visualisation of the model prediction traces showing the interaction effect of the thermal resistance (R_h) and ambient temperature (T_a) on the predicted thermal comfort. (a) When the temperature was low (20 °C), additional thermal resistance was perceived as comfortable. However, (b) when the temperature was high (30 °C), additional thermal resistance was perceived as uncomfortable. The values of the input variables were normalised in the range between -1 and 1, which correspond to low and high levels, respectively. Table 4.6 shows the average parameter estimates of the developed compact regression model (3) for the 15 test subjects.

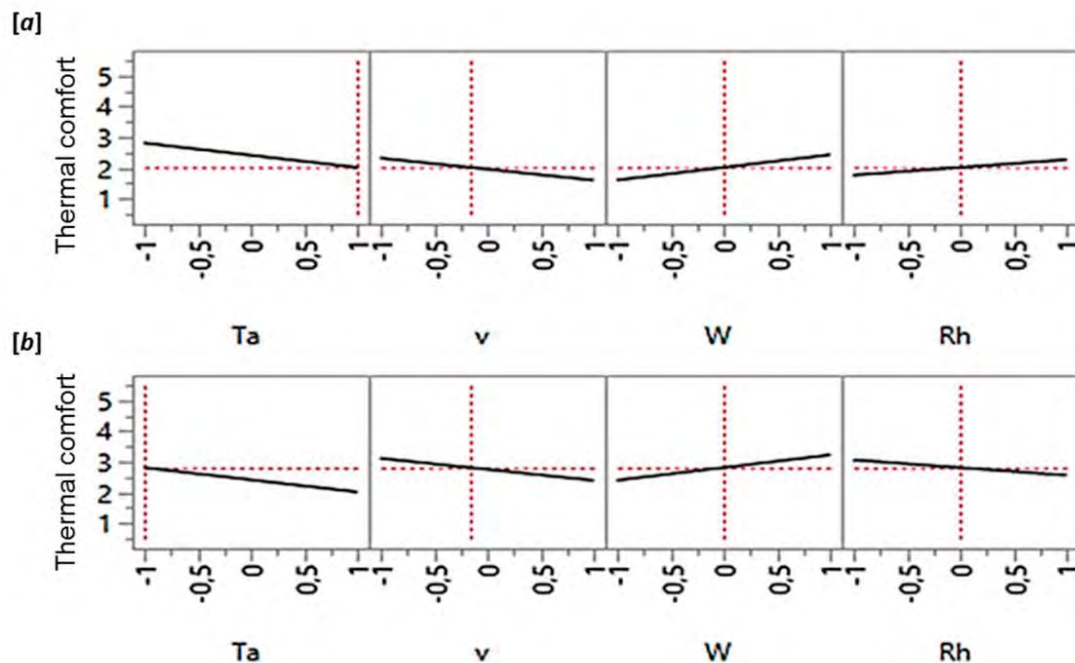


Table 4.6 | Estimation results.

The estimation results of the compact regression model (3) to predict thermal comfort, showing the average model estimates for the 15 test subjects.

Term	Parameter	Estimate	Std. Error	t-Ratio	P > t
intercept	A	1.86	0.21	13.61	<0.0001 *
ΔT	β_1	1.30	0.19	5.22	0.0031 *
HR	β_2	-0.62	0.13	-5.67	<0.0014 *
[TaRh]	β_3	0.35	0.07	2.52	0.0140 *

* significant ($p < 0.05$).

The prediction trace analysis ²⁰⁶ of the developed model (2) was based on computing the predicted response as one variable was changing while the others were held constant at certain values. The results showed that the effect of Rh was dependent on the level of T_a . At a low level (-1) of ambient air temperature ($T_a = 20$ °C), for a change in thermal resistance R_h from a low level (-1) (i.e., no-bicycle helmet) to a high level (1) (i.e., using the Lazer-Z1 Fast), the predicted thermal comfort scale (Table 4.2) decreased by 0.5 thermal comfort units but was perceived as comfortable. However, at a high level (1) of ambient air temperature ($T_a = 30$ °C), the comfort level increased by 0.5 thermal comfort units. This information is important for actively controlling under-helmet thermal comfort, which can be done by manipulating the helmet thermal resistance via, for instance, opening/closing some of the helmet's holes.

As expected, the heart rate (HR) of the test subjects was found to be highly correlated (Pearson's correlation coefficient, $r = 0.85$) with the power (P). Additionally, the heart rate was significantly correlated ($r = 0.68$) with the recorded thermal comfort for all 15 test subjects.

As expected, the temperature difference (ΔT) between the average air temperature beneath the helmet (\bar{T}_h) and the ambient air temperature (T_a) was correlated with both relative air velocity (v) and helmet thermal resistance (R_h), with $r = 0.82$ and 0.78 , respectively.

By employing both heart rate (H_R) and the temperature difference (ΔT) as input variables to the linear regression model, the best model structure that gave the highest average goodness of fit (with average $R^2 = 0.89 \pm 0.04$) and lowest Akaike information criterion (average $AIC = 123 \pm 7$) was as follows:

(3)

$$T_C = \alpha + \beta_1 \Delta T + \beta_2 H_R + \beta_3 [T_a R_h],$$

where $\Delta T = \bar{T}_h - T_a$ and \bar{T}_h is the average air temperature under the helmet, which is calculated from the four temperature sensors located under the helmet. It can be noticed that the structure of model (3) is more compact, consisting of three input variables, compared with the structure of model (2), which consisted of five input variables. Model (3) showed better prediction performance for the thermal comfort level than model (2), which had maximum mean absolute percentage errors (MAPEs) of 8.4% and 11%, respectively. The MAPE is given by

$$MAPE = \frac{100\%}{N} \sum_{k=1}^N \left| \frac{\hat{T}_C(k) - T_C(k)}{T_C(k)} \right|$$

where N is the number of data points and T_C is the predicted thermal comfort.

It can be noticed that both the mechanical work rate (P) and air velocity (v) disappeared from the compact model (3). The heart rate (H_R) variable included in the compact model (3) directly linked to the applied mechanical work rate (P), hence the effect of P , included in model (2), translated by the bioresponse represented by HR (e.g., ²⁰⁷) included in model (3). According to Newton's law of cooling, temperature difference (ΔT) is the driving force for the convective heat transfer (Q_h) between the cyclist's head and the ambient air. The heat flux (q) is proportional to ΔT and the convective heat transfer coefficient (h_c) links both variables as follows:

$$q = -h\Delta T \text{ [W}\cdot\text{m}^{-2}\text{]}.$$

The heat transfer coefficient ($h_c, \text{W}\cdot\text{m}^{-2}\cdot\text{°C}$) is a combination of the heat transfer coefficient of the air (h_{air}) and that of the helmet ($h_H=1/R_h$); hence,

$$\Delta T = -\left[\frac{1}{h_{air} + \frac{1}{R_h}} \right] q.$$

The heat transfer coefficients of the air (h_{air}) and the bicycle helmet ($1/R_h$) are dependent on air velocity (v). Hence, it is clear that the effect of ΔT is inherently connected to the effect of both v and helmet thermal resistance (R_h).

It can be concluded from the presented results that the input variables included in model (3), namely, temperature difference (ΔT), heart rate (H_R) of the cyclist and the interaction variable [$T_a R_h$] between ambient temperature (T_a) and helmet thermal resistance (R_h), were suitable enough to estimate the cyclist's thermal comfort (T_C) under the bicycle helmet. These selected variables were the basis for developing a reduced-order personalised model for real-time monitoring of a cyclist's thermal comfort under the helmet. Additionally, from a practical point of view, these three variables were suitable to be measured using integrated sensors in the cyclist's helmet, as is shown in the following subsection.

Testing the SmartHelmet Prototype and Validation of the Developed General Model

In Figure 4.6, the average ratings of perceived exertion (RPE), thermal comfort (T_C) and thermal sensation (T_S) values at the start and end times of the TT are presented for all seven test subjects. The average values (\pm standard deviation) of all used subjective ratings showed a significant ($p < 0.05$) increase at the end of the TT (RPE

= 17.6 ± 0.5 , $T_C = 2.6 \pm 0.5$ and $T_S = 4.4 \pm 0.6$) compared with their values at the start of the trial.

Figure 4.6 | Average values of RPE, TC, and TS.

Average values of ratings of perceived exertion (RPE), thermal comfort (T_C) and thermal sensation (T_S) between the start (PRE) and end (POST) times of the TT (* indicates a significant difference of $p < 0.05$).

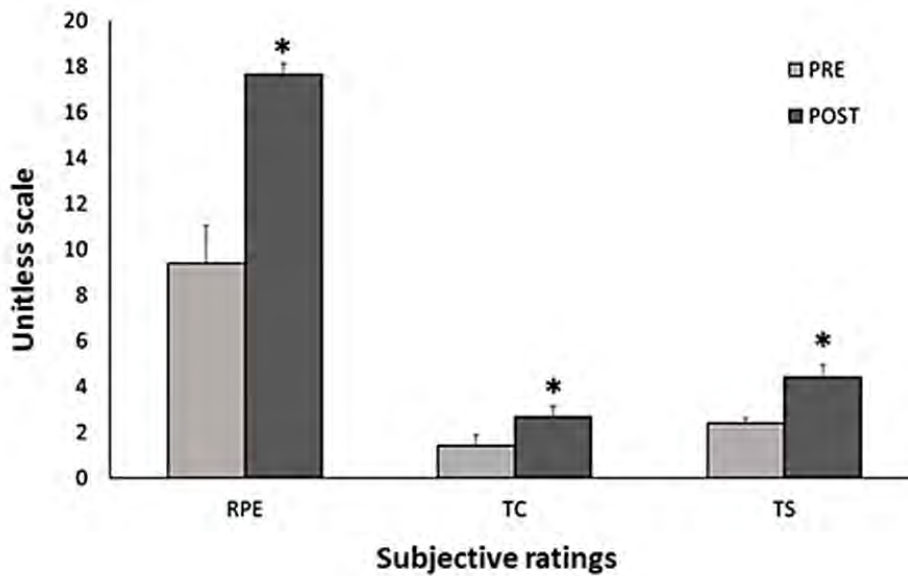
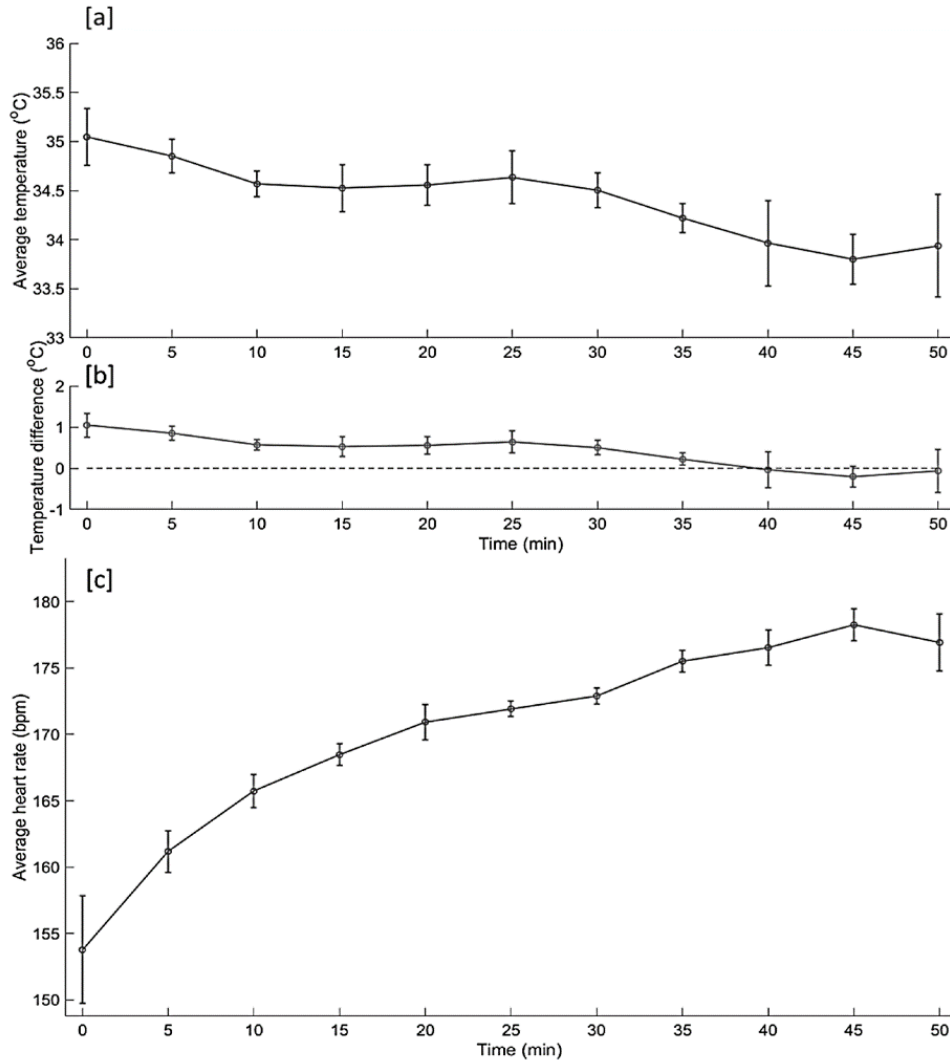


Figure 4.7 shows the real-time measured average temperatures (\bar{T}_h) under the helmet, average temperature difference (ΔT) between the average temperature under the helmet and the ambient air temperature and the average heart rate (HR) obtained during the TT from all seven test subjects using the developed prototype smart helmet.

Figure 4.7 | Obtained data during the TT.

(a) Average temperature (\bar{T}_h) beneath the helmet, (b) average temperature difference (ΔT) between the average temperature and the ambient air temperature and (c) average heart rate (HR) obtained during the TT from all test subjects.



The developed offline linear regression model (3) was used to estimate the thermal comfort (T_c) of all seven test subjects based on the measurements acquired from the SmartHelmet prototype and for comparison with the thermal comfort subjective rating. The model was able to estimate the thermal comfort from all test subjects and revealed an average R^2 of 0.84 (± 0.03). Model (3) was able to predict the cyclist's thermal comfort under the helmet and had a maximum MAPE of 10%. However, by retuning the model parameters using the data obtained from the TT experiment, the maximum MAPE was reduced to 7.8%.

The main advantage of the proposed model is that it is a conceptually simple yet very effective tool to explore linear relationships between a response variable (output) and a set of explanatory variables (input variables), which can be easily used for wearable technology such as the SmartHelmet. On the other hand, the disadvantage of such a model is the absence of the time component; in other words, the model is not able to explain the transient response of the output. Additionally, in practice, many factors can affect and change the relationship represented by the proposed model. These factors include helmet-related factors (e.g., helmet weight), other environmental conditions (e.g., wind direction) and personal-related factors, which were not included in the model (e.g., the surface area and contour of the cyclist's head). Hence, it is clear that such general models need to be adapted to new data (personal data) and different conditions for better performance. With the help of wearable sensing technologies (SmartHelmet) and streaming modelling algorithms, an adaptive personalised model can be developed for real-time monitoring of a cyclist's head thermal comfort.

In the following subsection, we introduce the framework of online model adaptation and personalisation (streaming algorithm) based on the easily measured variables obtained from the wearable sensors impeded in the SmartHelmet.

Introduction of Online Personalisation and Adaptive Modelling Algorithm

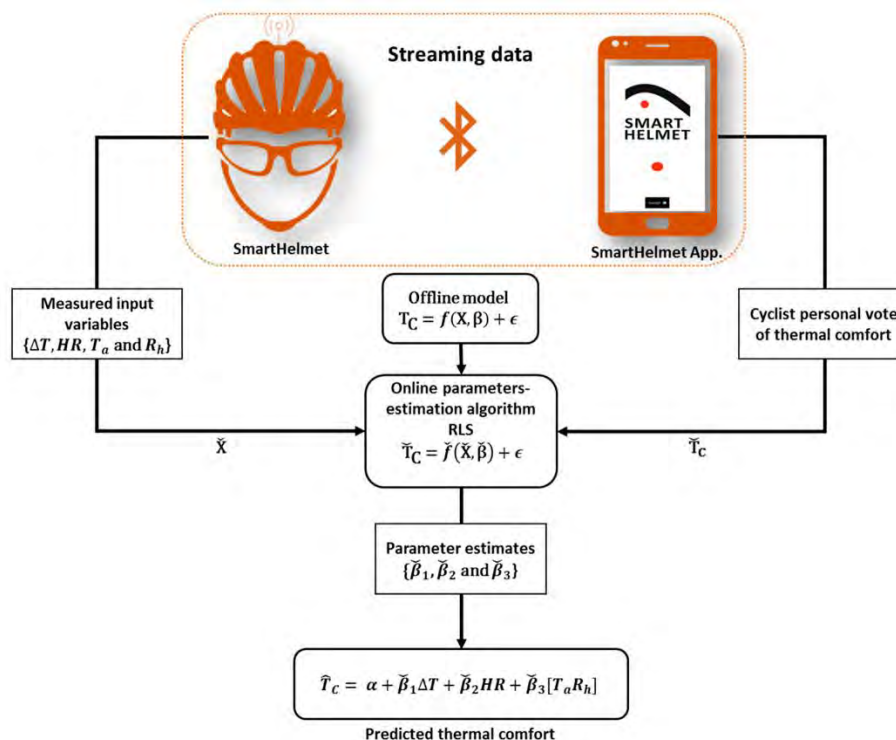
Most of the available thermal sensation and comfort predictive models (e.g.,^{160,208-214}) are static models. That is, they predict the average vote of a large group of people based on, for example, the 7-point thermal sensation scale instead of individual thermal comfort, and they only describe the overall thermal sensation/comfort of multiple occupants in a shared thermal environment. To overcome the disadvantages of static models, adaptive thermal comfort models aim to provide insights and opportunities to personalise the thermal comfort prediction of individuals²¹⁵. The idea behind adaptive models is that occupants and individuals are no longer regarded as

passive recipients of the thermal environment, but rather, they play an active role in creating their own thermal preferences ²¹⁶. The suggested linear regression model, represented by (3), in the present paper is considered as a global model, also called an offline model ^{217,218}, for an adaptive personalised model to assess and predict individual thermal comfort under a cyclist's helmet.

Figure 4.8 depicts the proposed steps for retuning and personalising the offline regression model (3). The suggested personalised adaptive tuning algorithm consists of the main components shown in Figure 4.8.

Figure 4.8 | Personalisation algorithm.

Schematic representation of the proposed online personalisation algorithm to predict thermal comfort under the helmet. The retuning and personalisation algorithm is based on data streaming obtained from the developed SmartHelmet prototype and the cyclist's personal vote of thermal comfort acquired from the developed SmartHelmet App. The streamed data is fed, together with the developed offline model, to an online parameter estimation algorithm based on a recursive least-squares (RLS) algorithm.



Offline Linear Regression Model

As mentioned earlier, the linear regression model (3), which was developed based on the data obtained from the 15 test subjects, is the offline base model for online prediction of personal under-helmet thermal comfort. The general form of the offline linear regression model (3) is as follows:

(4)

$$T_C = X\beta + \epsilon$$

and is subjected to $T_C \in \mathbb{R}^{n \times 1}$ and $X \in \mathbb{R}^{n \times 3}$, where T_C is the output vector (n samples of thermal comfort votes); ϵ is the model residual vector, which consists of independent and Gaussian-distributed entries; and β and X are the regression vector (of the size 3) and predictor matrix (of the size $n \times 3$), respectively, given by

$$X = \begin{bmatrix} 1 & \Delta T_1 & H_{R1} & (T_a R_h)_1 \\ 1 & \Delta T_2 & H_{R2} & (T_a R_h)_2 \\ \vdots & \vdots & \vdots & \vdots \\ 1 & \Delta T_n & H_{Rn} & (T_a R_h)_n \end{bmatrix} \text{ and } \beta = \begin{bmatrix} \alpha \\ \beta_1 \\ \beta_2 \\ \beta_3 \end{bmatrix}.$$

Streaming Data

The availability of real-time sensor data from the developed SmartHelmet prototype allows for streaming data, which is processed via an online algorithm (stream processing) to adapt the offline model ²¹⁹. The streaming data includes new \check{n} samples of measured sensor data (new input matrix \check{X}) acquired from the SmartHelmet sensors, and new personal thermal comfort votes (new output vector \check{T}_C) acquired through an interactive query provided by the developed SmartHelmet App.

Online Parameter Estimation Algorithm

As explained earlier (Section 2.1.3), the general setting of regression analysis is to identify a relationship between a response variable (Y) and one or several explanatory variables (predictors) (X) by using a learning sample ²²⁰. In a prediction

framework, the main assumption for predicting Y on a new sample of X observations is that the regression model (with the general form $Y = f(X) + \epsilon$, where ϵ represents the model residuals) is still valid. Unfortunately, this assumption is not valid in the present case, where the thermal comfort of the individual cyclist is strongly dependent on many personal- and time-dependent factors¹⁸⁹. Therefore, in this study, we adapted the original regression model (3) to a new sample (observations) by estimating a transformation^{218,220} between the original regression function ($f(X)$) and the new one ($\check{f}(\check{X})$) while still using the same model variables and structure. Ordinary least squares (LS) is one of the most popular regression techniques, which was used here for parameter estimation of the developed offline model. However, for the online parameter estimation and in the presence of unknown parameter changes, its adaptive versions—the sliding or moving LS, recursive least squares (RLS) and recursive partial least squares (PLS)—are widely used^{218,221,222}.

In the present paper, the RLS algorithm is suggested for online personalisation and adaptive modelling of under-helmet thermal comfort. The suggested RLS algorithm has the advantage of being simple and computationally efficient for wearable and adaptive sensing, which was the case in the present work. In the RLS algorithm, the new regression vector $\check{\beta}$, as in Equation (4), can be estimated recursively as follows^{203,223,224}.

(5)

$$\mathbf{P}_{n+1} = \mathbf{P}_n - \frac{\mathbf{P}_n(\mathbf{X}_{n+1})^T \mathbf{X}_{n+1} \mathbf{P}_n}{1 + \mathbf{X}_{n+1} \mathbf{P}_n (\mathbf{X}_{n+1})^T},$$

$$\check{\beta}_{n+1} = \check{\beta}_n + \mathbf{P}_{n+1}(\mathbf{X}_{n+1})^T (\check{T}_{C_{n+1}} - \mathbf{X}_{n+1} \check{\beta}_n)$$

(6)

where $\mathbf{P}_n = (\mathbf{X}_n^T \mathbf{X}_n)^{-1}$. This recursive algorithm is efficient for cases where the regression vector $\check{\beta}$ is a function of time (time varying). However, in the case of adaptive modelling with streaming data, due to the arrival of new samples, the influence of new

observations decreases gradually and the ability to track the changes in β will be lost. Hence, to mitigate this, the widely used and popular forgetting factor approach ²²⁵ is proposed in this paper. The approach of forgetting here is based on gradually discarding older data in favour of more recent information. In the least-squares method, forgetting can be viewed as giving less weight to older data and more weight to recent data ^{225,226}. Hence, the forgetting factor, λ , was introduced to (5) as follows ²¹⁸:

$$\mathbf{P}_{n+1} = \frac{1}{\lambda} \left(\mathbf{P}_n - \frac{\mathbf{P}_n (\mathbf{X}_{n+1})^T \mathbf{X}_{n+1} \mathbf{P}_n}{\lambda + \mathbf{X}_{n+1} \mathbf{P}_n (\mathbf{X}_{n+1})^T} \right) \quad (7)$$

where $\lambda \in (0, 1]$. The forgetting factor λ operates as a weight, which diminishes for more remote data and expands for more recent data ^{225,226}. The main difference here between (5) and (7) is that in conventional RLS (5), the covariance vanishes to zero with time, losing its capability to keep track of changes in the regression vector β . In (7), however, the covariance matrix is divided by $0 \leq \lambda < 1$ at each update. This slows down the fading out of the covariance matrix ²²⁶.

Conclusions

In the present work, we aimed to develop a general model approach to predict a cyclist's head thermal comfort using nonintrusive and easily measured variables, which can be measured using impeded sensors in a bicycle helmet. During the first experimental stage, 15 participants were exposed to different levels of mechanical activity, ambient temperatures, helmet thermal resistance and wind velocities in order to develop a general model to predict a cyclist's head thermal comfort. The results showed that ambient temperature, average air temperature under the helmet, cyclist heart rate, cyclist mechanical work and helmet thermal resistance significantly influenced the cyclist's head thermal comfort. A reduced-order general linear regression model with three input variables, namely, temperature difference between

ambient temperature and average under-helmet temperature, cyclist's heart rate and the interaction between ambient temperature and helmet thermal resistance, was the most suitable to predict the cyclist's head thermal comfort, showing a maximum MAPE of 8.4%. The developed general model structure was based on easily measured variables that can be measured continuously using impeded sensors in the bicycle helmet but is still of reduced order and low computational cost, which is suitable for streaming and adaptive modelling. Based on the selected model variables, a smart helmet prototype (SmartHelmet) was developed using impeded sensing technology as a proof of concept. The developed general model was validated using the developed SmartHelmet prototype. During the validation experimental phase, seven well-trained male cyclists were exposed to a hot (34 °C and 56% relative humidity) environment and completed a 30 km cycling TT inside an environmental chamber. The validation results showed that the developed general model was able to predict the thermal comfort of the seven participants and had a maximum MAPE of 10%. By retuning the model parameters, the maximum MAPE decreased to 7.8%. Finally, we introduced a calculation framework of an adaptive personalised model based on the developed general model to predict a cyclist's head thermal comfort based on streaming data from the SmartHelmet prototype.

Acknowledgments

We acknowledge the support from the European Union's Horizon 2020 research and innovation programme under the Marie Skłodowska-Curie grant agreement no. 645770.

Chapter 5

Night-Time Heart Rate Variability during an Expedition to Mt Everest: A Case Report

This work was conducted by Konstantinos Mantzios, Aggelos Pappas, Georgios-Ioannis Tsianos, and Andreas D. Flouris. We all participated in the conception and design of the study. I developed the prototype, performed the statistical analyses, data interpretation, and drafted and revised the manuscript critically for important intellectual content. I had full access to all of the data in the study and take responsibility for the integrity of the data and the accuracy of the data analysis.

As of February 2023, this paper⁴ has been published online by Sports MDPI as follows: Mantzios K., Pappas A., Tsianos G-I et al. Night-Time Heart Rate Variability during an Expedition to Mt Everest: A Case Report. Sports MDPI; [10.3390/sports11020048](https://doi.org/10.3390/sports11020048)

Abstract

Mt Everest has been gaining popularity from casual hiking athletes, climbers, and ultra-endurance marathon runners. However, living and sleeping at altitude increases the risk of injury and illness. This is because travel to high altitudes adversely affects human physiology and performance, with unfavourable changes in body composition, exercise capacity, and mental function. This is a case report of a climber who reached the summit of Mt Everest from the north side. During his 40-day expedition, we collected sleep quality data and night-time heart rate variability. During the night inside the tent, the air temperature ranged from -12.9 to 1.8 °C (-5.8 ± 4.9 °C) and the relative humidity ranged from 26.1 to 78.9% ($50.7 \pm 16.9\%$). Awake time was $17.1 \pm 6.0\%$ of every sleep-time hour and increased with altitude ($r = 0.42$). Sleep time ($r = -0.51$) and subjective quality ($r = 0.89$) deteriorated with altitude. Resting heart rate increased ($r = 0.70$) and oxygen saturation decreased ($r = -0.94$) with altitude. The mean NN, RMSSD, total power, LF/HF, and SD1 and SD2 were computed using the NN time series. Altitude reduced the mean NN ($r = -0.73$), RMSSD ($r = -0.31$), total power ($r = -0.60$), LF/HF ratio ($r = -0.40$), SD1 ($r = -0.31$), and SD2 ($r = -0.70$). In conclusion, this case report shows that sleeping at high altitudes above 5500 m results in progressively reduced HRV, increased awakenings, as well as deteriorated sleep duration and subjective sleep quality. These findings provide further insight into the effects of high altitude on cardiac autonomic function and sleep quality and may have implications for individuals who frequently spend time at high altitudes, such as climbers.

Introduction

Year on year, more than 800 climbers attempt to reach the highest peak on the planet: the summit of Mt Everest. In recent decades, Mt Everest has been gaining popularity from casual hiking athletes, climbers, and ultra-endurance marathon runners³⁹. Between 1990 and 2005, there were 2200 individuals who attempted the summit for the first time. However, this number has risen dramatically in recent years, with over 3600 first-time climbers attempting the summit between 2006 and 2019²²⁷. However, living and sleeping at altitude increases the risk of injury and illness^{39,228}. More than 300 people are injured annually while attempting to climb Mt Everest²²⁹. The mortality rate among climbers at altitudes higher than the Base Camp is 1.3%, and the majority of these deaths (82.3%) occur on or after the summit attempt²³⁰. This rate ranges from 10 to 12.6 deaths per 100 mountaineers climbing above 6000 m in the Himalayas²³¹. The cause of these grim statistics is that travel to high altitudes adversely affects human physiology and performance^{232,233}, with unfavourable changes in body composition, exercise capacity, and mental function^{233,234}. It also leads to symptoms such as fatigue, headaches, and difficulty concentrating, as the body has to work harder to perform the same tasks due to hypoxemia²³⁵. The limited available evidence suggests that acute exposure to high altitude significantly increases the activity of the sympathetic nervous system²³⁶. This is accompanied by a decrease in heart rate variability (HRV)²³⁷. HRV is a widely recognized noninvasive method for evaluating the balance between the parasympathetic and sympathetic nervous systems in the regulation of cardiac function. The ability to assess HRV in individuals has significant clinical implications, as it can provide insights into an individual's cardiovascular health and risk for disease²³⁸.

Night-time HRV is associated with sleep quality because sleep in healthy individuals is characterized by attenuated sympathetic and increased parasympathetic nervous activity^{239,240}. As such, sleep problems are linked with autonomic imbalance

^{240,241}. This ability of HRV to assess sleep quality can be of value for climbers since the ascent to high altitudes leads to reduced sleep time and subjective sleep quality, as well as increased night-time awakenings ^{233,234,242}. This is due to the decrease in oxygen levels at high altitude, which can cause respiratory disturbances during sleep. Compared to sea level, sleep at high altitude is associated with decreased slow-wave sleep and REM sleep, sleep efficiency, and total sleep time, and increased waking time ²³³. A previous study showed that the ascent to Everest North Base Camp (5180 m) decreased vagal tone and increased sympathetic activity, a phenomenon that was reversed with acclimatization ²⁴², further supporting the disruption of normal HRV during the ascent to high altitude. An autonomic imbalance during sleep, characterized by increased sympathetic activation, may contribute to the development of acute mountain sickness and other negative health outcomes ²³⁶. However, autonomic nervous system fluctuations have not been studied at altitudes beyond 5500 m, which is where the body's physiology is significantly challenged ^{243,244}. In this case study, we aimed to explore night-time HRV fluctuations and oxygen saturation at altitudes beyond 5500 m during an expedition to Mt Everest.

Materials and Methods

The participant of this study was an experienced male climber and ultra-endurance athlete (age 44 years; height 183 cm; body mass 85 kg). He had previously climbed Mt Everest from the north side. Additionally, he had completed multiple extreme ultra-endurance events including the Marathon des Sables run in the Sahara Desert, a race that covers more than 250 km of harsh terrain in extreme heat ¹¹². He had also swum the English Channel (34 km of cold, open water), and had swum non-stop across the Aegean Sea: a distance of 101 km.

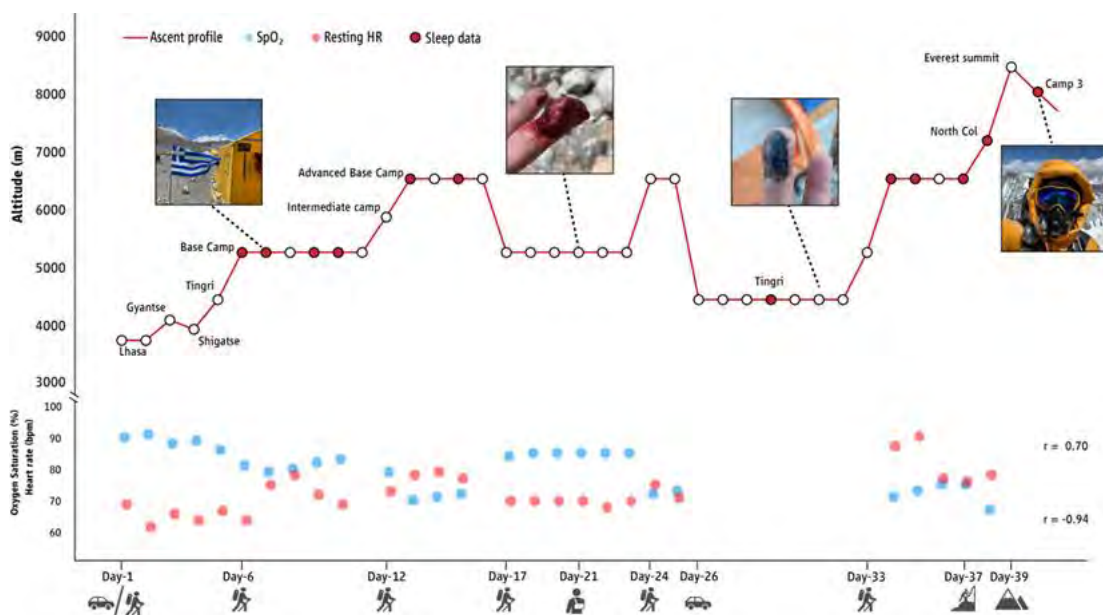
Thirty days before the ascent to Mt Everest, the athlete followed a 4-week altitude acclimation protocol at the FAME Laboratory (Trikala, Greece). The daily protocol was designed to simulate the physical demands of a high-altitude environment

and included a combination of running and cycling that were performed over a period of 4 h. The daily protocol included 2 h of running in normobaric normoxia and 2 h of cycling in normobaric hypoxia. This type of hypoxia simulates altitudes between 5000 and 6000 m. The hypoxia environment was achieved using the Everest Summit II (Hypoxico Inc, Gardiner, NY, USA).

The outline of the climber's ascent profile is illustrated in Figure 5.1. In brief, he remained at Base Camp (BC) for 6 days (days 6–11) and during this time he performed daily aerobic exercise (stationary running and stepping) for approximately 1 h every day. During days 12–13, he climbed to 6340 m (Advanced Base Camp) where he spent three days and then returned to BC (day 17). He had planned to continue moving between 5000 and 6500 m until weather would permit him to ascend to the summit. Alas, four days after returning to BC (on day 21), he fell while descending from a training climb and injured his finger (Figure 5.1). He sustained an extensive laceration to the distal palmar aspect of his right middle finger. The injury required 10 sutures and the procedure was undertaken at BC. On day 23, he climbed again to 6340 m, but the hypoxic conditions caused a significant deterioration of his injury, which forced him to descend to Tingri (4348 m) and visit the local hospital for further assessment and treatment with several antibiotic regimes and analgesia. Seven days later, on day 32, he trekked back to the BC. Seven days thereafter (day 39), he successfully reached the summit from the north side. Then, he descended to Camp 3 (8300 m; day 40) and proceeded to lower altitudes.

Figure 5.1 | 40-day Mt Everest expedition.

GPS tracking of the 40-day Mt Everest expedition and results for morning oxygen saturation (SpO_2) and resting heart rate (HR). Circles indicate nights during the expedition. Red circles indicate assessment of heart rate variability during night-time sleep. Correlation coefficients (r) indicate associations with altitude.



During the expedition, a custom-built GPS-logger was used to track the location of the climber. This device was developed using an Arduino microcontroller and was equipped with a NEO-6M GPS antenna (Somerville, MA, USA). The GPS-logger was essential in recording the climber's movements throughout the expedition, providing accurate location data. The device was powered by a 9-volt lithium battery that was specially designed with extra protection for cold temperatures, ensuring that the GPS-logger would function correctly even in the harsh conditions of the expedition. In addition, a small, portable weather station (Kestrel Drop D3, Nielsen-Kellerman Co., Boothwyn, PA, USA) was used to record weather data (air temperature and relative humidity) at various locations and altitudes throughout the expedition. Additionally, oxygen saturation and resting heart rate were collected every morning upon waking up (NONIN GO2 Achieve 9570 finger pulse oximeter, Nonin Medical Inc., Plymouth, MN,

USA). During the 40-day expedition, we employed a specific protocol for collecting data on night-time HRV. For 12 nights, the climber wore a modified heart rate monitor (Polar Team 2, Polar Electro Oy, Kempele, Finland) while he slept. This device was powered by a specially designed 3.7 V and 2000 mAh lithium battery with dimensions 6.7 × 44 × 63 mm that was equipped with extra protection to withstand cold temperatures. This allowed us to gather continuous HRV data throughout the night, providing a comprehensive understanding of the climber's autonomic nervous system activity during sleep. This method was chosen for its non-invasive nature, its ability to capture long-term patterns in HRV, and the device's ability to operate in extremely cold temperatures.

In the collected HRV series, we removed observations that did not fit within a set range from our dataset and replaced them with linear interpolation to maintain the continuity of the signal. This important preprocessing step helps cleaning up the data and removing noise that may be present due to movement, waking, or coughing²³⁸. The databased cleaning and analysis of the beat-by-beat series of RR intervals for each entire night was performed with the HRV-library written in Python (<https://pypi.org/project/hrv-analysis/> (accessed on August 16, 2021)) using a 5-min window analysis with 2.5 min time step throughout the night-time for every different night. Using the normal-to-normal (NN) time series, we computed the mean NN, the root mean square of successive differences between normal heartbeats (RMSSD), the total power, the low-frequency to high-frequency (in normalized units) ratio (LF/HF), as well as the Poincaré SD1 and SD2 and their ratio (SD1/SD2)^{245,246}. In long-term recordings, such as the ones performed in our study, the RMSSD and Poincaré SD1 reflect primarily parasympathetic drive, while the total power, LF/HF, Poincaré SD2, and Poincaré SD1/SD2 are sensitive to both parasympathetic and sympathetic tones^{238,246,247}. Finally, after the expedition, we analyzed the climber's diary and had an extended discussion with him to extract information on sleep quality based on the

Stanford Sleepiness Scale (SSS)²⁴⁸. Due to the small sample size and non-normal data distribution, we used the Spearman correlation coefficient to detect potential associations between altitude and oxygen saturation, resting heart rate, and HRV parameters.

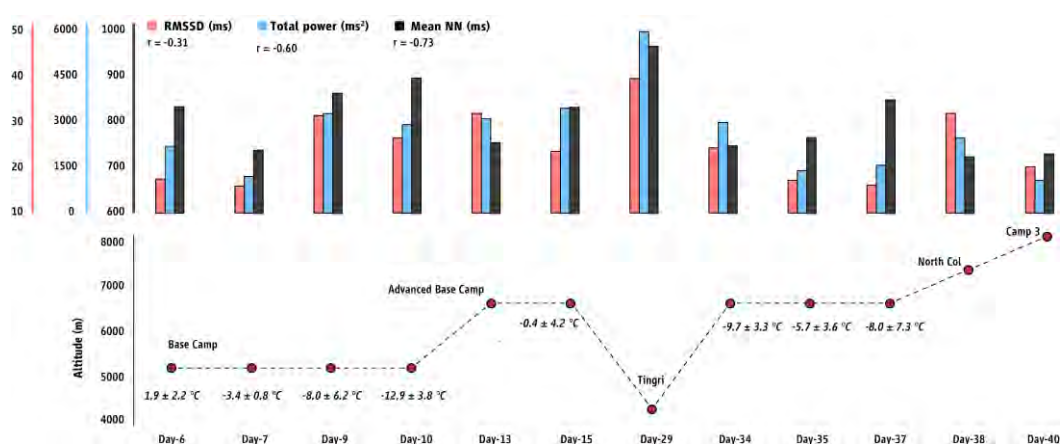
Results

During the night inside the tent, the air temperature ranged from -12.9 to 1.8 °C (-5.8 ± 4.9 °C) and the relative humidity ranged from 26.1 to 78.9% ($50.7 \pm 16.9\%$). Awakenings were very frequent during the recorded sleeping patterns. For every hour of night-time sleep, the average awake time ranged from 9 to 26.5% ($17.1 \pm 6.0\%$) and was linearly associated with altitude ($r = 0.42$). The heart rate data recorded during awakening were not included in the HRV analysis. We found that the altitude level was positively correlated with the resting heart rate ($r = 0.70$) and negatively correlated with oxygen saturation ($r = -0.94$) (Figure 5.1). After removing all of the awakening time, the average time used for the HRV analysis was 226.8 ± 97.1 min ranging from 117.5 to 455.0 min and was negatively associated with altitude ($r = -0.51$). Additionally, altitude reduced the mean NN during sleep ($r = -0.73$; Figure 5.2), which was 813.0 ± 42.3 ms at 5400 m (BC; Day 6) compared to 948.2 ± 69.4 ms at 4348 m (Tingri; Day 29). The same was also observed for the other parameters of HRV [RMSSD ($r = -0.31$); total power ($r = -0.60$); LF/HF ratio ($r = -0.40$); Poincaré SD1 ($r = -0.31$); Poincaré SD2 ($r = -0.70$); Poincaré SD1/SD2 ($r = -0.24$)]. Subjective sleep quality deteriorated while ascending at higher altitudes ($r = 0.89$; higher SSS scores indicate lower subjective sleep quality), being high (1.2 ± 0.4 in the SSS, indicating feeling active, vital, alert, or wide awake during the day) at altitudes 4348–5440 m, moderate (2.2 ± 0.4 in the SSS, indicating functioning at high levels, but not fully alert during the day) at 6340 m, and low (4.0 ± 2.1 in the SSS, indicating being somewhat foggy, or let down during the day) at altitudes 7050–8300 m. Acclimatization to altitude at 5400 m

(BC; days 7–10) and at 6340 m (days 13–15 and 34–37) increased the mean NN (average change: 76.44 ± 17.72 ms). This also correlated with subjective sleep quality, which improved during habituation at specific altitudes (i.e., SSS scores were higher on the first day at a given altitude, compared to subsequent days at the same altitude).

Figure 5.2 | Results for the HRV values.

Results for the root mean square of successive differences between normal heartbeats (RMSSD), the total power, and the mean normal-to-normal (NN) beats during night-time sleep at different altitudes. Correlation coefficients (r) indicate associations with altitude. Numbers in italics indicate mean \pm SD ambient temperature in the tent during night-time sleep.



Discussion

This case report presents the first evidence of night-time HRV fluctuations at altitudes beyond 5500 m during an expedition to Mt Everest [in our case, Advanced Base Camp (6340 m), the North Col (7020 m), and Camp 3 (8300 m)]. To our knowledge, this is the first study to directly observe the autonomic nervous system activity at this altitude, filling a significant gap in the literature, as previous studies were either conducted in simulated conditions or on animal subjects²³⁶. The findings of our case study are valuable, as they provide new insight into the human response to high altitude, and the expected differences in autonomic nervous system activity above 5500 m. A decrease in HRV is linked to a higher likelihood of experiencing acute mountain sickness²⁴⁹. Our climber experienced decreased HRV during sleep at these high altitudes, and this was

associated with reduced sleep duration and lower subjective sleep quality. These findings confirm previous studies assessing night-time HRV, which reported that the rapid ascent to altitudes up to 5500 m causes sleep apneas and increased sympathetic drive²⁴². The latter is triggered by peripheral chemoreceptor stimulation aiming to offset the attenuated arterial oxygen content²⁴².

Within 3–4 days of acclimatization to altitude at 5400 m (BC) and at 6340 m, we recorded favourable adaptations in HRV and subjective sleep quality. Based on previous reports, acclimatization at 5180 m increases the ventilatory response to hypoxemia²⁵⁰ and the time domain of the HRV²⁴². Our results support this conclusion, as we observed adaptation patterns in the NN, but not in other HRV domains. During the first days of acclimatization at 5400 m (BC), we found an improvement (~4%) in oxygen saturation. This pattern was not systematically observed during the remaining phases of the expedition, which may be explained by the disruption in the pre-planned 1-month acclimatization protocol caused by the injury and the need to descend to a lower altitude. Nevertheless, it is logical to suspect that improvements in sleep quality and HRV time domain measures were caused by favorable adaptations in oxygen delivery. It would have been interesting to confirm this notion with added analyses using daytime HRV data. Unfortunately, our study design did not allow exploring daytime HRV adaptations.

When reading our results for LF/HF, it is important to consider that this parameter is influenced by breathing rate, which was not assessed/controlled in our study. As such, we recommend caution when interpreting our results for the LF/HF ratio as a measure of parasympathetic and sympathetic tones. To address this, we also calculated the Poincaré SD1/SD2 ratio which is not influenced by the respiratory rate. The results of Poincaré SD1/SD2 showed similar, yet less pronounced, effects to those of LF/HF.

Conclusions

In conclusion, our case report presented here demonstrates that sleeping at high altitudes above 5500 m results in progressively reduced HRV, increased awakenings, as well as deteriorated sleep duration and subjective sleep quality. These findings provide further insight into the effects of high altitude on cardiac autonomic function and sleep quality and may have implications for individuals who frequently spend time at high altitudes, such as climbers.

Acknowledgments

The climber was sponsored for the expedition to Mt Everest by Evnia, Fleet Complete, Dioratikotita, North Face Hellas. None of the sponsors had any input on the protocols, findings, or data analysis of this research.

Chapter 6

Free Web Tool for Heat Strain Mitigation: Aligning with ISO 7933:2018 Standards

This work was conducted by Konstantinos Mantzios, Leonidas G. Ioannou, Alexandros Mantzios, Giorgos Gkikas, and Andreas D. Flouris. The study is currently under preparation and has not been published yet. My role involved developing the web interface for the online software, carrying out field studies, and collecting data. I have also performed statistical analyses, interpreted the data, and drafted and revised the manuscript. I maintain full access to all algorithms, codes, and data used in the study and assume responsibility for the integrity of the data and the accuracy of the data analysis.

Abstract

Introduction: This research aimed to develop and validate FL-WebPHS, a web-based software designed to estimate heat strain in individuals under diverse environmental conditions. We focused on long-distance runners, a group frequently exposed to heat strain. **Methods:** The study involved eight long-distance runners. During their races, we recorded core temperatures and environmental conditions and compared these with core temperature predictions from the FL-WebPHS software. **Results:** The FL-WebPHS showed a moderate agreement between observed and predicted core temperatures, reflected by a Pearson's correlation coefficient of $r=0.58$ ($p<0.001$) and Willmott's Index of Agreement of 0.63. The average difference between observed and predicted values was 0.59°C , and the software's 95% limits of agreement for core temperature predictions ranged from -1.57 to 0.38°C . **Conclusion:** The FL-WebPHS provides an effective tool for estimating heat strain for athletes and workers under known and environmental conditions. This software could assist physiologists, event organizers, coaches, industrial hygienists, and occupational physicians in optimizing health and performance through strategic heat mitigation.

Introduction

The human capacity for performing physical and mental tasks has been consistently demonstrated to be adversely affected in hot environments^{26,45,88,251}. A growing body of evidence emphasizes the impact of weather parameters on athletic performance, particularly in endurance running competitions, which have experienced a surge in popularity in recent years^{1,49,53,252-254}. Heat stress has been shown to affect several parameters vital for exercise endurance, leading to performance impairment in endurance races^{54,55}. Athletes participating in these events frequently face considerable thermoregulatory strain, as they must maintain high-intensity exercise for extended periods under environmental heat stress^{81,255,256}. Overall performance tends to decrease as core and skin temperatures increase^{93,257-259}, emphasizing the importance of accurately measuring body core temperature in determining an athlete's thermoregulatory strain during exercise²⁶⁰. Considering the significant influence of heat stress on athletic performance and the growing interest in endurance sports, it becomes crucial to implement effective strategies for mitigating the adverse effects of heat on athletes^{1,261,262}. The integration of pre-cooling techniques, hydration optimization, and heat acclimatization protocols into training regimens has proven beneficial in addressing heat stress^{263,264}. Moreover, advanced algorithms and software designed to predict heat strain have emerged as invaluable tools, enabling professionals to make data-driven decisions and implement tailored interventions to ensure optimal athletic performance and safety in high-temperature environments^{9,73}.

In our earlier work the FAME Lab PHS Calculator software (PHS_{FL}) was designed and implemented as a new tool to calculate the Predicted Heat Strain (PHS) for a group of individuals based on ISO 7933:2018^{8,45}. Optimized for physiologists, industrial hygienists, and occupational physicians, PHS_{FL} calculates the required environmental and physiological parameters using other ISO standards (7726:1998²⁶⁵, 8996:2004⁴³, and 7730:1994²⁶⁶) and published literature^{160,267}. PHS_{FL} tool has been

successfully tested and applied in various occupational settings, providing valuable insights into the physiological implications of heat stress on workers. In this study, our primary objective was to design and implement the new FAME Lab PHS web tool (FL-WebPHS), a software based on ISO 7933:2018 and the existing PHS_{FL} software. Moreover, we aimed to assess the construct validity of the FL-WebPHS by comparing its results against those obtained through field experiments performed on running athletes participating in endurance races. This research seeks to enhance our understanding of the physiological implications of heat stress on athletic performance and provide a practical tool for professionals in the field to better evaluate and manage heat strain in athletes.

Methods

Development of the FL-WebPHS.

The FL-WebPHS is a browser-based software developed using HTML, CSS, and JavaScript (Chapter 1.8). It contains two main components: the first is based on a modified version of the ISO 7933:2018 standard called PHS_{FL}⁸, and the second is based on the ISO 7933:2018 standard⁴⁵. It is an online tool available for free at <https://bit.ly/PHSwebtool> designed for use on a range of devices like laptops, desktop computers, and smartphones and compatible with various operating systems such as Windows, Unix, MacOS, IOS, and Android. The main screen features 38 buttons and input-boxes (Figure 6.1), described in detail in Table 6.1.

Table 6.1 | FL-WebPHS software.

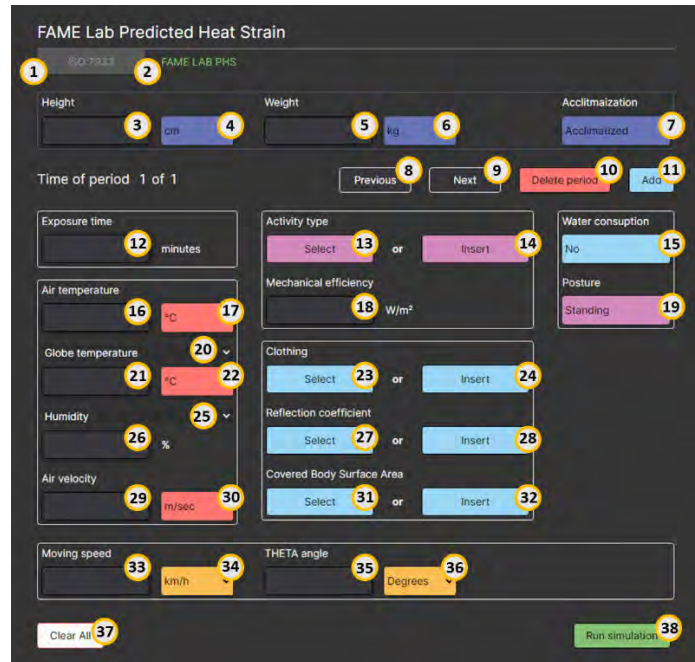
Explanation of the 38 different options/buttons provided on the main screen of the FL-WebPHS software, as shown in Figure 6.1.

#	Name	Description
1	ISO:7933	Navigate to the web app's second component, based on the ISO 7933:2018 standard.
2	FAME LAB PHS	Access the web app's current component, based on the PHS _{FL} .

3	Height	Enter the height of the simulated individual.
4	Height-unit	Select the height unit: cm or inch.
5	Weight	Enter the weight of the simulated individual.
6	Weight-unit	Select the weight unit: kg or lb.
7	Acclimatization	Choose the acclimatization status: "Acclimatized" or "Non-Acclimatized".
8	Previous	Navigate to the previous time period, if available.
9	Next	Navigate to the next time period, if available.
10	Delete period	Remove the current period and its data.
11	Add	Add a new period with predefined data from the current period.
12	Exposed time	Enter the duration (minutes) spent on the simulated task.
13	Select Activity	Open a new window to choose an activity from the compendium of physical activities list ⁴⁷ .
14	Insert Activity	Open a new input field to enter the metabolic rate.
15	Water consumption	Select whether the individual can drink water freely during the exposure time: "Yes" or "No".
16	Air temperature	Enter the air temperature.
17	Temperature-unit	Select the temperature unit: °C or °F.
18	Mechanical efficiency	Input the mechanical efficiency value.
19	Posture select	Choose the individual's posture: "Standing" or "Sitting" or "Crouching"
20	Select Globe-Radian Temperature	Choose between Globe and Radian temperature.
21	Globe or Radian temperature	Enter the selected temperature value.
22	Temperature-unit	Select the temperature unit: °C or °F.
23	Select clothing	Choose clothing type from ASHRAE list ⁴⁶ .
24	Insert Clothing	Input clothing insulation value.
25	Select Humidity or Vapor pressure	Choose between humidity or vapor pressure.
26	Humidity or Vapor pressure value	Enter the selected humidity or vapor pressure value.
27	Select Reflection coefficient	Choose a reflection coefficient option.
28	Insert Reflection coefficient	Input the reflection coefficient value.
29	Air velocity	Enter the air velocity.
30	Air velocity-unit	Select the air velocity unit: m/s or ft/min.
31	Select Covered BSA	Choose the covered body surface area (BSA) option.
32	Insert Covered BSA	Input the covered BSA value.
33	Moving Speed	Enter the individual's moving speed.
34	Moving Speed-unit	Select the moving speed unit: m/s or ft/min.
35	THETA angle	Input the THETA angle value.
36	THETA angle-unit	Select the THETA angle unit: degrees or radians.
37	Clear all	Reset all input fields.
38	Run simulation	Run the simulation and navigates to results section.

Figure 6.1 | FL-WebPHS main screen.

The FL-WebPHS main screen, featuring 38 buttons and input-boxes. The buttons titled "Select" open a new window offering additional options, while the buttons labeled "Insert" enable users to input specific values.



FL-WebPHS optimization.

Upon completing the development of the two primary components of the FL-WebPHS, we proceeded to make various additions and modifications to improve its overall functionality and user experience. It is important to note that the second component is based on the original code as specified in ISO 7933:2018⁴⁵. Any kind of modifications are made in the PHS_{FL}-based version.

Unlimited different time periods:

A significant improvement in FL-WebPHS is the expansion of its capabilities to handle time periods. While the first version (PHS_{FL}) was constrained to only 10 different time periods, the web-based version (FL-WebPHS) has been designed to accommodate an unlimited number of time periods. The final predicted values from each interval are utilized as initial data for the following period. New input values are taken into account

during this process, while the remaining attributes of the software, such as equations and code, are maintained without any alterations. This feature allows for greater flexibility and adaptability, enabling users to model various scenarios more effectively and accurately.

Unit conversion flexibility:

In the newly developed software, we have introduced a feature to increase user experience by providing the functionality to switch between units. The software now supports both imperial and metric units for all available input parameters.

Expanded results and export capabilities:

We have also created better data visualization, making it easier to interpret the results. Additionally, we have updated the results section to provide users with a more comprehensive understanding of heat stress exposure by incorporating three new key outputs:

1. "Time to reach 38°C core body temperature safety limit (valid for 95% of people)"
2. "Time to reach 2% body mass dehydration state (valid for 95% of people)"
3. "Average sweat rate"

Furthermore, we have implemented functionality that allows users to save their simulation data and charts in a convenient and accessible format. The charts can be saved as .png files, while the minute-by-minute data can be exported as .csv files.

Validating FL-WebPHS for athletes

The construct validity, which refers to a measurement being associated with variables assessing the same (or similar) characteristic²⁶⁸, of the FL-WebPHS was assessed by comparing its results with those obtained via field experiments conducted on human participants. While the first version of PHS_{FL} was tested in the context of construction

work⁸, the current study aimed to evaluate its applicability to athletes, specifically long-distance runners. The experimental protocol for the field studies was approved by the Bioethics Review Board of the University of Thessaly Department of Physical Education and Sport Science (protocol no. 3-3/9-6-2021; Annex A). Our study involved monitoring a group of eight experienced and acclimatized runners. Before their participation in the study, written informed consent was obtained from all volunteer runners after providing a detailed explanation of the procedures involved.

In the morning before the race started, self-reported age, body stature (Seca 213; seca GmbH & Co. KG; Hamburg, Germany), and body mass (BC1000, Tanita Corporation, Tokyo, Japan) were collected from the participants. During the race, continuous core temperature data were gathered using wireless telemetric capsules (BodyCap, Caen, France). Moreover, continuous environmental data, including air temperature, globe temperature, relative humidity, and air velocity, were obtained using a portable weather station (Kestrel 5400FW, Nielsen-Kellerman, Pennsylvania, USA). Image recordings were utilized to calculate clothing insulation and covered body surface area. Specifically, all clothes worn by runners were photo-recorded and matched with known clothing insulation values found in the literature⁴⁶, and the fraction of the covered body surface area of workers was determined by summing the regions of their body covered by garments. The ratios of the area of different body regions to the total body surface area were obtained from ISO 7933:2018⁴⁵. All participating athletes were equipped with personal smartwatches throughout the race, which enabled the collection of detailed activity files (.gpx) upon completion. These files included essential data such as satellite coordinates, speed, and grade, which facilitated the accurate calculation of each athlete's walking speed and metabolic rate during the race. The metabolic rate calculations were performed using the American College of Sports Medicine (ACSM) equations²⁶⁹.

The collected raw data was used to calculate half-hourly mean values. These averages were used to conduct eight (i.e., one simulation per runner) three-period (i.e., warm-up, race, cool-down) simulations using the FL-WebPHS. To assess the relationship between observed and predicted values, various statistical methods were employed. First, Willmott's Index of Agreement was calculated to provide an estimate of the model's accuracy, followed by Pearson's correlation coefficient. To evaluate potential differences between the observed and predicted values, mean differences, root mean squared errors (RMSE), and absolute mean errors (MAE) were computed. Lastly, the Bland-Altman 95% limits of agreement, along with the associated percent coefficient of variation, were calculated to further assess and visualize the between-method differences. Statistical analyses were performed using Python programming language version 3.9.12, specifically employing libraries such as NumPy, SciPy, and Seaborn for data manipulation, analysis, and visualization. The level of significance for these analyses was set at $p < 0.05$.

Results

Eight long-distance runners (age: 46.9 ± 5.2 years; height: 175.6 ± 8.9 cm; weight: 76.5 ± 10.7 kg) participated in the study. Four of them completed the "*Athens Marathon the Authentic*" (42,195m) with an average finish time of $04:14 \pm 00:19$ hours, while the remaining four participated in a 30k race, finishing with an average time of $02:59 \pm 00:12$ hours. During the marathon, runners experienced environmental conditions of air temperature $18.60 \pm 1.10^\circ\text{C}$, globe temperature $20.85 \pm 2.84^\circ\text{C}$, relative humidity $66.24 \pm 4.47\%$, and air velocity 0.14 ± 0.30 m/s. In contrast, the 30k race runners faced conditions of air temperature $20.95 \pm 1.42^\circ\text{C}$, globe temperature $25.23 \pm 4.17^\circ\text{C}$, relative humidity $80.88 \pm 8.92\%$, and air velocity 0.18 ± 0.38 m/s. All participants wore clothing with a thermal insulation value of 0.29clo and a clothing coverage of 44% of the body surface area. Their average walking speed was 2.8 ± 0.2 m/s, and they had an average metabolic rate of 612.5 ± 37.2 watts/m².

The Willmott's Index of Agreement between observed and predicted core temperature was 0.63, indicating a moderate agreement. Pearson's correlation coefficient revealed a moderate positive linear relationship between the observed ($38.23 \pm 0.59^\circ\text{C}$) and predicted ($38.88 \pm 0.44^\circ\text{C}$) core temperature ($r=0.58$, $p<0.001$) (Figure 6.2 and 6.3). The mean difference of 0.59°C suggested that the predicted values were, on average, higher than the observed values (RMSE: 0.77°C ; MAE: 0.65°C). The 95% limits of agreement between measured and predicted core temperature ranged from -1.57 to 0.38°C , with the corresponding percentage coefficients of variation at 2.55% (Figure 6.4). To visualize the performance and accuracy of the FL-WebPHS, the violin plot (Figure 6.5) illustrates the distribution of the differences between the observed and predicted core temperatures, providing further insight into the variability of the data.

Figure 6.2 | Linear relationship.

Scatter plot illustrates the moderate positive linear relationship between observed and predicted core temperatures. The data points represent half-hourly averaged individual observations.

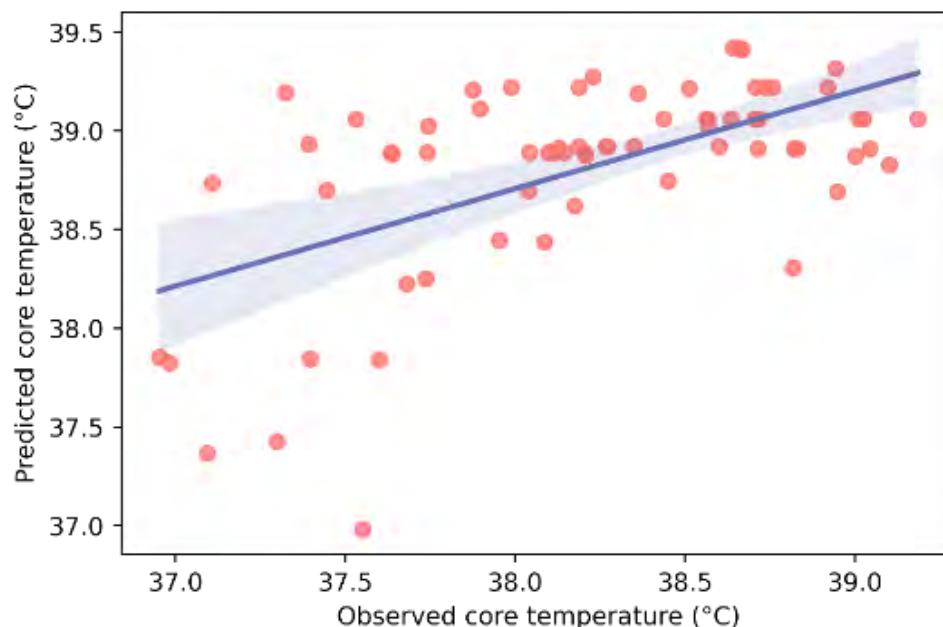


Figure 6.3 | Average observed and predicted values.

The chart displays the average observed and predicted core temperatures for all runners, with the shaded area representing the standard deviation.

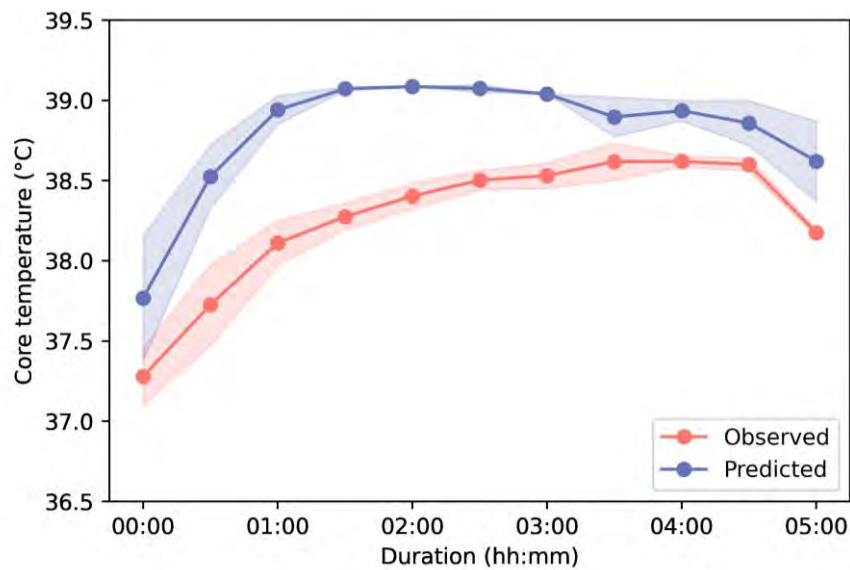


Figure 6.4 | 95% limits of agreement.

Half-hourly averaged differences between observed and predicted core temperatures across all runners, represented by red circles. The black dashed line represents the bias, or the average difference between the two methods. The yellow dashed lines indicate the 95% limits of agreement, providing a range for the expected differences between the observed and predicted values.

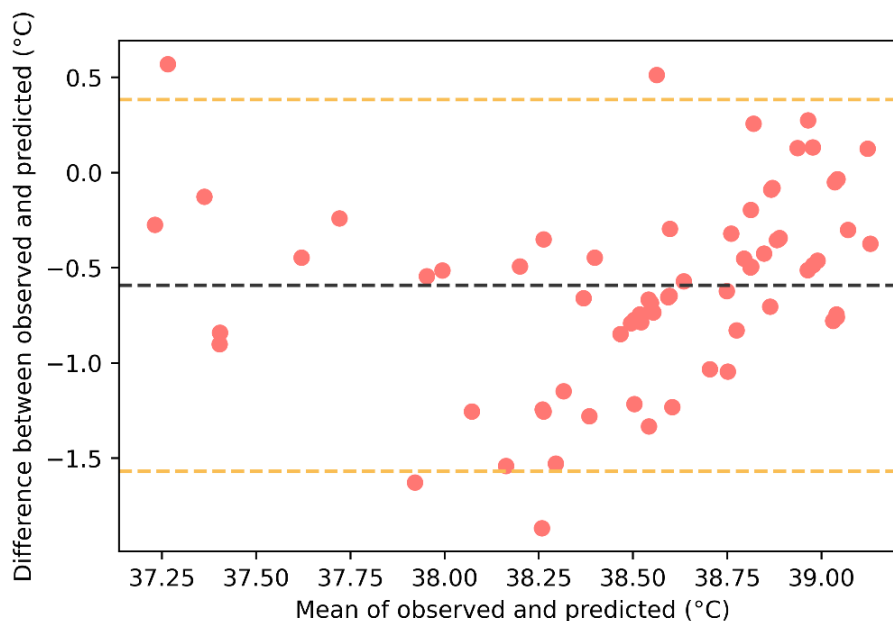
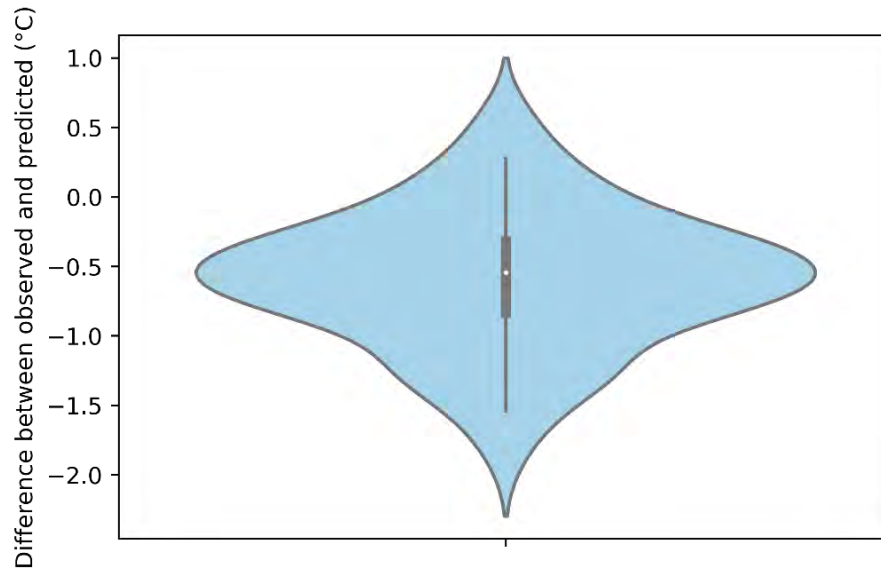


Figure 6.5 | Violin plot.

Violin plot illustrates the distribution of the differences between the observed and predicted core temperatures. The width of the violin at any given point along the y-axis corresponds to the density of data points at that specific difference value. The wider the violin at a particular point, the more data points are present at that difference level.



Discussion

In this study, we designed the FL-WebPHS, a web-based software that calculates the heat strain experienced by a person in given environmental conditions based on ISO 7933:2018 and the existing PHS_{FL} software^{8,45}. The new software is a browser-based tool, offering numerous features that improve its practicality and user-experience. Our validation analyses, shows that the estimations made by FL-WebPHS are close to results derived from field tests conducted on human participants, specifically long-distance runners during races in moderate¹ environments.

The FL-WebPHS software incorporates several elements. The software now allows unlimited different time periods, enabling users to model various scenarios more effectively and accurately, while the previous version (PHS_{FL}) was constrained to only 10 different time periods. This improvement offers greater flexibility for users to create

more detailed and realistic heat strain assessments. Additionally, the FL-WebPHS was equipped with the functionality to switch between units, making it easier for users to work with the software according to their preferences and needs. The software also features improved data visualization, allowing users to better understand and interpret the results of their heat strain assessments.

Our findings demonstrated a moderate agreement between the predicted core temperatures using FL-WebPHS and the observed core temperatures measured during field experiments in marathon and 30k race runners. Furthermore, the 95% limits of agreement indicate that a core temperature of 38°C, as measured by a gastrointestinal thermistor during a marathon, could be estimated at a maximum of 38.38°C (38 + 0.38) in the worst-case scenario when using the FL-WebPHS. This range provides a reasonably accurate estimation of the heat strain experienced by athletes during endurance races, taking into consideration the variability in individual physiological responses to heat stress.

Our validation assessment found a moderate positive linear relationship between the observed and predicted core temperatures ($r=0.58$, $p<0.001$). Interestingly, this correlation coefficient is comparable to those reported in the development and validation of the PHS model ($r=0.594$ for field experiments and $r=0.659$ for laboratory experiments). This similarity in correlation coefficients demonstrates that our FL-WebPHS software maintains a similar level of predictive accuracy as the original PHS model. Furthermore, it is also comparable to the correlation coefficient found in our previous study validating the software in human participants during work in the heat ($r=0.573$)⁸.

Despite the promising results of our study, there are some limitations that should be considered. First, we could not examine potential differences in sweat rate between the predicted and observed data, as the runners drank water throughout the

race. This made it unfeasible to accurately measure the precise volume of water consumed and its impact on sweat rate. Secondly, the validation of observed mean skin temperature with the predicted values was disrupted because light rain during the two races affected the measurements. The rainwater in contact with the sensors caused an underestimation of skin temperature. Additionally, some skin temperature sensors were lost on the road, during the race, as the adhesive tape unrolled from the skin due to the rain, making it impossible to calculate the mean skin temperature without all the data. Lastly, our study has limitations since we computed core temperature values as half-hourly averages in order to minimize the effect of momentary occurrences, such as consuming water, splashing water on the body, or consumption electrolytes throughout the race. While this approach reduces the impact of these factors on the overall analysis, it may also limit the detail of the data and our understanding of the immediate physiological responses to heat stress during the race.

In conclusion, we developed the FL-WebPHS, an online tool available for free at <https://bit.ly/PHSwebtool>, which estimates heat strain for both athletes and workers in known and fluctuating environmental conditions, drawing on ISO 7933:2018 and the PHS_{FL} software. This user-friendly software can assist physiologists, event organizers, coaches, industrial hygienists, and occupational physicians in optimizing health and performance by employing effective heat mitigation strategies. The FL-WebPHS aims to contribute to improved athletic performance and work productivity while promoting awareness of heat strain management in various environments.

General Conclusions

This PhD research explored the intersection of technological advancements and their application in optimizing human performance and health under varied environmental conditions. Hardware prototypes (e.g., Smart Helmet and Web Thermometer Tracker) were created in conjunction with software prototypes (e.g., Task Analysis App, FL-WebPHS). These technologies, suitable for deployment in both laboratory and field studies, facilitated real-time data collection and analysis, thereby aiding in understanding human responses in diverse environmental conditions. Moreover, they assisted in assessing health status, performance, and productivity, and in evaluating and predicting physiological heat strain.

Leveraging machine learning methods, the first study utilized a decision tree regressor algorithm to investigate the impact of weather factors on athletic performance. The analysis of 1258 races across 84 locations and 42 countries revealed that more than one-quarter of endurance running events were conducted in moderate, high, or extreme heat. This machine learning analysis demonstrated that among various weather parameters, air temperature has the most significant effect on athletic performance. However, the findings also suggested that considering air temperature alone was not sufficient. Coaches, athletes, and organizers should evaluate all four weather parameters, including air temperature, relative humidity, wind speed, and solar radiation, as decision trees based just on air temperature accounted for a relatively low percentage of variability in performance.

In a follow-up study, similar machine learning techniques were employed to conduct an in-depth risk assessment for heat stress during work and leisure activities. This analysis identified work duration and body mass index as significant factors of individuals' exposure to heat stress. Addressing these risk factors could lead to significant healthcare savings by reducing occupational heat illness, and mortality associated with heat strain. This is especially necessary for industries that rely heavily on manual labor performed outdoors, often in hot

conditions. Implementing appropriate strategies, such as adjusting work-rest ratios, ensuring sufficient hydration, wearing suitable clothing, and providing shading, could help mitigate the heat strain experienced by workers. As environmental heat stress increases due to climate change, a worldwide effort involving fields like science, health and safety, and labor is needed.

Progressing, the focus shifted to exploring more specific applications of the developed technologies and methodologies. The objective was the optimization of athletic performance and protection in hot environments. This led to the creation of a model to predict athletes' head thermal comfort, utilizing simple and easily measurable variables. These variables can be monitored continuously using sensors embedded in a bicycle helmet. In the first experimental stage, various factors, including ambient temperature, under-helmet temperature, cyclist heart rate, cyclist mechanical work, and helmet thermal resistance, were identified as significantly influencing a cyclist's head thermal comfort. From this, a streamlined linear regression model was established, demonstrating a maximum MAPE of 8.4%. This model, despite its reduced complexity and low computational cost, provided reliable and real-time data, making it ideal for continuous and adaptive modeling. Based on the selected variables from this model, a smart helmet prototype, named SmartHelmet, was created using embedded sensor technology. The model was validated using the SmartHelmet prototype in a controlled hot environment during a 30 km cycling Time Trial. The results validated the model's effectiveness in predicting thermal comfort with a maximum MAPE of 10%, which further reduced to 7.8% after refining the model parameters. Finally, we introduced a calculation framework for an adaptive personalized model, based on streaming data from the SmartHelmet prototype, to predict a cyclist's head thermal comfort in real-time.

Extending the investigation into the varied aspects of human performance and well-being, the study also probed the effects of high altitude. Specifically, it examined the impacts of high altitude on cardiac autonomic function and sleep quality, using time and frequency analysis algorithms for HRV analysis. The findings underscored the importance of

understanding physiological adaptations and changes in sleep patterns that occur at high altitudes. For individuals regularly navigating such environments, this understanding becomes particularly significant. In the case study reported, sleeping at high altitudes above 5500 meters led to a gradual decline in HRV and an increase sleep awakenings. Both the sleep duration and the subjective quality of sleep were negatively affected. These insights reveal how high altitude affects cardiac autonomic function and sleep quality. This is a crucial understanding for individuals, such as climbers, who often experience high altitudes. It could provide information for strategies to improve their health and well-being.

In an effort to provide a practical tool for physiologists, industrial hygienists, occupational physicians, coaches, and event organizers to optimize human health, performance, and productivity, we designed and implemented the FL-WebPHS. This online tool is specifically created to estimate heat strain for both athletes and workers. It integrates the ISO 7933:2018 standards with PHS_{FL} software, aids in the effective implementation of heat mitigation strategies. Our validation assessment revealed a moderate positive linear relationship between observed and predicted core temperatures ($r=0.58$, $p<0.001$). Interestingly, this correlation is comparable to those reported during the development and validation of the original PHS (ISO 7933:2018) model ($r=0.594$ for field experiments and $r=0.659$ for laboratory experiments), indicating that our FL-WebPHS software maintains a similar level of predictive accuracy. The correlation coefficient also aligns with our previous study validating the software in human participants during work in the heat ($r=0.573$), further underscoring the reliability of this tool in managing heat strain

This PhD research explored the intersection of these technological advancements and their application in optimizing human performance and protecting health under various environmental conditions. It delved into how these tools could be harnessed to understand and mitigate the impact of challenging environments on human health and performance, and how they were used to develop strategies and solutions that enhanced safety, productivity,

performance, and overall wellbeing. Future studies should continue to explore the correlation between environmental conditions and human health and performance. As wearable technology becomes more integrated in our daily lives, the multitude of data points we collect every day provides researchers with a unique opportunity. It enables them to better understand how diverse environmental conditions influence health and performance. Upcoming research should focus on integrating technologies like artificial intelligence to effectively analyze this data. By doing so, we can build more accurate predictive models, refine performance strategies, and better handle the risks associated with varying environmental conditions.

Future Directions

As participation in endurance events grows among recreational athletes, the significance of technological advancements such as real-time performance feedback and prediction algorithms is increasing, particularly in the context of climate change and challenging weather conditions. Devices like the SmartHelmet could offer real-time performance feedback, alerting athletes, for instance, to boost their hydration intake in response to increased thermal stress. In addition, the findings from this PhD research regarding the influence of weather parameters on athletic performance could be integrated into these systems, improving their predictive capabilities and the accuracy of their recommendations. Moreover, this knowledge could assist event organizers in strategically scheduling endurance events during the cooler night hours, potentially mitigating heat-related risks. Additionally, the FL-WebPHS by estimating an athlete's total water loss grounded on individual and environmental parameters could be used to develop unique personalized hydration strategies for each athlete during training and competition to improve performance and protect health across a diverse range of environmental conditions.

Climate change also impact a number of workers on different industries across the globe, increasing the need for effective heat stress mitigation strategies. Among the 18 factors

influencing heat stress, BMI and work duration play significant roles. For example, workers with higher BMI may be more vulnerable to heat stress, highlighting the need for more frequent breaks. The FL-WebPHS algorithm is based on ISO standards that consider six of 18 factors influencing heat stress including personalized anthropometrics, environmental conditions work duration, clothing, metabolic demands and acclimatization. This algorithm can be used to develop personalized guides for the duration and timing of breaks, along with hydration strategies for each worker. Employers can use FL-WebPHS to mitigate heat-related health issues and increase productivity.

With the growing popularity of high-altitude climbing and other extreme activities, the need for better and safer preparation, including proper acclimatization, has become more and more important. The findings from this PhD research on the physiological impacts of high altitudes can be effectively implemented to ensure optimal acclimatization during high-altitude expeditions. Climbers could use wearable technologies, equipped with altimeters and biometric sensors, to continuously monitor health indicators, including HRV. These devices can be used for real-time monitoring of physiological responses and feedback. For example, a decrease in HRV detected during the climber's sleep could trigger an alert. Such immediate feedback would allow climbers to adapt their ascent plans appropriately, allowing them a safer and more effective acclimatization process.

Limitations

Despite the significant progress achieved in this PhD research, there are a few limitations to be considered. Specifically, we have employed decision tree regressor algorithms to explore the impact of weather factors on athletic performance. Though these algorithms are easier to employ and offer lower computational efficiency, they can be greatly affected by minor variations in the data, potentially resulting in lower accuracy of predictions. This sensitivity of decision trees to data changes is a native characteristic. Machine learning algorithms such as “Random Forests” or “Gradient Boosting” can mitigate this concern by utilizing multiple tree

techniques. However, they have also their own challenges, such as increased computational power and requirements.

Furthermore, it should be noted that the machine learning models employed in the PhD studies were trained and validated using historical weather data and world records, assuming that future data will include similar patterns. To address this concern, advanced algorithms such as deep learning analysis could be utilized. These algorithms have the ability to capture complex patterns in the data, potentially decreasing this limitation. However, it is important to note that implementing deep learning models requires larger datasets and higher computational power.

Epilogue

In a world facing climate change and rising global temperatures, my PhD journey focused on the role of technology in optimizing human health and performance across varied environmental conditions. This odyssey, enriched by collaborations with distinct laboratories and research teams worldwide, provided a complete perspective on the dynamic interaction between environment and human performance. Highlighting the importance of teamwork across different fields, the combined knowledge of researchers, universities, and industry experts is crucial. These partnerships serve as catalysts, accelerating progress in our understanding of environmental impacts on humans. By working together, we keep discovering new insights and creating innovative solutions for challenges faced by humans. As we explore this exciting field of science, this joint work and varied skills will be vital in directing our path in a quickly changing environment.

References

1. Mantzios K, Ioannou LG, Panagiotaki Z, et al. Effects of Weather Parameters on Endurance Running Performance: Discipline-specific Analysis of 1258 Races. *Med Sci Sports Exerc* 2022;54(1):153-161. DOI: 10.1249/MSS.0000000000002769.
2. Ioannou LG, Gkikas G, Mantzios K, Tsoutsoubi L, Flouris AD. Chapter 32 - Risk assessment for heat stress during work and leisure. In: Tsatsakis AM, ed. *Toxicological Risk Assessment and Multi-System Health Impacts from Exposure*: Academic Press; 2021:373-385.
3. Youssef A, Colon J, Mantzios K, et al. Towards model-based online monitoring of cyclist's head thermal comfort: smart helmet concept and prototype. *Applied Sciences* 2019;9(15):3170.
4. Mantzios K, Pappas A, Tsianos GI, Flouris AD. Night-Time Heart Rate Variability during an Expedition to Mt Everest: A Case Report. *Sports (Basel)* 2023;11(2). DOI: 10.3390/sports11020048.
5. CISBETI 2019 - International Congress of Health, Well-Being, Technology and Innovation. *BMC Health Services Research* 2019;19(1):448. DOI: 10.1186/s12913-019-4213-z.
6. Wasunna AE, Wyper DY. Technology for health in the future. *World Health Stat Q* 1998;51(1):33-43. (In eng).
7. Silbergliitt R, Antón PS, Howell DR, Wong A. *The Global Technology Revolution 2020, In-Depth Analyses: Bio/Nano/Materials/Information Trends, Drivers, Barriers, and Social Implications*. 2002.
8. Ioannou LG, Tsoutsoubi L, Mantzios K, Flouris AD. A free software to predict heat strain according to the ISO 7933:2018. *Ind Health* 2019;57(6):711-720. DOI: 10.2486/indhealth.2018-0216.
9. Ioannou LG, Mantzios K, Tsoutsoubi L, et al. Indicators to assess physiological heat strain - Part 1: Systematic review. *Temperature (Austin)* 2022;9(3):227-262. DOI: 10.1080/23328940.2022.2037376.
10. Ringuet-Riot CJ, Hahn A, James DA. A structured approach for technology innovation in sport. *Sports Technology* 2013;6(3):137-149. DOI: 10.1080/19346182.2013.868468.
11. Crang ZL, Duthie G, Cole MH, Weakley J, Hewitt A, Johnston RD. The Validity and Reliability of Wearable Microtechnology for Intermittent Team Sports: A Systematic Review. *Sports Medicine* 2021;51(3):549-565. DOI: 10.1007/s40279-020-01399-1.
12. Petersen PE. Global policy for improvement of oral health in the 21st century--implications to oral health research of World Health Assembly 2007, World Health Organization. *Community Dent Oral Epidemiol* 2009;37(1):1-8. (In eng). DOI: 10.1111/j.1600-0528.2008.00448.x.
13. Reid CR, Schall MC, Amick RZ, et al. Wearable Technologies: How Will We Overcome Barriers to Enhance Worker Performance, Health, And Safety? *Proceedings of the Human Factors and Ergonomics Society Annual Meeting* 2017;61:1026 - 1030.
14. Maltseva K. Wearables in the workplace: The brave new world of employee engagement. *Business Horizons* 2020;63(4):493-505. DOI: <https://doi.org/10.1016/j.bushor.2020.03.007>.
15. Borden KA, Cutter SL. Spatial patterns of natural hazards mortality in the United States. *International Journal of Health Geographics* 2008;7(1):64. DOI: 10.1186/1476-072X-7-64.
16. Mora C, Dousset B, Caldwell IR, et al. Global risk of deadly heat. *Nature Climate Change* 2017;7(7):501-506. DOI: 10.1038/nclimate3322.

17. Luber G, McGeehin M. Climate change and extreme heat events. *Am J Prev Med* 2008;35(5):429-35. (In eng). DOI: 10.1016/j.amepre.2008.08.021.
18. Stillman JH. Heat Waves, the New Normal: Summertime Temperature Extremes Will Impact Animals, Ecosystems, and Human Communities. *Physiology* 2019;34 2:86-100.
19. International Labour Organization. Working on a warmer planet: The impact of heat stress on labour productivity and decent work. Geneva: Publications Production Unit, International Labour Organization; 2019.
20. Ioannou LG, Tsoutsoubi L, Mantzios K, et al. The Impacts of Sun Exposure on Worker Physiology and Cognition: Multi-Country Evidence and Interventions. *International Journal of Environmental Research and Public Health* 2021;in press.
21. Ioannou LG, Testa DJ, Tsoutsoubi L, et al. Migrants from Low-Income Countries have Higher Heat-Health Risk Profiles Compared to Native Workers in Agriculture. *Journal of Immigrant and Minority Health* 2023. DOI: 10.1007/s10903-023-01493-2.
22. Luczak H. Work under extreme conditions. *Ergonomics* 1991;34 6:687-720.
23. Karthick S, Kermanshachi S, Pamidimukkala A, Namian M. A review of construction workforce health challenges and strategies in extreme weather conditions. *International Journal of Occupational Safety and Ergonomics* 2022;29:773 - 784.
24. Ioannou LG, Tsoutsoubi L, Samoutis G, et al. Time-motion analysis as a novel approach for evaluating the impact of environmental heat exposure on labor loss in agriculture workers. *Temperature (Austin)* 2017;4(3):330-340. (In eng). DOI: 10.1080/23328940.2017.1338210.
25. Brookfield H, Allen BJ. HIGH-ALTITUDE OCCUPATION AND ENVIRONMENT. *Mountain Research and Development* 1989;9:201.
26. Flouris AD, Dinas PC, Ioannou LG, et al. Workers' health and productivity under occupational heat strain: a systematic review and meta-analysis. *Lancet Planet Health* 2018;2(12):e521-e531. DOI: 10.1016/S2542-5196(18)30237-7.
27. Guogao Z, Hanzhen H, Zhi-en W, Rongtai C, Chengkun L, Wei Z. Health and safety measures for working in extremely hot environments. *Acta Academiae Medicinae Wuhan* 2008;3:104-109.
28. Lukowicz P, Timm-Giel A, Lawo M, Herzog O. WearIT@work: Toward Real-World Industrial Wearable Computing. *IEEE Pervasive Computing* 2007;6.
29. Nunneley SA, Troutman SJ, Webb P. Head cooling in work and heat stress. *Aerospace medicine* 1971;42 1:64-8.
30. Frank MR, Autor D, Bessen J, et al. Toward understanding the impact of artificial intelligence on labor. *Proceedings of the National Academy of Sciences of the United States of America* 2019;116:6531 - 6539.
31. Chatzitofis A, Zarpalas D, Daras P. A Computerized System for Real-Time Exercise Performance Monitoring and e-Coaching Using Motion Capture Data. 2018.
32. Li RT, Kling SR, Salata MJ, Cupp SA, Sheehan J, Voos JE. Wearable Performance Devices in Sports Medicine. *Sports Health* 2016;8:74 - 78.
33. Howard RM. Wireless Sensor Devices in Sports Performance. *IEEE Potentials* 2016;35:40-42.
34. Gawli S, Ubale I, Damekar S. Personalized AI Dietitian and Fitness Trainer. *International Journal for Research in Applied Science and Engineering Technology* 2022.
35. Taware G, Kharat RS, Dhende P, Jondhalekar P, Agrawal R. AI-Based Workout Assistant and Fitness Guide. 2022 6th International Conference On Computing, Communication, Control And Automation (ICCUBEA 2022:1-4.
36. Vihma T. Effects of weather on the performance of marathon runners. *International Journal of Biometeorology* 2010;54:297-306.

37. Böcker L, Dijst M, Prillwitz J. Impact of Everyday Weather on Individual Daily Travel Behaviours in Perspective: A Literature Review. *Transport Reviews* 2013;33:71 - 91.
38. Chan CB, Ryan DAJ. Assessing the Effects of Weather Conditions on Physical Activity Participation Using Objective Measures. *International Journal of Environmental Research and Public Health* 2009;6:2639 - 2654.
39. Letchford A, Paudel R, Thomas OD, Booth AS, Imray CH. Acute Mountain Sickness (AMS) Knowledge Among High Altitude Marathon Runners Competing in the Everest Marathon. *Wilderness Environ Med* 2016;27(1):111-6. (In eng). DOI: 10.1016/j.wem.2015.09.021.
40. Knoth C, Knechtle B, Rüst CA, Rosemann TJ, Lepers R. Participation and performance trends in multistage ultramarathons—the ‘Marathon des Sables’ 2003–2012. *Extreme Physiology & Medicine* 2012;1:13 - 13.
41. Scheer V. Participation Trends of Ultra Endurance Events. *Sports Medicine and Arthroscopy Review* 2019;27:3–7.
42. Mantzios K. Design, Implementation, and Verification of Validity and Reliability of a Software for the Protection of Health and Improvement of Performance in a Hot Environment. In: Flouris AD, ed. Thessaly: University of Thessaly; 2019.
43. ISO 8996. Determination of metabolic rate. International Standard; 2004.
44. Flouris AD, Ioannou LG, Dinas PC, et al. Assessment of occupational heat strain and mitigation strategies in Qatar. Doha, Qatar: International Labour Organization, 2019. (FL/2019/13).
45. ISO/DIS 7933. Ergonomics of the thermal environment — Analytical determination and interpretation of heat stress using the predicted heat strain model. Geneva: International Organization for Standardization; 2018.
46. McCullough EA, Jones BW, Huck J. A comprehensive data base for estimating clothing insulation. *Ashrae Trans* 1985;91(2):29-47.
47. Ainsworth BE, Haskell WL, Whitt MC, et al. Compendium of physical activities: an update of activity codes and MET intensities. *Med Sci Sports Exerc* 2000;32(9 Suppl):S498-504. DOI: 10.1097/00005768-200009001-00009.
48. Gaid N. Most cities too hot to host 2088 summer Olympics. *Nature News* 2016.
49. Smith KR, Woodward A, Lemke B, et al. The last Summer Olympics? Climate change, health, and work outdoors. *Lancet* 2016;388(10045):642-4. DOI: 10.1016/S0140-6736(16)31335-6.
50. Thorsson S, Rayner D, Palm G, et al. Is Physiological Equivalent Temperature (PET) a superior screening tool for heat stress risk than Wet-Bulb Globe Temperature (WBGT) index? Eight years of data from the Gothenburg half marathon. *Br J Sports Med* 2020. DOI: 10.1136/bjsports-2019-100632.
51. Shultz D. What will it take to break the 2-hour marathon? *Science Magazine*. May 8 (www.sciencemag.org/news/2017/05/what-will-it-take-break-2-hour-marathon).
52. Thurber C, Dugas LR, Ocobock C, Carlson B, Speakman JR, Pontzer H. Extreme events reveal an alimentary limit on sustained maximal human energy expenditure. *Sci Adv* 2019;5(6):eaaw0341. DOI: 10.1126/sciadv.aaw0341.
53. Roberts WO. Determining a "do not start" temperature for a marathon on the basis of adverse outcomes. *Med Sci Sports Exerc* 2010;42(2):226-32. DOI: 10.1249/MSS.0b013e3181b1cddf.
54. McCann DJ, Adams WC. Wet bulb globe temperature index and performance in competitive distance runners. *Med Sci Sports Exerc* 1997;29(7):955-61. DOI: 10.1097/00005768-199707000-00016.

55. Ely MR, Cheuvront SN, Roberts WO, Montain SJ. Impact of weather on marathon-running performance. *Med Sci Sports Exerc* 2007;39(3):487-93. DOI: 10.1249/mss.0b013e31802d3aba.
56. Suping Z, Guanglin M, Yanwen W, Ji L. Study of the relationships between weather conditions and the marathon race, and of meteorotropic effects on distance runners. *International journal of biometeorology* 1992;36(2):63-68.
57. Trapasso LM, Cooper JD. Record performances at the Boston Marathon: biometeorological factors. *International journal of biometeorology* 1989;33(4):233-237.
58. Vihma T. Effects of weather on the performance of marathon runners. *International journal of biometeorology* 2010;54(3):297-306.
59. Maughan R. Distance running in hot environments: a thermal challenge to the elite runner. *Scandinavian journal of medicine & science in sports* 2010;20:95-102.
60. Maughan RJ, Watson P, Shirreffs SM. Heat and cold. *Sports Medicine* 2007;37(4-5):396-399.
61. Weller A, Millard C, Stroud M, Greenhaff P, Macdonald I. Physiological responses to a cold, wet, and windy environment during prolonged intermittent walking. *American Journal of Physiology-Regulatory, Integrative and Comparative Physiology* 1997;272(1):R226-R233.
62. Villiers MDd. How does the wind affect road-running achievement? *The Physics Teacher* 1991;29(5):286-289. DOI: 10.1119/1.2343319.
63. Ely MR, Cheuvront SN, Montain SJ. Neither cloud cover nor low solar loads are associated with fast marathon performance. *Med Sci Sports Exerc* 2007;39(11):2029.
64. Jago L, Chalip L, Brown G, Mules T, Ali S. Building events into destination branding: Insights from experts. *Event Management* 2003;8:3-14.
65. Misailidi M, Mantzios K, Papakonstantinou C, Ioannou LG, Flouris AD. Environmental and Psychophysical Heat Stress in Adolescent Tennis Athletes. *Int J Sports Physiol Perform* 2021:1-6. DOI: 10.1123/ijsp.2020-0820.
66. Gilbert MM. *Renewable and efficient electric power systems*: John Wiley & Sons, 2004.
67. Ioannou LG, Mantzios K, Tsoutsoubi L, et al. Effect of a Simulated Heat Wave on Physiological Strain and Labour Productivity. *International Journal of Environmental Research and Public Health* 2021;18(6):3011. (<https://www.mdpi.com/1660-4601/18/6/3011>).
68. Hardy B. ITS-90 formulations for vapor pressure, frostpoint temperature, dewpoint temperature, and enhancement factors in the range -100 to +100 C. *The Proceedings of the Third International Symposium on Humidity & Moisture*, Teddington, London, England 1998:1-8.
69. Smagorinsky J. On the dynamical prediction of large-scale condensation by numerical methods. *Geophys Monogr* 1960;5:71-78.
70. Khatib T, Elmenreich W. *Modeling of the solar source. Modeling of photovoltaic systems using Matlab: Simplified green codes*. Hoboken, NJ, USA: John Wiley & Sons, Inc.; 2016:17-53.
71. Kasten F, Czeplak G. Solar and terrestrial radiation dependent on the amount and type of cloud. *Solar energy* 1980;24(2):177-189.
72. American College of Sports Medicine. Prevention of thermal injuries during distance running. *The Physician and Sportsmedicine* 1984;12(7):43-51. DOI: 10.1080/00913847.1984.11701899.

73. Liljegren JC, Carhart RA, Lawday P, Tschopp S, Sharp R. Modeling the wet bulb globe temperature using standard meteorological measurements. *J Occup Environ Hyg* 2008;5(10):645-55. DOI: 10.1080/15459620802310770.
74. Yamasawa F, Fischetto G, Bermon S, et al. Competition Medical Guidelines. 2013.
75. Pedregosa F, Varoquaux G, Gramfort A, et al. Scikit-learn: Machine learning in Python. *the Journal of machine Learning research* 2011;12:2825-2830.
76. Seabold S, Perktold J. Statsmodels: Econometric and statistical modeling with python. *Proceedings of the 9th Python in Science Conference: Austin, TX; 2010:61.*
77. Timpka T, Jacobsson J, Bargarora V, et al. Preparticipation predictors for championship injury and illness: cohort study at the Beijing 2015 International Association of Athletics Federations World Championships. *Br J Sports Med* 2017;51(4):271-276. DOI: 10.1136/bjsports-2016-096580.
78. Flouris AD, Friesen BJ, Herry CL, Seely AJE, Notley SR, Kenny GP. Heart rate variability dynamics during treatment for exertional heat strain when immediate response is not possible. *Exp Physiol* 2019;104(6):845-854. DOI: 10.1113/EP087297.
79. Kenny GP, Wilson TE, Flouris AD, Fujii N. Heat exhaustion. *Handb Clin Neurol* 2018;157:505-529. DOI: 10.1016/B978-0-444-64074-1.00031-8.
80. Racinais S, Alonso JM, Coutts AJ, et al. Consensus recommendations on training and competing in the heat. *Br J Sports Med* 2015;49(18):1164-73. DOI: 10.1136/bjsports-2015-094915.
81. Racinais S, Moussay S, Nichols D, et al. Core temperature up to 41.5 masculineC during the UCI Road Cycling World Championships in the heat. *Br J Sports Med* 2019;53(7):426-429. DOI: 10.1136/bjsports-2018-099881.
82. Racinais S, Nichols D, Travers G, et al. Health status, heat preparation strategies and medical events among elite cyclists who competed in the heat at the 2016 UCI Road World Cycling Championships in Qatar. *Br J Sports Med* 2020;54(16):1003-1007. DOI: 10.1136/bjsports-2019-100781.
83. Alonso JM, Edouard P, Fischetto G, Adams B, Depiesse F, Mountjoy M. Determination of future prevention strategies in elite track and field: analysis of Daegu 2011 IAAF Championships injuries and illnesses surveillance. *Br J Sports Med* 2012;46(7):505-14. DOI: 10.1136/bjsports-2012-091008.
84. Alonso JM, Tscholl PM, Engebretsen L, Mountjoy M, Dvorak J, Junge A. Occurrence of injuries and illnesses during the 2009 IAAF World Athletics Championships. *Br J Sports Med* 2010;44(15):1100-5. DOI: 10.1136/bjism.2010.078030.
85. Mountjoy M, Alonso JM, Bergeron MF, et al. Hyperthermic-related challenges in aquatics, athletics, football, tennis and triathlon. *Br J Sports Med* 2012;46(11):800-4. DOI: 10.1136/bjsports-2012-091272.
86. Montain SJ, Ely MR, Chevront SN. Marathon performance in thermally stressing conditions. *Sports Med* 2007;37(4-5):320-3. DOI: 10.2165/00007256-200737040-00012.
87. Periard JD, Eijsvogels TMH, Daanen HAM. Exercise under heat stress: thermoregulation, hydration, performance implications and mitigation strategies. *Physiol Rev* 2021. DOI: 10.1152/physrev.00038.2020.
88. Flouris AD, Schlader ZJ. Human behavioral thermoregulation during exercise in the heat. *Scand J Med Sci Sports* 2015;25 Suppl 1:52-64. DOI: 10.1111/sms.12349.
89. Flouris AD. Functional architecture of behavioural thermoregulation. *Eur J Appl Physiol* 2011;111(1):1-8. DOI: 10.1007/s00421-010-1602-8.
90. Junge N, Jorgensen R, Flouris AD, Nybo L. Prolonged self-paced exercise in the heat - environmental factors affecting performance. *Temperature (Austin)* 2016;3(4):539-548. DOI: 10.1080/23328940.2016.1216257.

91. James CA, Hayes M, Willmott AGB, et al. Defining the determinants of endurance running performance in the heat. *Temperature (Austin)* 2017;4(3):314-329. DOI: 10.1080/23328940.2017.1333189.
92. Cairns MA, Burdett RG, Pisciotta JC, Simon SR. A biomechanical analysis of racewalking gait. *Med Sci Sports Exerc* 1986;18(4):446-53. (In eng).
93. Mora-Rodriguez R, Ortega JF, Hamouti N. In a hot-dry environment racewalking increases the risk of hyperthermia in comparison to when running at a similar velocity. *European Journal of Applied Physiology* 2011;111(6):1073-1080. DOI: 10.1007/s00421-010-1733-y.
94. Menier DR, Pugh LG. The relation of oxygen intake and velocity of walking and running, in competition walkers. *J Physiol* 1968;197(3):717-21. (In eng). DOI: 10.1113/jphysiol.1968.sp008584.
95. Petersson J, Kuklane K, Gao C. Is There a Need to Integrate Human Thermal Models with Weather Forecasts to Predict Thermal Stress? *Int J Environ Res Public Health* 2019;16(22). DOI: 10.3390/ijerph16224586.
96. Maia PA, Ruas AC, Bitencourt DP. Wet-bulb globe temperature index estimation using meteorological data from Sao Paulo State, Brazil. *Int J Biometeorol* 2015;59(10):1395-403. DOI: 10.1007/s00484-014-0949-7.
97. World Health Organization. Quantitative risk assessment of the effects of climate change on selected causes of death, 2030s and 2050s. Geneva, Switzerland: World Health Organization, 2014.
98. Flouris AD, Kenny GP. Heat remains unaccounted for in thermal physiology and climate change research. *F1000Research* 2017;6:221. DOI: 10.12688/f1000research.10554.2.
99. Nybo L, Kjellstrom T, Bogataj LK, Flouris AD. Global heating: Attention is not enough; we need acute and appropriate actions. *Temperature (Austin)* 2017;4(3):199-201. DOI: 10.1080/23328940.2017.1338930.
100. Borden KA, Cutter SL. Spatial patterns of natural hazards mortality in the United States. *Int J Health Geogr* 2008;7:64. DOI: 10.1186/1476-072X-7-64.
101. Quiller G, Krenz J, Ebi K, et al. Heat exposure and productivity in orchards: Implications for climate change research. *Archives of environmental & occupational health* 2017;0. DOI: 10.1080/19338244.2017.1288077.
102. Sahu S, Sett M, Kjellstrom T. Heat exposure, cardiovascular stress and work productivity in rice harvesters in India: implications for a climate change future. *Ind Health* 2013;51(4):424-31. (In eng).
103. Kjellstrom T, Lemke B, Otto M, Hyatt O, K. D. Occupational heat stress: contribution to WHO project on "Global assessment of the health impacts of climate change", which started in 2009. Mapua, New Zealand: Health and Environment International Trust, 2014. (http://www.climatechip.org/sites/default/files/publications/TP2014_4_Occupational_Heat_Stress_WHO.pdf).
104. Kjellstrom T, Lemke B, Otto M, Hyatt O, Briggs D, Freyberg C. Threats to occupational health, labor productivity and the economy from increasing heat during climate change: an emerging global health risk and a challenge to sustainable development and social equity. Mapua, New Zealand: Health and Environment International Trust, 2014.
105. Casanueva A, Burgstall A, Kotlarski S, et al. Overview of Existing Heat-Health Warning Systems in Europe. *International journal of environmental research and public health* 2019;16(15):2657. (In eng). DOI: 10.3390/ijerph16152657.

106. Morabito M, Messeri A, Noti P, et al. An Occupational Heat-Health Warning System for Europe: The HEAT-SHIELD Platform. *Int J Environ Res Public Health* 2019;16(16) (In eng). DOI: 10.3390/ijerph16162890.
107. Lowe D, Ebi KL, Forsberg B. Heatwave early warning systems and adaptation advice to reduce human health consequences of heatwaves. *Int J Environ Res Public Health* 2011;8(12):4623-48. (Research Support, Non-U.S. Gov't Review) (In eng). DOI: 10.3390/ijerph8124623.
108. Zander KK, Botzen WJ, Oppermann E, Kjellstrom T, Garnett ST. Heat stress causes substantial labour productivity loss in Australia. *Nature Climate Change* 2015;5(7):647.
109. Périard J, Racinais S, Sawka MN. Adaptations and mechanisms of human heat acclimation: applications for competitive athletes and sports. *Scandinavian journal of medicine & science in sports* 2015;25:20-38.
110. Sotiridis A, Debevec T, McDonnell AC, Ciuha U, Eiken O, Mekjavic IB. Exercise cardiorespiratory and thermoregulatory responses in normoxic, hypoxic, and hot environment following 10-day continuous hypoxic exposure. *Journal of Applied Physiology* 2018;125(4):1284-1295. DOI: 10.1152/jappphysiol.01114.2017.
111. Périard JD, Travers GJS, Racinais S, Sawka MN. Cardiovascular adaptations supporting human exercise-heat acclimation. *Autonomic Neuroscience* 2016;196:52-62. DOI: <https://doi.org/10.1016/j.autneu.2016.02.002>.
112. Ioannou LG, Tsoutsoubi L, Nybo L, Tsianos GI, Flouris AD. Habitual heat exposure and acclimatization associated with athletic performance in the multistage marathon des sables. *Journal of Human Performance in Extreme Environments* 2018;14(1):9. DOI: 10.7771/2327-2937.1107.
113. Radakovic SS, Maric J, Surbatovic M, et al. Effects of Acclimation on Cognitive Performance in Soldiers during Exertional Heat Stress. *Military Medicine* 2007;172(2):133-136. DOI: 10.7205/milmed.172.2.133.
114. ISO 7243. Hot environments: estimation of the heat stress on working man, based on the WBGT-index (wet bulb globe temperature). 2nd ed. Geneva, Switzerland: International Organization for Standardization, 1989.
115. Flouris AD, McGinn R, Poirier MP, et al. Screening criteria for increased susceptibility to heat stress during work or leisure in hot environments in healthy individuals aged 31–70 years. *Temperature* 2018;5(1):86-99. DOI: 10.1080/23328940.2017.1381800.
116. Carrillo AE, Flouris AD, Herry CL, et al. Age-related reductions in heart rate variability do not worsen during exposure to humid compared to dry heat: A secondary analysis. *Temperature* 2019;6(4):341-345. DOI: 10.1080/23328940.2019.1684791.
117. Notley SR, Poirier MP, Hardcastle SG, et al. Aging Impairs Whole-Body Heat Loss in Women under Both Dry and Humid Heat Stress. *Medicine and science in sports and exercise* 2017;49(11):2324-2332. (In eng). DOI: 10.1249/mss.0000000000001342.
118. Stapleton JM, Poirier MP, Flouris AD, et al. Aging impairs heat loss, but when does it matter? *Journal of Applied Physiology* 2015;118(3):299-309. DOI: 10.1152/jappphysiol.00722.2014.
119. Meade RD, Notley SR, Kenny GP. Aging and human heat dissipation during exercise-heat stress: an update and future directions. *Current Opinion in Physiology* 2019;10:219-225. DOI: <https://doi.org/10.1016/j.cophys.2019.07.003>.
120. ISO 7933. Ergonomics of the Thermal Environment - Analytical Determination and Interpretation of Heat Stress Using Calculation of the Predicted Heat Strain. Geneva, Switzerland 2004.
121. Havenith G. Clothing and thermoregulation. *Textiles and the Skin Curr Probl Dermatol Basel, Karger* 2003;31:35-49.

122. Mäkinen H. 17 - Firefighters' protective clothing. In: Horrocks AR, Price D, eds. *Advances in Fire Retardant Materials*: Woodhead Publishing; 2008:467-491.
123. Bishop P, Ray P, Reneau P. A review of the ergonomics of work in the US military chemical protective clothing. *International Journal of Industrial Ergonomics* 1995;15(4):271-283. DOI: [https://doi.org/10.1016/0169-8141\(94\)00041-Z](https://doi.org/10.1016/0169-8141(94)00041-Z).
124. Havenith G, Fiala D, Błazejczyk K, et al. The UTCI-clothing model. *International Journal of Biometeorology* 2012;56(3):461-470. DOI: 10.1007/s00484-011-0451-4.
125. Błazejczyk K. New indices to assess thermal risks outdoors. *Proceedings of 11th International Conferences on Environmental Ergonomics, May2005*:22-26.
126. ACGIH. 2012 TLVs and BEIs—based on the documentation of the threshold limit values for chemical substances and physical agents & biological exposure indices. American Conference of Governmental Industrial Hygienists Cincinnati, OH; 2012.
127. Shkolnik A, Taylor CR, Finch V, Borut A. Why do Bedouins wear black robes in hot deserts? *Nature* 1980;283(5745):373-375. DOI: 10.1038/283373a0.
128. Luetkemeier MJ, Allen DR, Huang M, et al. Skin tattooing impairs sweating during passive whole body heating. *Journal of Applied Physiology* 2020;129(5):1033-1038. DOI: 10.1152/jappphysiol.00427.2019.
129. Manjunath G, Aravindhakshan R, Varghese S. Effect of fasting during Ramadan on thermal stress parameters. *East Mediterr Health J* 2019;25(1):34-39. (In eng). DOI: 10.26719/emhj.18.013.
130. Havenith G. Interaction of clothing and thermoregulation. *Exogenous Dermatology* 2002;1(5):221-230.
131. Kluger N. Epidemiology of tattoos in industrialized countries. *Curr Probl Dermatol* 2015;48:6-20. (In eng). DOI: 10.1159/000369175.
132. Westerterp KR. Diet induced thermogenesis. *Nutrition & Metabolism* 2004;1(1):5. DOI: 10.1186/1743-7075-1-5.
133. Piil JF, Lundbye-Jensen J, Christiansen L, et al. High prevalence of hypohydration in occupations with heat stress—Perspectives for performance in combined cognitive and motor tasks. *PLOS ONE* 2018;13(10):e0205321. DOI: 10.1371/journal.pone.0205321.
134. Sawka MN, Montain SJ, Latzka WA. Hydration effects on thermoregulation and performance in the heat. *Comparative Biochemistry and Physiology Part A: Molecular & Integrative Physiology* 2001;128(4):679-690. DOI: [https://doi.org/10.1016/S1095-6433\(01\)00274-4](https://doi.org/10.1016/S1095-6433(01)00274-4).
135. Brucker DL, Houtenville AJ. People With Disabilities in the United States. *Archives of Physical Medicine and Rehabilitation* 2015;96(5):771-774. DOI: <https://doi.org/10.1016/j.apmr.2015.02.024>.
136. Vornholt K, Uitdewilligen S, Nijhuis FJ. Factors affecting the acceptance of people with disabilities at work: a literature review. *J Occup Rehabil* 2013;23(4):463-75. (In eng). DOI: 10.1007/s10926-013-9426-0.
137. Price MJ, Trbovich M. Chapter 50 - Thermoregulation following spinal cord injury. In: Romanovsky AA, ed. *Handbook of Clinical Neurology*: Elsevier; 2018:799-820.
138. Webb LH, Parsons KC. Case studies of thermal comfort for people with physical disabilities. *Transactions-American Society of Heating Refrigerating and Air Conditioning Engineers* 1998;104:883-895.
139. Cuddy ML. The effects of drugs on thermoregulation. *AACN Clin Issues* 2004;15(2):238-53. (In eng). DOI: 10.1097/00044067-200404000-00010.
140. Hari Shanker S, Per-Ove S, Syed FA. Drugs of Abuse-Induced Hyperthermia, Blood-Brain Barrier Dysfunction and Neurotoxicity: Neuroprotective Effects of a New

- Antioxidant Compound H-290/51. *Current Pharmaceutical Design* 2007;13(18):1903-1923. DOI: <http://dx.doi.org/10.2174/138161207780858375>.
141. Lomax P, Schönbaum E. The effects of drugs on thermoregulation during exposure to hot environments. *Prog Brain Res* 1998;115:193-204. (In eng). DOI: 10.1016/s0079-6123(08)62037-3.
142. Crandall CG, Vongpatanasin WV, Ronald G. Mechanism of Cocaine-Induced Hyperthermia in Humans. *Annals of Internal Medicine* 2002;136(11):785-791. DOI: 10.7326/0003-4819-136-11-200206040-00006 %m 12044126.
143. Smith RB, Wright G. Anesthesia and methadone maintenance: case reports. *Anesth Prog* 1972;19(3):80-81. (In eng) (<https://pubmed.ncbi.nlm.nih.gov/4502985> <https://www.ncbi.nlm.nih.gov/pmc/articles/PMC2515655/>).
144. Al-Adwani A, Basu N. Methadone and excessive sweating. *Addiction* 2004;99(2):259-264. DOI: 10.1046/j.1360-0443.2004.00637.x.
145. Yaglou C, Minaed D. Control of heat casualties at military training centers. *Arch Indust Health* 1957;16(4):302-16.
146. DiPasquale DM, Kolkhorst FW, Buono MJ. Acute Normobaric Hypoxia Reduces Body Temperature in Humans. *High Altitude Medicine & Biology* 2015;16(1):61-66. DOI: 10.1089/ham.2014.1098.
147. Stahn AC, Werner A, Opatz O, et al. Increased core body temperature in astronauts during long-duration space missions. *Scientific Reports* 2017;7(1):16180. DOI: 10.1038/s41598-017-15560-w.
148. Daanen HAM, Van Marken Lichtenbelt WD. Human whole body cold adaptation. *Temperature* 2016;3(1):104-118. DOI: 10.1080/23328940.2015.1135688.
149. Raj SM, Pagani L, Gallego Romero I, Kivisild T, Amos W. A general linear model-based approach for inferring selection to climate. *BMC Genet* 2013;14:87. (In eng). DOI: 10.1186/1471-2156-14-87.
150. Montagna W, Carlisle K. The architecture of black and white facial skin. *Journal of the American Academy of Dermatology* 1991;24(6):929-937. DOI: 10.1016/0190-9622(91)70148-U.
151. Havenith G, Griggs K, Qiu Y, Dorman L, Kulasekaran V, Hodder S. Higher comfort temperature preferences for anthropometrically matched Chinese and Japanese versus white-western-middle-European individuals using a personal comfort / cooling system. *Building and Environment* 2020;183:107162. DOI: <https://doi.org/10.1016/j.buildenv.2020.107162>.
152. Morris NB, Jay O, Flouris AD, et al. Sustainable solutions to mitigate occupational heat strain – an umbrella review of physiological effects and global health perspectives. *Environmental Health* 2020;19(1):95. DOI: 10.1186/s12940-020-00641-7.
153. World Health Organization. Cardiovascular diseases (CVDs). May 17th, 2017 (<https://www.who.int/news-room/fact-sheets/detail/cardiovascular-diseases-cvds>).
154. International Diabetes Federation. *IDF diabetes atlas*. 9th ed 2019.
155. Moghadamnia MT, Ardalan A, Mesdaghinia A, Keshtkar A, Naddafi K, Yekaninejad MS. Ambient temperature and cardiovascular mortality: a systematic review and meta-analysis. *PeerJ* 2017;5:e3574. DOI: <https://doi.org/10.7717/peerj.3574>.
156. Ioannou LG, Tsoutsoubi L, Amorim T, Samoutis G, Flouris AD. Links between Night-Time Thermoneutral Zone and Mortality from Circulatory Causes in the Elderly Population of Cyprus. *Geriatric Medicine and Gerontology* 2018;4(1). DOI: doi.org/10.23937/2469-5858/1510040.

157. Cai H, Harrison DG. Endothelial Dysfunction in Cardiovascular Diseases: The Role of Oxidant Stress. *Circulation Research* 2000;87(10):840-844. DOI: doi:10.1161/01.RES.87.10.840.
158. Stansberry KB, Shapiro SA, Hill MA, McNitt PM, Meyer MD, Vinik AI. Impaired Peripheral Vasomotion in Diabetes. *Diabetes Care* 1996;19(7):715-721. DOI: 10.2337/diacare.19.7.715.
159. Flouris AD, Schlader ZJ. Human behavioral thermoregulation during exercise in the heat. *Scandinavian Journal of Medicine & Science in Sports* 2015;25(S1):52-64. DOI: <https://doi.org/10.1111/sms.12349>.
160. Fiala D. Dynamic simulation of human heat transfer and thermal comfort. De Montfort University Leicester, UK; 1998.
161. Ioannou LG, Tsoutsoubi L, Samoutis G, et al. Time-motion analysis as a novel approach for evaluating the impact of environmental heat exposure on labor loss in agriculture workers. *Temperature (Austin)* 2017;4(3):330-340. (In eng). DOI: 10.1080/23328940.2017.1338210.
162. Mora-Rodriguez R. Influence of Aerobic Fitness on Thermoregulation During Exercise in the Heat. *Exercise and Sport Sciences Reviews* 2012;40(2):79-87. DOI: 10.1097/JES.0b013e318246ee56.
163. World Health Organization. How to make policies more gender-sensitive. Gender, women, and the tobacco epidemic. Geneva 2010.
164. Kaciuba-Uscilko H, Gruzca R. Gender differences in thermoregulation. *Current Opinion in Clinical Nutrition & Metabolic Care* 2001;4(6) (https://journals.lww.com/co-clinicalnutrition/Fulltext/2001/11000/Gender_differences_in_thermoregulation.12.aspx).
165. Boivin DB, Boudreau P. Impacts of shift work on sleep and circadian rhythms. *Pathologie Biologie* 2014;62(5):292-301. DOI: <https://doi.org/10.1016/j.patbio.2014.08.001>.
166. Dzeng R-J, Wang S-H, Fang Y-C. Quantitative evaluation of the impact of night shifts and alcohol consumption on construction tiling quality. *Applied Ergonomics* 2015;50:226-236. DOI: <https://doi.org/10.1016/j.apergo.2015.03.008>.
167. Jun DH, El-Rayes K. Optimizing the utilization of multiple labor shifts in construction projects. *Automation in Construction* 2010;19(2):109-119. DOI: <https://doi.org/10.1016/j.autcon.2009.12.015>.
168. Arditi D, Lee D-E, Polat G. Fatal accidents in nighttime vs. daytime highway construction work zones. *Journal of Safety Research* 2007;38(4):399-405. DOI: <https://doi.org/10.1016/j.jsr.2007.04.001>.
169. Bohle P, Pitts C, Quinlan M. Time to call it quits? The safety and health of older workers. *Int J Health Serv* 2010;40(1):23-41. (In eng). DOI: 10.2190/HS.40.1.b.
170. Lim J, Dinges DF. A meta-analysis of the impact of short-term sleep deprivation on cognitive variables. *Psychol Bull* 2010;136(3):375-389. (In eng). DOI: 10.1037/a0018883.
171. Wagstaff AS, Lie J-AS. Shift and night work and long working hours - a systematic review of safety implications. *Scandinavian Journal of Work, Environment & Health* 2011;37(3):173-185. (<http://www.jstor.org/stable/41151541>).
172. Raslear TG, Hursh SR, Van Dongen HP. Predicting cognitive impairment and accident risk. *Prog Brain Res* 2011;190:155-67. (In eng). DOI: 10.1016/b978-0-444-53817-8.00010-4.

173. d'Errico A, Costa G. Socio-demographic and work-related risk factors for medium- and long-term sickness absence among Italian workers. *Eur J Public Health* 2012;22(5):683-8. (In eng). DOI: 10.1093/eurpub/ckr140.
174. Zhou X, Ferguson SA, Matthews RW, et al. Mismatch between subjective alertness and objective performance under sleep restriction is greatest during the biological night. *J Sleep Res* 2012;21(1):40-9. (In eng). DOI: 10.1111/j.1365-2869.2011.00924.x.
175. David B, Robert A, Edmund R, Brian B. Occupational heat illness in Washington State, 1995–2005. *American Journal of Industrial Medicine* 2007;50(12):940-950. DOI: doi:10.1002/ajim.20517.
176. M. GD, Brooke AG, L. HK. Characterizing occupational heat-related mortality in the United States, 2000–2010: An analysis using the census of fatal occupational injuries database. *American Journal of Industrial Medicine* 2015;58(2):203-211. DOI: doi:10.1002/ajim.22381.
177. Nybo L, Kjellstrom T, Bogataj LK, Flouris AD. Global heating: Attention is not enough; we need acute and appropriate actions. *Temperature* 2017;4(3):199-201. DOI: 10.1080/23328940.2017.1338930.
178. Feeling the heat. *Nature Climate Change* 2018;8(5):347-347. DOI: 10.1038/s41558-018-0169-y.
179. Oja P, Titze S, Bauman A, et al. Health benefits of cycling: a systematic review. *Scandinavian journal of medicine & science in sports* 2011;21(4):496-509.
180. Zentner J, Franken H, Löbbecke G. Head injuries from bicycle accidents. *Clinical neurology and neurosurgery* 1996;98(4):281-285.
181. Elvik R. Publication bias and time-trend bias in meta-analysis of bicycle helmet efficacy: a re-analysis of Attewell, Glase and McFadden, 2001. *Accident Analysis & Prevention* 2011;43(3):1245-1251.
182. Shinar D, Bogerd C, Chliaoutakis J, et al. Final report of Working Group 2: Traffic psychology. COST Action TU1101/HOPE. 2015.
183. Finnoff JT, Laskowski ER, Altman KL, Diehl NN. Barriers to bicycle helmet use. *Pediatrics* 2001;108(1):e4-e4.
184. Bogerd CP, Aerts J-M, Annaheim S, et al. A review on ergonomics of headgear: Thermal effects. *International journal of industrial ergonomics* 2015;45:1-12.
185. Underwood L, Vircondelet C, Jermy M. Thermal comfort and drag of a streamlined cycling helmet as a function of ventilation hole placement. *Proceedings of the Institution of Mechanical Engineers, Part P: Journal of Sports Engineering and Technology* 2018;232(1):15-21.
186. Mayor T, Couto S, Psikuta A, Rossi RM. Advanced modelling of the transport phenomena across horizontal clothing microclimates with natural convection. *International journal of biometeorology* 2015;59:1875-1889.
187. ASHRAE A. ASHRAE standard 55–2010; Thermal Environmental Conditions for Human Occupancy. American Society of Heating, Refrigerating, and Airconditioning Engineers, Inc: Atlanta, GA, USA 2010.
188. Gagge AP, Stolwijk J, Hardy J. Comfort and thermal sensations and associated physiological responses at various ambient temperatures. *Environmental research* 1967;1(1):1-20.
189. Kenneth C, Parsons C. *Human Thermal Environments: The Effects of Hot, Moderate, and Cold Environments on Human Health, Comfort, and Performance*. CRC Press: Boca Raton, FL, USA; 2014.
190. Fanger PO. *Thermal comfort. Analysis and applications in environmental engineering. Thermal comfort Analysis and applications in environmental engineering* 1970.

191. Enescu D. Models and indicators to assess thermal sensation under steady-state and transient conditions. *Energies* 2019;12(5):841.
192. Koelblen B, Psikuta A, Bogdan A, Annaheim S, Rossi R. Thermal sensation models: a systematic comparison. *Indoor Air* 2017;27(3):680-689.
193. Rugh JP, Farrington RB, Bharathan D, et al. Predicting human thermal comfort in a transient nonuniform thermal environment. *European journal of applied physiology* 2004;92:721-727.
194. Havenith G, Fiala D. Thermal indices and thermophysiological modeling for heat stress. *Comprehensive Physiology* 2011;6(1):255-302.
195. Youssef A, Truyen P, Brode P, Fiala D, Aerts J-M. Towards Real-Time Model-Based Monitoring and Adoptive Controlling of Indoor Thermal Comfort. *Proceedings of the Ventilating Healthy Low-Energy Buildings, Nottingham, UK 2017*:13-14.
196. De Bruyne G, Aerts J-M, Vander Sloten J, Goffin J, Verpoest I, Berckmans D. Quantification of local ventilation efficiency under bicycle helmets. *International journal of industrial ergonomics* 2012;42(3):278-286.
197. Tanner R, Gore C. *Physiological tests for elite athletes: Human kinetics*, 2012.
198. Billat VL, Sirvent P, Py G, Koralsztein J-P, Mercier J. The concept of maximal lactate steady state: a bridge between biochemistry, physiology and sport science. *Sports medicine* 2003;33:407-426.
199. Beneke R. Methodological aspects of maximal lactate steady state—implications for performance testing. *European journal of applied physiology* 2003;89:95-99.
200. Sibernagl S. *Atlas van de Fysiologie*. SESAM/HBuitgevers: Baarn, The Netherlands 2008.
201. Fitts RH. Cellular mechanisms of muscle fatigue. *Physiological reviews* 1994;74(1):49-94.
202. Mukunthan S, Vleugels J, Huysmans T, De Bruyne G. Latent heat loss of a virtual thermal manikin for evaluating the thermal performance of bicycle helmets. *Advances in Human Factors in Simulation and Modeling: Proceedings of the AHFE 2018 International Conferences on Human Factors and Simulation and Digital Human Modeling and Applied Optimization, Held on July 21–25, 2018, in Loews Sapphire Falls Resort at Universal Studios, Orlando, Florida, USA 9*: Springer; 2019:66-78.
203. Soong TT. *Fundamentals of probability and statistics for engineers*: John Wiley & Sons, 2004.
204. Borg GA. Psychophysical bases of perceived exertion. *Medicine & science in sports & exercise* 1982.
205. Box GE, Draper NR. *Empirical model-building and response surfaces*: John Wiley & Sons, 1987.
206. Institute S. *JMP 11 Profilers*: SAS Institute, 2013.
207. Zinoubi B, Zbidi S, Vandewalle H, Chamari K, Driss T. Relationships between rating of perceived exertion, heart rate and blood lactate during continuous and alternated-intensity cycling exercises. *Biology of sport* 2018;35(1):29-37.
208. Fiala D, Lomas KJ, Stohrer M. First principles modeling of thermal sensation responses in steady-state and transient conditions. *ASHRAE transactions* 2003;109:179.
209. Guan YD, Hosni MH, Jones BW, Giolda TP. Investigation of human thermal comfort under highly transient conditions for automotive applications-Part 2: Thermal sensation modeling. *Ashrae Transactions* 2003;109:898.
210. Guan YD, Hosni MH, Jones BW, Giolda TP. Investigation of human thermal comfort under highly transient conditions for automotive applications-Part 1: Experimental design and human subject testing implementation. *Ashrae Transactions* 2003;109:885.

211. Kingma B, Schellen L, Frijns A, van Marken Lichtenbelt W. Thermal sensation: a mathematical model based on neurophysiology. *Indoor air* 2012;22(3):253-262.
212. Nilsson HO. Comfort climate evaluation with thermal manikin methods and computer simulation models 2004.
213. Takada S, Matsumoto S, Matsushita T. Prediction of whole-body thermal sensation in the non-steady state based on skin temperature. *Building and Environment* 2013;68:123-133.
214. Zhang H. Human thermal sensation and comfort in transient and non-uniform thermal environments: University of California, Berkeley, 2003.
215. Lu S, Wang W, Wang S, Cochran Hameen E. Thermal comfort-based personalized models with non-intrusive sensing technique in office buildings. *Applied Sciences* 2019;9(9):1768.
216. De Dear R, Brager GS. Developing an adaptive model of thermal comfort and preference. 1998.
217. Kadlec P, Grbić R, Gabrys B. Review of adaptation mechanisms for data-driven soft sensors. *Computers & chemical engineering* 2011;35(1):1-24.
218. Sharma S, Khare S, Huang B. Robust online algorithm for adaptive linear regression parameter estimation and prediction. *Journal of Chemometrics* 2016;30(6):308-323.
219. Zimmer AM, Kurze M, Seidl T. Adaptive model tree for streaming data. 2013 IEEE 13th International Conference on Data Mining: IEEE; 2013:1319-1324.
220. Bouveyron C, Jacques J. Adaptive linear models for regression: improving prediction when population has changed. *Pattern Recognition Letters* 2010;31(14):2237-2247.
221. Jiang J, Zhang Y. A revisit to block and recursive least squares for parameter estimation. *Computers & Electrical Engineering* 2004;30(5):403-416.
222. Young PC. Recursive estimation and time-series analysis: An introduction for the student and practitioner: Springer Science & Business Media, 2011.
223. Benesty J, Paleologu C, Gänsler T, et al. Recursive least-squares algorithms. A perspective on stereophonic acoustic echo cancellation 2011:63-69.
224. Plackett RL. Some theorems in least squares. *Biometrika* 1950;37(1/2):149-157.
225. Johnson CR. Lectures on adaptive parameter estimation. Prentice Hall Advanced Reference Series 1988:160-163.
226. Vahidi A, Stefanopoulou A, Peng H. Recursive least squares with forgetting for online estimation of vehicle mass and road grade: theory and experiments. *Vehicle System Dynamics* 2005;43(1):31-55.
227. Huey RB, Carroll C, Salisbury R, Wang JL. Mountaineers on Mount Everest: Effects of age, sex, experience, and crowding on rates of success and death. *PLoS One* 2020;15(8):e0236919. DOI: 10.1371/journal.pone.0236919.
228. Maggiorini M, Bühler B, Walter M, Oelz O. Prevalence of acute mountain sickness in the Swiss Alps. *BMJ* 1990;301(6756):853-5. (In eng). DOI: 10.1136/bmj.301.6756.853.
229. Nemethy M, Pressman AB, Freer L, McIntosh SE. Mt Everest Base Camp Medical Clinic "Everest ER": epidemiology of medical events during the first 10 years of operation. *Wilderness Environ Med* 2015;26(1):4-10. DOI: 10.1016/j.wem.2014.07.011.
230. Firth PG, Zheng H, Windsor JS, et al. Mortality on Mount Everest, 1921-2006: descriptive study. *BMJ* 2008;337:a2654. DOI: 10.1136/bmj.a2654.
231. Windsor J, Firth P, Grocott M, Rodway GW, Montgomery H. Mountain mortality: a review of deaths that occur during recreational activities in the mountains. *Postgrad Med J* 2009;85(1004):316-321.
232. Huey RB, Eguskitza X. Limits to human performance: elevated risks on high mountains. *J Exp Biol* 2001;204(Pt 18):3115-9. (In eng).

233. de Aquino Lemos V, Antunes HK, dos Santos RV, Lira FS, Tufik S, de Mello MT. High altitude exposure impairs sleep patterns, mood, and cognitive functions. *Psychophysiology* 2012;49(9):1298-306. (In eng). DOI: 10.1111/j.1469-8986.2012.01411.x.
234. San T, Polat S, Cingi C, Eskiizmir G, Oghan F, Cakir B. Effects of high altitude on sleep and respiratory system and theirs adaptations. *Scientif World J* 2013;2013:241569. DOI: 10.1155/2013/241569.
235. Porcelli MJ, Gugelchuk GM. A trek to the top: a review of acute mountain sickness. *J Am Osteopath Assoc* 1995;95(12):718-20. (In eng).
236. Hainsworth R, Drinkhill MJ, Rivera-Chira M. The autonomic nervous system at high altitude. *Clin Auton Res* 2007;17(1):13-9. DOI: 10.1007/s10286-006-0395-7.
237. Zuzewicz K, Biernat B, Kempa G, Kwarecki K. Heart rate variability in exposure to high altitude hypoxia of short duration. *Int J Occup Saf Ergon* 1999;5(3):337-46. DOI: 10.1080/10803548.1999.11076424.
238. Heart rate variability: standards of measurement, physiological interpretation and clinical use. Task Force of the European Society of Cardiology and the North American Society of Pacing and Electrophysiology. *Circulation* 1996;93(5):1043-65. (In eng).
239. Jackowska M, Dockray S, Endrighi R, Hendrickx H, Steptoe A. Sleep problems and heart rate variability over the working day. *J Sleep Res* 2012;21(4):434-40. DOI: 10.1111/j.1365-2869.2012.00996.x.
240. Meerlo P, Sgoifo A, Suchecki D. Restricted and disrupted sleep: effects on autonomic function, neuroendocrine stress systems and stress responsivity. *Sleep Med Rev* 2008;12(3):197-210. DOI: 10.1016/j.smrv.2007.07.007.
241. Chamorro R, Algarin C, Rojas O, et al. Night-time cardiac autonomic modulation as a function of sleep-wake stages is modified in otherwise healthy overweight adolescents. *Sleep Med* 2019;64:30-36. DOI: 10.1016/j.sleep.2019.06.008.
242. Insalaco G, Salvaggio A, Pomidori L, Cogo A, Romano S. Heart rate variability during sleep at high altitude: effect of periodic breathing. *Sleep Breath* 2016;20(1):197-204. DOI: 10.1007/s11325-015-1205-z.
243. Brown JP, Grocott MP. Humans at altitude: physiology and pathophysiology. *Cont Ed Anesth Crit Care Pain* 2012;13(1):17-22. DOI: 10.1093/bjaceaccp/mks047.
244. Magalhães J, Ascensão A, Viscor G, et al. Oxidative stress in humans during and after 4 hours of hypoxia at a simulated altitude of 5500 m. *Aviat Space Environ Med* 2004;75(1):16-22. (In eng).
245. Di Rienzo M, Castiglioni P, Rizzo F, et al. Linear and fractal heart rate dynamics during sleep at high altitude. Investigation with textile technology. *Methods Inf Med* 2010;49(5):521-5. DOI: 10.3414/ME09-02-0053.
246. Flouris AD, Poirier MP, Bravi A, et al. Changes in heart rate variability during the induction and decay of heat acclimation. *Eur J Appl Physiol* 2014;114(10):2119-28. DOI: 10.1007/s00421-014-2935-5.
247. Kaltsatou A, Flouris AD, Herry CL, et al. Heart rate variability in older workers during work under the Threshold Limit Values for heat exposure. *Am J Ind Med* 2020;63(9):787-795. DOI: 10.1002/ajim.23156.
248. Hoddes E, Zarcone V, Dement W. Stanford sleepiness scale. *Enzyklopädie der Schlafmedizin* 1972;1184(1).
249. Karinen HM, Uusitalo A, Vaha-Ypya H, et al. Heart rate variability changes at 2400 m altitude predicts acute mountain sickness on further ascent at 3000-4300 m altitudes. *Front Physiol* 2012;3:336. DOI: 10.3389/fphys.2012.00336.
250. Calbet JA, Lundby C. Air to muscle O₂ delivery during exercise at altitude. *High Alt Med Biol* 2009;10(2):123-34. DOI: 10.1089/ham.2008.1099.

251. Piil JF, Lundbye-Jensen J, Christiansen L, et al. High prevalence of hypohydration in occupations with heat stress-Perspectives for performance in combined cognitive and motor tasks. *PLoS One* 2018;13(10):e0205321. DOI: 10.1371/journal.pone.0205321.
252. Cushman DM, Markert M, Rho M. Performance trends in large 10-km road running races in the United States. *J Strength Cond Res* 2014;28(4):892-901. DOI: 10.1519/JSC.0000000000000249.
253. El Helou N, Tafflet M, Berthelot G, et al. Impact of environmental parameters on marathon running performance. *PLoS One* 2012;7(5):e37407. DOI: 10.1371/journal.pone.0037407.
254. Thorsson S, Rayner D, Palm G, et al. Is Physiological Equivalent Temperature (PET) a superior screening tool for heat stress risk than Wet-Bulb Globe Temperature (WBGT) index? Eight years of data from the Gothenburg half marathon. *Br J Sports Med* 2021;55(15):825-830. DOI: 10.1136/bjsports-2019-100632.
255. Misailidi M, Mantzios K, Papakonstantinou C, Ioannou LG, Flouris AD. Environmental and Psychophysical Heat Stress in Adolescent Tennis Athletes. *Int J Sports Physiol Perform* 2021;16(12):1895-1900. DOI: 10.1123/ijsp.2020-0820.
256. Vihma T. Effects of weather on the performance of marathon runners. *Int J Biometeorol* 2010;54(3):297-306. DOI: 10.1007/s00484-009-0280-x.
257. Ioannou LG, Tsoutsoubi L, Samoutis G, et al. Time-motion analysis as a novel approach for evaluating the impact of environmental heat exposure on labor loss in agriculture workers. *Temperature* 2017;4:1-11.
258. ELY BR, CHEUVRONT SN, KENEFICK RW, SAWKA MN. Aerobic Performance Is Degraded, Despite Modest Hyperthermia, in Hot Environments. *Medicine & Science in Sports & Exercise* 2010;42(1):135-141. DOI: 10.1249/MSS.0b013e3181adb9fb.
259. Allnutt MF, Allan JR. The effects of core temperature elevation and thermal sensation on performance. *Ergonomics* 1973;16 2:189-96.
260. Eggenberger P, MacRae BA, Kemp S, Burgisser M, Rossi RM, Annaheim S. Prediction of Core Body Temperature Based on Skin Temperature, Heat Flux, and Heart Rate Under Different Exercise and Clothing Conditions in the Heat in Young Adult Males. *Front Physiol* 2018;9:1780. DOI: 10.3389/fphys.2018.01780.
261. Nybo L, Rasmussen P, Sawka MN. Performance in the heat-physiological factors of importance for hyperthermia-induced fatigue. *Compr Physiol* 2014;4(2):657-89. DOI: 10.1002/cphy.c130012.
262. Periard JD, Racinais S, Sawka MN. Adaptations and mechanisms of human heat acclimation: Applications for competitive athletes and sports. *Scand J Med Sci Sports* 2015;25 Suppl 1:20-38. DOI: 10.1111/sms.12408.
263. American College of Sports M, Sawka MN, Burke LM, et al. American College of Sports Medicine position stand. Exercise and fluid replacement. *Med Sci Sports Exerc* 2007;39(2):377-90. DOI: 10.1249/mss.0b013e31802ca597.
264. Tyler CJ, Reeve T, Hodges GJ, Cheung SS. The Effects of Heat Adaptation on Physiology, Perception and Exercise Performance in the Heat: A Meta-Analysis. *Sports Med* 2016;46(11):1699-1724. DOI: 10.1007/s40279-016-0538-5.
265. ISO 7726. Ergonomics of the thermal environment - Instruments for measuring physical quantities. International Standard; 1998.
266. ISO 7730. Moderate thermal environments - Determination of the PMV and PPD indices and specification of the conditions for thermal comfort. International Standard; 1994.
267. National Weather Service. Vapor Pressure. (<https://www.weather.gov/media/epz/wxcalc/vaporPressure.pdf>).

268. Bland JM, Altman DG. Statistics Notes: Validating scales and indexes. *BMJ* 2002;324(7337):606-7. DOI: 10.1136/bmj.324.7337.606.
269. Glass S, Dwyer GB, Medicine ACoS. ACSM's metabolic calculations handbook: Lippincott Williams & Wilkins, 2007.

Appendixes

Appendix A: Detailed Visualization and Functional Description of the FL-WebPHS Software Components

Figure A.1 | Component based on ISO 7933:2018.

This figure showcases the user interface of the second component of the FL-WebPHS, which is built using the original ISO 7933:2018 algorithm. It emphasizes the structured data entry approach required for precise computations.

Predicted Heat Strain ISO:7933

ISO:7933 FAME LAB PHS

Exposure time minutes

Air temperature

Globe temperature

Humidity %

Air velocity

Metabolic rate W/m²

Mech. efficiency W/m²

Height

Weight

Clothing clo

Reflection coefficient -

Covered BSA %

Moving speed

THETA angle

Acclitmaization


Water consumption

Posture

Clear All Save Run simulation

Figure A.2 | Covered Body Surface Area.

This figure highlights the "Covered Body Surface Area" calculation feature. It uses a checkbox system representing various body areas that users can select to denote which areas are covered.



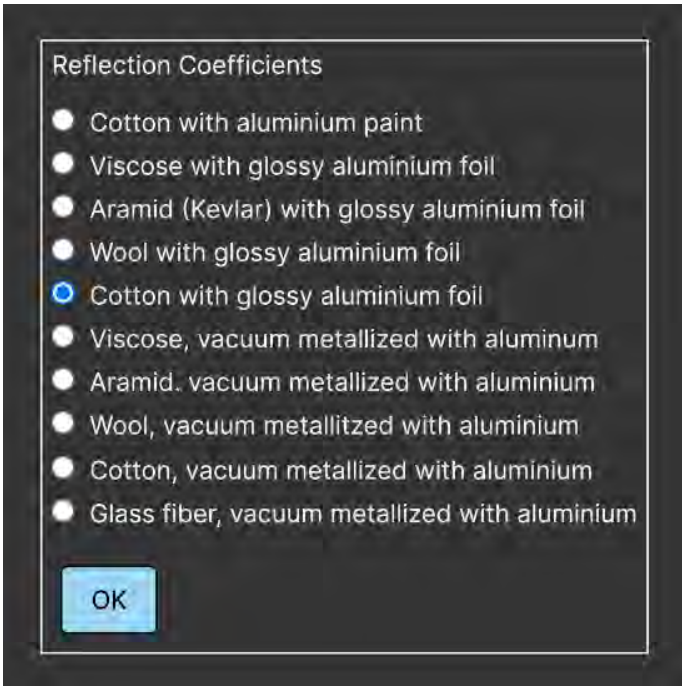
Covered Body Surface Area

- Head and face
- Thorax and abdomen
- Back
- Arms
- Hands
- Thigh
- Legs
- Feet

75.00 % OK

Figure A.3 | Reflection Coefficients.

This figure presents the selection process for reflection coefficients of clothing materials.



Reflection Coefficients

- Cotton with aluminium paint
- Viscose with glossy aluminium foil
- Aramid (Kevlar) with glossy aluminium foil
- Wool with glossy aluminium foil
- Cotton with glossy aluminium foil
- Viscose, vacuum metallized with aluminium
- Aramid, vacuum metallized with aluminium
- Wool, vacuum metallized with aluminium
- Cotton, vacuum metallized with aluminium
- Glass fiber, vacuum metallized with aluminium

OK

Figure A.4 | Clothing Insulation.

This figure presents the selection process for clothing insulation based on the American Society of Heating, Refrigerating and Air-Conditioning Engineers (ASHRAE) standards. It showcases the wide array of garment types, including shirts, sweaters, jackets, trousers, skirts, dresses, sleepwear, robes, and underwear, for which insulation calculations can be accurately made.

The screenshot shows a software window titled "ASHRAE: A Comprehensive Data Base for Estimating Clothing Insulation". At the top, there is a horizontal menu with tabs for "Shirts", "Sweaters", "Jackets", "Trousers", "Skirts", "Dresses", "Sleepwear", "Robes", and "Underwear". The "Trousers" tab is currently selected. Below the menu, there is a list of clothing items, each with a checkbox:

- Straight, long, fitted (denim)
- Straight, long, Htted (tweed)
- Straight, long, loose (denim)
- Straight, long, loose (tweed)
- Walking shorts(denim)
- Walking shorts (tweed)
- Short shorts (denim)
- Sweat pants (fleece-backed knit)
- Work pants (duck)
- Overalls (denim)
- Coveralls (gabardine)
- Insulated coveralls (multicomponent)

At the bottom left, there is a text input field containing the value "0.40". To its right is a dropdown menu showing "clo" with a downward arrow. At the bottom right, there is a blue "OK" button.

Figure A.5 | Metabolic Rate.

This figure presents the feature that calculates metabolic rate, leveraging the Compendium of Physical Activities. The Compendium presents all activities in metabolic equivalents, which we convert to W/m^2 by multiplying by 58.15, as described in ISO 7730:1994²⁶⁶.

Compendium of Physical Activities

Select your activity

Activity: 1020 - bicycling METS: 6.8 Metabolic Rate: 395.4 W/m^2

CODE	METS	MAJOR BRADING	SPECIFIC ACTIVITIES
1003	14	bicycling	bicycling, mountain, uphill, vigorous
1004	16	bicycling	bicycling, mountain, competitive, racing
1008	8.5	bicycling	bicycling, BMX
1009	8.5	bicycling	bicycling, mountain, general
1010	4	bicycling	bicycling,
1011	6.8	bicycling	bicycling, to/from work, self selected pace
1013	5.8	bicycling	bicycling, on dirt or farm road, moderate pace
1015	7.5	bicycling	bicycling, general
1018	3.5	bicycling	bicycling, leisure, 5.5 mph
1019	5.8	bicycling	bicycling, leisure, 9.4 mph
1020	6.8	bicycling	bicycling, 10-11.9 mph, leisure, slow, light effort
1030	8	bicycling	bicycling, 12-13.9 mph, leisure, moderate effort
1040	10	bicycling	bicycling, 14-15.9 mph, racing or leisure, fast, vigorous effort
1050	12	bicycling	bicycling, 16-19 mph, racing/not drafting or > 19 mph drafting, very fast, racing general
1060	15.8	bicycling	bicycling, > 20 mph, racing, not drafting
1065	8.5	bicycling	bicycling, 12 mph, seated, hands on brake hoods or bar drops, 80 rpm
1066	9	bicycling	bicycling, 12 mph, standing, hands on brake hoods, 80 rpm

Figure A.6 | FL-WebPHS Results.

This figure displays the results obtained from the modified PHS_{FL} algorithm. It includes four charts predicting rectal temperature, core temperature, skin temperature, and total sweat rate, with both initial and final values.



Figure A.7 | Raw data table.

This figure presents a detailed, minute-by-minute table of the data derived from the first component of the software. It provides a comprehensive view of the user's physiological parameters over time.

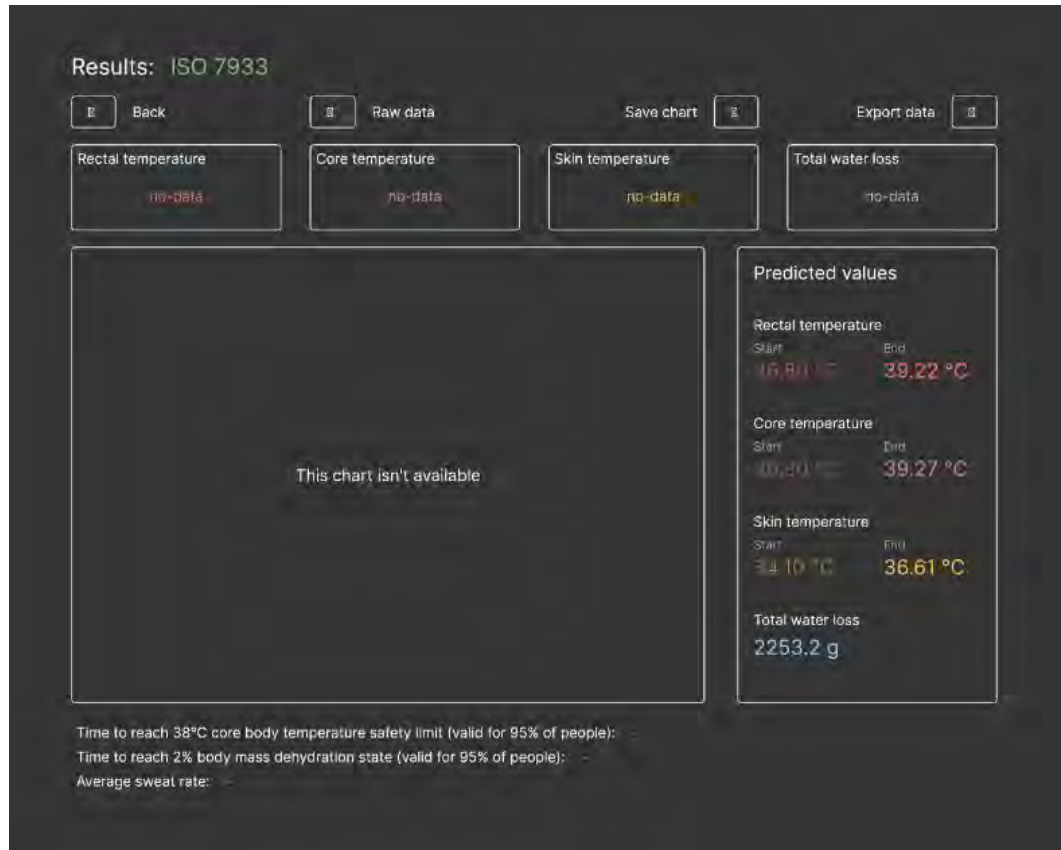
Results: FAME Lab PHS

Back Charts Save chart Export data

Duration (min)	Rectal temperature (°C)	Core temperature (°C)	Skin temperature (°C)	Total water loss (g)
1	36.80	36.74	34.99	1.10
2	36.81	36.82	34.99	2.68
3	36.84	36.90	34.99	4.74
4	36.88	36.97	35.00	7.27
5	36.92	37.03	35.01	10.29
6	36.97	37.09	35.02	13.77
7	37.02	37.14	35.04	17.73
8	37.07	37.19	35.06	22.15
9	37.12	37.24	35.08	27.01
10	37.17	37.28	35.11	32.32
11	37.21	37.32	35.13	38.06
12	37.25	37.35	35.16	44.22
13	37.30	37.39	35.18	50.78
14	37.33	37.42	35.21	57.73
15	37.37	37.44	35.23	65.06
16	37.40	37.47	35.25	72.75
17	37.44	37.49	35.28	80.78
18	37.47	37.51	35.30	89.15
19	37.49	37.53	35.32	97.82
20	37.52	37.55	35.33	106.80
21	37.54	37.57	35.35	116.06
22	37.56	37.58	35.37	125.59
23	37.58	37.60	35.38	135.38
24	37.60	37.61	35.40	145.40

Figure A.8 | ISO 7933:2018 Results.

This figure shows the results generated by the second component of the software, using the ISO 7933:2018¹²⁰ standard algorithm. It provides the initial and final predicted values, offering valuable insights despite its less detailed approach.



Appendix B: Effects of weather parameters on endurance running performance: discipline specific analysis of 1258 races

Table B1 | Official websites of each competition.

Official websites of each competition for which results for the marathon, 50km race-walk, 20km race-walk, 10,000m, 5,000m and 3,000m-steeplechase were obtained from.

Competition	Website
1. Olympic Games	www.worldathletics.org/competitions/olympic-games www.olympic.org/athletics
2. World Championships	www.worldathletics.org/competitions/world-athletics-championships
3. World Athletics Continental Cup	www.worldathletics.org/competitions/world-athletics-continental-cup
4. Commonwealth Games	www.worldathletics.org/results/commonwealth-games
5. Diamond Leagues	www.worldathletics.org/competitions/diamond-league
6. World Athletics Race Walking Team Championships	www.worldathletics.org/competitions/world-athletics-race-walking-team-championshi
7. World Athletics Gold Label Races	www.worldathletics.org/competitions/world-athletics-label-road-races
o TCS Amsterdam Marathon	www.tcsamsterdammarathon.nl/
o Athens Marathon The Authentic	www.athensauthenticmarathon.gr/site/index.php/en/
o CFLD Beijing Marathon	www.beijing-marathon.com/en/guicheng.html
o BMW Berlin-Marathon	www.bmw-berlin-marathon.com/en/
o B.A.A. Boston Marathon	www.baa.org/
o Bank of America Chicago Marathon	www.chicagomarathon.com/
o KBC Dublin Marathon	www.kbcdublinmarathon.ie/
o Fukuoka International Open Marathon	www.fukuoka-marathon.com/en/
o Gold Coast Marathon	www.goldcoastmarathon.com.au/
o Standard Chartered Hong Kong Marathon	www.hkmarathon.com/
o Jerusalem Marathon	www.jerusalem-marathon.com/en/home-page/
o Virgin Money London Marathon	www.virginmoneylondonmarathon.com/
o Maratón Ciudad de México	www.maraton.cdmx.gob.mx/
o Tata Mumbai Marathon	www.tatamumbaiarathon.procam.in/
o TCS New York City Marathon	www.nyrr.org/tcsnycmarathon
o Lake Biwa Mainichi Marathon	www.lakebiwa-marathon.com/indexe.html
o Scotiabank Ottawa Marathon	www.runottawa.ca/races-and-events/scotiabank-ottawa-marathon
o Schneider Electric Marathon de Paris	www.schneiderelectricparismarathon.com/en
o Philadelphia Marathon Weekend	www.philadelphiamarathon.com/
o NN Marathon Rotterdam	www.nnmarathonrotterdam.org/
o Seoul Marathon	www.seoul-marathon.com/eng/index.php

○ Shanghai International Marathon	www.shang-ma.com/#/dashboard
○ Blackmores Sydney Marathon	www.sydneyrunningfestival.com.au/
○ Tokyo Marathon	www.marathon.tokyo/en/
○ Scotiabank Toronto Waterfront Marathon	www.torontowaterfrontmarathon.com/
○ Maratón Valencia Trinidad Alfonso EDP	www.valenciaciudadelrunning.com/en/marathon/
○ Vienna City Marathon	www.vienna-marathon.com/
○ Xiamen Marathon	www.xmim.org/homes/home.html

Table B2 | Summary of best hyperparameters and testing estimations for each event.

Event	criterion	max_depth	max_leaf_n odes	min_samples_l eaf	min_samples _split	R ²	RMSE (%)
Overall	"mse"	15	150	10	45	0.33	2.55
Marathon	"mse"	10	150	10	18	0.30	2.67
50km race-walk	"mse"	6	20	10	2	0.50	3.32
20km race-walk	"mse"	8	30	10	4	0.58	2.36
10,000m	"mse"	6	200	10	9	0.24	1.92
5,000m	"mse"	15	70	10	10	0.39	1.89
3,000m-steeplechase	"mse"	20	150	10	27	0.21	2.41

Key: R² = coefficient of determination; RMSE=Root mean square error.

Table B3 | Cross validity statistics.

Cross validity statistics for the weather data reported by the race organizers and the associated data collected from the closest weather stations for 140 races (11% of total races: 2% of marathons; 33% of 50km race-walks; 39% of 20km race-walks; 21% of 10,000m; 20% of 5,000m; and 30% of 3,000m-steeplechase races).

	Reported (mean±sd °C)	Weather station (mean±sd °C)	Difference (mean±sd °C)	RMSE (mean±sd °C)	Effect size (Cohen's d)	Wilcoxon test (Z score ^{p-value})	Spearman correlation (rho ^{p-value})
Air temperature	23.6 ± 4.8	22.8 ± 5.3	-1.3 ± 3.1	2.5 ± 2.2	0.14	-2.92 ^(0.004)	0.82 ^(<0.001)
Simplified WBGT	24.0 ± 4.7	23.7 ± 5.0	-0.7 ± 2.2	1.6 ± 1.6	0.06	-3.19 ^(<0.001)	0.92 ^(<0.001)
Heat Index	24.0 ± 6.3	23.4 ± 7.0	-1.5 ± 3.8	2.8 ± 2.9	0.06	-3.31 ^(<0.001)	0.85 ^(<0.001)

Note: Difference = Value of weather station minus value reported by organizers; RMSE=Root mean square error

Table B4 | Competition statistics.

Number of athletes as well as the Wet-Bulb Globe Temperature (WBGT) and performance across each competition and event (mean \pm SD [min / max]).

Competition	Event	Athletes (n)	Temperature (°C)	WBGT (°C)	Performance decrement (%)
1 Olympic Games	Marathon	196	21.9 \pm 4.4 [14.2 / 31]	20.5 \pm 3.8 [11.7 / 29.8]	2.6 \pm 2.3 [-4.2 / 10.2]
	50km race-walk	120	22 \pm 5.4 [12.8 / 31.3]	20.6 \pm 5.2 [12.4 / 27.2]	2.1 \pm 4.5 [-6.7 / 15.1]
	20km race-walk	130	22.7 \pm 5 [14.0 / 30.4]	22.2 \pm 4.1 [13.2 / 29.3]	1.1 \pm 3.2 [-4.8 / 9.4]
	10,000m	220	20.1 \pm 4 [13.2 / 29.0]	17.6 \pm 3.6 [11.4 / 24.9]	0.9 \pm 1.4 [-2.4 / 4.5]
	5,000m	170	20.2 \pm 4.7 [12.2 / 27.2]	17.3 \pm 4.3 [10.2 / 25.9]	1.6 \pm 2.2 [-3.2 / 8.1]
	3,000m steeplechase	150	21 \pm 4.9 [10.0 / 29.0]	18.2 \pm 4.2 [8.0 / 24.8]	3.4 \pm 2.5 [-0.5 / 12.1]
2 World Championships	Marathon	320	23.8 \pm 5.9 [10.3 / 33.1]	21.4 \pm 4.3 [10.8 / 28.4]	4.3 \pm 2.7 [-2.1 / 15.2]
	50km race-walk	160	23.9 \pm 5.9 [14.0 / 32.4]	22.0 \pm 4.8 [14.0 / 29.3]	4.9 \pm 4.0 [-2.2 / 19.1]
	20km race-walk	270	25.5 \pm 5 [17.2 / 35.0]	22.2 \pm 4.0 [16.0 / 33.4]	4.5 \pm 3.5 [-3.3 / 16.4]
	10,000m	290	22.8 \pm 4.9 [13.0 / 32.4]	20.0 \pm 4.2 [11.3 / 28.2]	2.5 \pm 2.0 [-2.2 / 8.6]
	5,000m	240	21.8 \pm 5.2 [1.0 / 31.5]	18.8 \pm 4.3 [0.5 / 27.8]	2.7 \pm 2.3 [-1.5 / 8.6]
	3,000m steeplechase	170	24.1 \pm 4.8 [15.0 / 32.0]	20.7 \pm 4.7 [12.9 / 29.8]	2.3 \pm 1.4 [-2.1 / 5.6]
3 World Athletics Continental Cup	5,000m	75	21.7 \pm 6.3 [8.1 / 31.0]	18.1 \pm 4.4 [7.6 / 27.5]	4.5 \pm 5.2 [-6.7 / 16.7]
	3,000m steeplechase	73	22.4 \pm 6.2 [7.6 / 31.0]	18.9 \pm 4.4 [5.7 / 26.4]	3.7 \pm 3.7 [-3.1 / 18.0]
4 Commonwealth Games	Marathon	139	20.4 \pm 6.4 [14.0 / 33.4]	18.9 \pm 4.5 [13.3 / 26.0]	6.9 \pm 4.0 [-0.4 / 22.1]
	50km race-walk	14	23.7 \pm 5.5 [18.3 / 29.0]	20.5 \pm 2.4 [18.2 / 22.9]	4.2 \pm 10.1 [-7.0 / 32.2]
	20km race-walk	58	24.7 \pm 6 [16.9 / 33.6]	21.8 \pm 4.4 [16.6 / 28]	5.6 \pm 5.6 [-6.0 / 20.5]
	10,000m	156	18.8 \pm 3.9 [13.0 / 25.8]	16.4 \pm 3.1 [11.4 / 24.7]	2.9 \pm 2.5 [-1.6 / 9.9]
	5,000m	139	18.5 \pm 4.7 [12.0 / 28.8]	18.1 \pm 4.2 [12.9 / 30.0]	3.9 \pm 4.2 [-8.5 / 18.8]
	3,000m steeplechase	127	19.4 \pm 4.1 [11.0 / 26.8]	17.3 \pm 3.7 [10.1 / 23.5]	3.5 \pm 3.3 [-4.3 / 12.5]
5 Diamond Leagues	5,000m	838	17.8 \pm 4.5 [6.7 / 29.0]	15.2 \pm 4.2 [2.5 / 23.1]	3.2 \pm 1.9 [-0.8 / 11.3]
	3,000m steeplechase	289	20.1 \pm 5 [7.2 / 30.0]	16.9 \pm 4.3 [3.2 / 26.3]	4.5 \pm 2.0 [-0.9 / 11.8]
6 World Athletics Race Walking Team Championships	50km race-walk	100	17.8 \pm 3.8 [9.8 / 22.0]	17.6 \pm 4.7 [8.4 / 25.4]	5.3 \pm 2.9 [-1.7 / 11.2]
	20km race-walk	190	19.8 \pm 4.4 [12.0 / 29.2]	18.3 \pm 4.6 [11.1 / 31.8]	3.3 \pm 2.6 [-1.1 / 11.6]
7 World Athletics Gold Label Races	Marathon	1933	12.1 \pm 5.6 [5.0 / 29.8]	10.8 \pm 5.2 [- 7.0 / 29.9]	2.4 \pm 2.9 [-3.7 / 23.6]
	Marathon _{WT}	1300	12.1 \pm 5.6 [5.0 / 29.8]	10.8 \pm 5.2 [- 7.0 / 29.9]	24.2 \pm 11.1 [5.0 / 62.9]
Overall	Marathon	2588	13.3 \pm 6.6 [5.0 / 33.4]	12.0 \pm 6.0 [- 7.0 / 29.9]	10.0 \pm 12.2 [-4.2 / 62.9]

	50km race-walk	394	21.8 ± 5.8 [9.8 / 32.4]	20.4 ± 5.1 [8.4 / 29.3]	4.1 ± 4.5 [-7.0 / 32.2]
	20km race-walk	648	23.2 ± 5.5 [12.0 / 35.0]	21.1 ± 4.6 [11.1 / 33.4]	3.6 ± 3.7 [-6.0 / 20.5]
	10,000m	666	21 ± 4.7 [13.0 / 32.4]	18.3 ± 4.1 [11.3 / 28.2]	2.1 ± 2.1 [-2.4 / 9.9]
	5,000m	1462	19.1 ± 5 [1.0 / 31.5]	16.5 ± 4.5 [0.5 / 30.0]	3.0 ± 2.7 [-8.5 / 18.8]
	3,000m	809	21.3 ± 5.3	18.2 ± 4.5	3.6 ± 2.6
	steeplechase		[7.2 / 32.0]	[3.2 / 29.8]	[-4.3 / 18.0]

Key: Marathon_{WT} = marathon (well-trained runners)

Table B5 | World Athletics Gold Label Races.

Number of elite athletes as well as the Wet-Bulb Globe Temperature (WBGT) and performance across the World Athletics Gold Label Races (mean \pm SD [min / max]).

Race	Location (City, Country)	First/Collected year	Athletes (n)	Temperature (°C)	WBGT (°C)	Performance decrement (%)	
1	TCS Amsterdam Marathon	Amsterdam, Netherlands	1975/ 1989	92	12.0 \pm 4.0 [1.0 / 19.0]	11 \pm 3.9 [0.7 / 18.6]	1.5 \pm 1.8 [-1.1 / 6.9]
2	Athens Marathon The Authentic	Athens, Greece	1972/ 1987	75	18.5 \pm 4.1 [8.0 / 24.6]	16 \pm 4.3 [4.1 / 23.8]	4.0 \pm 4.0 [-0.9 / 15.8]
3	CFLD Beijing Marathon	Beijing, China	1981/ 1993	78	18.7 \pm 4.2 [7.0 / 27.0]	13.7 \pm 3.2 [5.4 / 19.7]	3.2 \pm 1.9 [-0.3 / 7.1]
4	BMW Berlin-Marathon	Berlin, Germany	1974/ 1989	84	14.3 \pm 3.0 [10.0 / 22.0]	13 \pm 2.6 [9.1 / 18.2]	1.3 \pm 1.5 [-1.7 / 7.0]
5	B.A.A. Boston Marathon	Boston, USA	1974/ 1989	85	8.1 \pm 3.8 [1.1 / 18.3]	8.5 \pm 3.8 [1.4 / 18.7]	3.2 \pm 3.0 [-2.3 / 12.6]
6	Bank of America Chicago Marathon	Chicago, USA	1977/ 1991	87	8.9 \pm 5.9 [-1.0 / 23.3]	7.9 \pm 5.4 [- 1.3 / 22.6]	2.3 \pm 2.3 [-1 / 8.4]
7	KBC Dublin Marathon	DUBLIN, Ireland	1980/ 1993	81	8.8 \pm 3.6 [2.7 / 15.6]	8.3 \pm 3.4 [2.2 / 14.7]	2.5 \pm 2.3 [-1.9 / 10]
8	Fukuoka International Open Marathon	Fukuoka, Japan	1947/ 1971	147	11.1 \pm 3.3 [3.1 / 16.9]	9.3 \pm 3.1 [1.4 / 14.7]	1.6 \pm 1.2 [-1.4 / 4.5]
9	Gold Coast Marathon	Gold Coast, Australia	1979/ 1992	84	16.8 \pm 1.9 [13 / 21.1]	14.1 \pm 1.9 [10.2 / 17.2]	3.3 \pm 2.5 [-0.7 / 9.1]
10	Standard Chartered Hong Kong Marathon	Hong Kong, China	1997/ 2004	48	19.2 \pm 5.0 [8.0 / 27.7]	16.3 \pm 4.3 [7.0 / 23.7]	2.1 \pm 2.0 [-1.3 / 8.9]
11	Jerusalem Marathon	Jerusalem, Israel	2011/ 2013	17	10.8 \pm 2.2 [8.5 / 15.1]	8.6 \pm 1.1 [7.4 / 10.4]	1.3 \pm 1.7 [-2.4 / 3.9]
12	Virgin Money London Marathon	London, Great Britain	1981/ 1993	65	11.8 \pm 3.8 [7.0 / 21]	12.3 \pm 3.9 [6.8 / 22.1]	0.8 \pm 1.0 [-1.1 / 3.7]
13	Maratón Ciudad de México	Mexico City, Mexico	1983/ 1995	68	14.4 \pm 2.3 [8.0 / 17.4]	14.6 \pm 2.8 [7.7 / 19.6]	3.3 \pm 2.1 [-1.2 / 12.5]
14	Tata Mumbai Marathon	Mumbai, India	2004/ 2009	33	26.8 \pm 1.7 [25.0 / 29.8]	25.7 \pm 2.2 [22.5 / 29.9]	0.4 \pm 0.9 [-1.5 / 1.9]
15	TCS New York City Marathon	New York City, USA	1970/ 1986	99	9.7 \pm 3.7 [3.3 / 16.1]	8.9 \pm 4.2 [-0.8 / 15.7]	2.0 \pm 1.5 [-2.1 / 5.7]
16	Lake Biwa Mainichi Marathon	Otsu, Japan	1946/ 1970	75	8.4 \pm 4.1 [0.0 / 18.8]	8.7 \pm 4.5 [0.1 / 21.6]	1.5 \pm 1.2 [-1.3 / 5.0]
17	Scotiabank Ottawa Marathon	Ottawa, Canada	1975/ 1989	80	11.1 \pm 4.0 [2.0 / 20.4]	11.3 \pm 3.6 [3.4 / 19.0]	3.1 \pm 3.7 [-1.0 / 14.5]
18	Schneider Electric Marathon de Paris	Paris, France	1976/ 1990	67	11.5 \pm 4.9 [5.0 / 24.1]	9.8 \pm 4.3 [3.6 / 20.4]	0.7 \pm 0.9 [-1.3 / 2.2]
19	Philadelphia Marathon Weekend	Philadelphia, USA	1954/ 1975	90	5.2 \pm 4.2 [- 4.0 / 16.1]	3.8 \pm 4.2 [- 5.4 / 15.4]	3.9 \pm 2.8 [-1.9 / 10.1]
20	NN Marathon Rotterdam	Rotterdam, Netherlands	1981/ 1993	81	11.7 \pm 3.8 [6.9 / 23.3]	10.7 \pm 3.4 [6.0 / 20.4]	1.4 \pm 1.2 [-1.1 / 4.1]
21	Seoul Marathon	Seoul, Korea	1993/ 2001	57	8.9 \pm 4.7 [- 5.0 / 16.5]	5.8 \pm 4.2 [-7.0 / 13.1]	1.2 \pm 1.3 [-1.0 / 5.1]
22	Shanghai International Marathon	Shanghai, China	2000/ 2006	39	15.8 \pm 4.5 [8.0 / 24]	12.5 \pm 3.7 [6.7 / 19.6]	0.9 \pm 1.4 [-2.7 / 4.9]
23	Blackmores Sydney Marathon	Sydney, Australia	2001/ 2007	39	15.9 \pm 3.6 [9.0 / 23.3]	13.9 \pm 3.2 [7.5 / 19.0]	3.4 \pm 4 [-2.1 / 14.3]
24	Tokyo Marathon	Tokyo, Japan	2007/ 2011	23	8.2 \pm 3.6 [3.2 / 16.5]	7.2 \pm 3.4 [1.2 / 14.6]	0.6 \pm 0.7 [-1.4 / 1.6]

25	Scotiabank Toronto Waterfront Marathon	Toronto, Canada	1977/ 1991	55	9.4 ± 3.6 [2.0 / 16.0]	9.4 ± 3.9 [1.8 / 16.7]	9.9 ± 6.2 [-3.7 / 23.6]
26	Maratón Valencia Trinidad Alfonso EDP	Valencia, Spain	1981/ 1993	73	9.7 ± 2.5 [5.0 / 15.0]	9.6 ± 2.5 [5.2 / 15.4]	1.3 ± 2.3 [-1.4 / 11.6]
27	Vienna City Marathon	Vienna, Austria	1984/ 1995	75	14.7 ± 4.6 [3.0 / 24.7]	13.5 ± 4.5 [1.9 / 22.8]	2.1 ± 1.8 [-1.0 / 5.9]
28	Xiamen Marathon	Xiamen, China	2003/ 2008	36	17.5 ± 2.8 [13.0 / 24.0]	14.5 ± 2.5 [10.1 / 20.0]	1.2 ± 1.6 [-1.0 / 4.1]

Table B6 | Decision tree analysis.

Testing estimations of machine learning decision tree analysis between air temperature and Wet Bulb Globe Temperature for each event.

Event	Air temperature		Wet Bulb Globe Temperature	
	R ²	RMSE (%)	R ²	RMSE (%)
Overall	0.17	-2.86	0.19	-2.81
Marathon	0.21	-2.85	0.13	-2.98
50km race-walk	0.23	-4.11	0.36	-3.74
20km race-walk	0.34	-2.98	0.47	-2.67
10,000m	0.17	-2.00	0.11	-2.08
5,000m	0.15	-2.23	0.15	-2.23
3,000m-steeplechase	0.04	-2.65	0.11	-2.56

Key: R² = coefficient of determination; RMSE=Root mean square error.

Table B7 | Regression equations.

Regression equations and indicators for each of the models developed through linear and non-linear regression analyses using the least squares method. The exploratory models estimate performance decrement (percent difference between an athlete's finish time and the competition's standing record) for every degree Celsius in air temperature, Heat Index, Simplified WBGT, and WBGT across the studied events. The confirmatory models repeated the analysis using multiple non-linear regression with the number of races for each degree WBGT inserted in each model as a covariate. In this case, the aim was not to derive formulas but to confirm that the exploratory models were not affected by the number of races held at different weather conditions.

Event	Type	Equation	R ²	F _(p)	AIC	BIC
Marathon (elite runners)	exploratory	$3.3744 - 0.22334 \cdot T_{air} + 0.01031 \cdot T_{air}^2$	0.72	16.93(<0.001)	46.86	49.18
		$3.25875 - 0.17453 \cdot HI + 0.00802 \cdot HI^2$	0.85	43.57(<0.001)	43.23	45.90
		$2.26656 - 0.08563 \cdot SWBGT + 0.00654 \cdot SWBGT^2$	0.71	13.63(<0.001)	42.60	44.52
		$2.65558 - 0.10119 \cdot WBGT + 0.00688 \cdot WBGT^2$	0.87	45(<0.001)	28.83	31.15
	confirmatory	---	0.58	2.78(0.08)	52.52	57.15
Marathon (well-trained runners)	exploratory	$19.59283 + 0.48737 \cdot WBGT$	0.90	36.32(<0.001)	42.82	44.01
	confirmatory	---	0.92	11.30(0.009)	46.63	49.02
50km race-walk	exploratory	$0.77154 + 0.09802 \cdot T_{air} + 0.002 \cdot T_{air}^2$	0.43	2.61(0.14)	42.83	43.74
		$4.51546 - 0.31142 \cdot HI + 0.01172 \cdot HI^2$	0.58	5.54(0.03)	46.89	48.08
		$16.19115 - 1.3821 \cdot SWBGT + 0.03534 \cdot SWBGT^2$	0.80	12.01(0.007)	30.27	30.87
		$6.22243 - 0.40987 \cdot WBGT + 0.0129 \cdot WBGT^2$	0.31	1.55(0.28)	45.10	46.01
	Confirmatory	---	0.82	2.92(0.200)	48.48	49.66
20km race-walk	exploratory	$3.23086 - 0.31683 \cdot T_{air} + 0.01303 \cdot T_{air}^2$	0.88	26.66(<0.001)	30.28	31.18
		$2.60931 - 0.22993 \cdot HI + 0.01045 \cdot HI^2$	0.94	59.36(<0.001)	26.67	27.86
		$9.88573 - 0.96482 \cdot SWBGT + 0.028 \cdot SWBGT^2$	0.88	19.13(0.004)	25.33	25.56
		$3.72957 - 0.4045 \cdot WBGT + 0.01698 \cdot WBGT^2$	0.96	57.94(<0.001)	13.66	13.90
	confirmatory	---	0.96	23.14(0.005)	27.14	28.96
10,000m	exploratory	$0.04628 + 0.14899 \cdot T_{air} - 0.00204 \cdot T_{air}^2$	0.39	1.6(0.29)	15.97	16.21
		$3.90221 - 0.1974 \cdot HI + 0.0051 \cdot HI^2$	0.23	1.07(0.39)	27.78	28.69
		$0.64516 + 0.03449 \cdot SWBGT - 0.0015 \cdot SWBGT^2$	0.94	43.9(<0.001)	-2.22	-1.98

		$-0.07927 + 0.14515 \cdot$ $WBGT - 0.00132 \cdot$ $WBGT^2$	0.72	6.57 _(0.04)	11.39	11.63
	confirmatory	---	0.92	2.48 _(0.446)	-7.53	-7.86
5,000m		$6.61155 - 0.52001 \cdot Tair +$ $0.01644 \cdot Tair^2$	0.71	8.66 _(0.013)	25.68	26.59
	exploratory	$5.35413 - 0.34045 \cdot HI +$ $0.01107 \cdot HI^2$	0.51	4.18 _(0.057)	29.37	30.56
		$5.76537 - 0.40724 \cdot$ $WBGT + 0.01391 \cdot$ $WBGT^2$	0.50	3.02 _(0.12)	19.45	20.04
	confirmatory	---	0.48	0.94 _(0.52)	42.05	44.43

Note: the least squares fit criterion was satisfied in all models ($p = 0.005$), confirming that in each case the data and the model with the best-fit parameters are consistent.
 Key: R^2 = coefficient of determination; $F_{(p)}$ = F statistic and associated probability; AIC = Akaike information criterion; BIC = Bayesian information criterion.

Figure B.1 | Performance decrement (competition’s standing record)

Performance decrement (percent difference between an athlete’s finish time and the competition’s standing record) for every degree Wet-Bulb Globe Temperature (WBGT) across the studied events based on linear and non-linear regression analyses using the least squares method. Performance is always negative (indicating impaired average performance) because, on average, the percent difference from the standing record was negative. The coefficient of determination (R^2) as well as the probability (p) from the ANOVA test are illustrated in each model. Detailed information on the regression equation and the indicators of each model are provided Table B4.

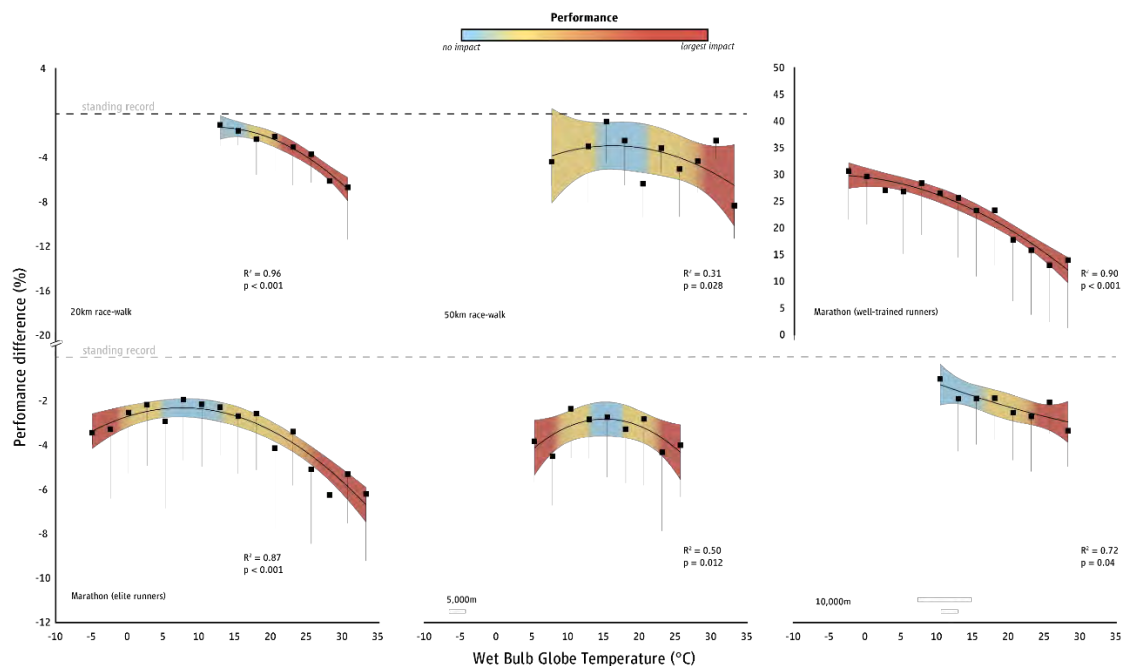


Figure B.2 | Performance decrement (event's world record).

Performance decrement (percent difference between an athlete's finish time and the event's world record) for every degree Wet-Bulb Globe Temperature (WBGT) across the studied events based on linear and non-linear regression analyses using the least squares method. Performance is always negative (indicating impaired average performance) because, on average, the percent difference from the standing record was negative. The coefficient of determination (R^2) as well as the probability (p) from the ANOVA test are illustrated in each model.

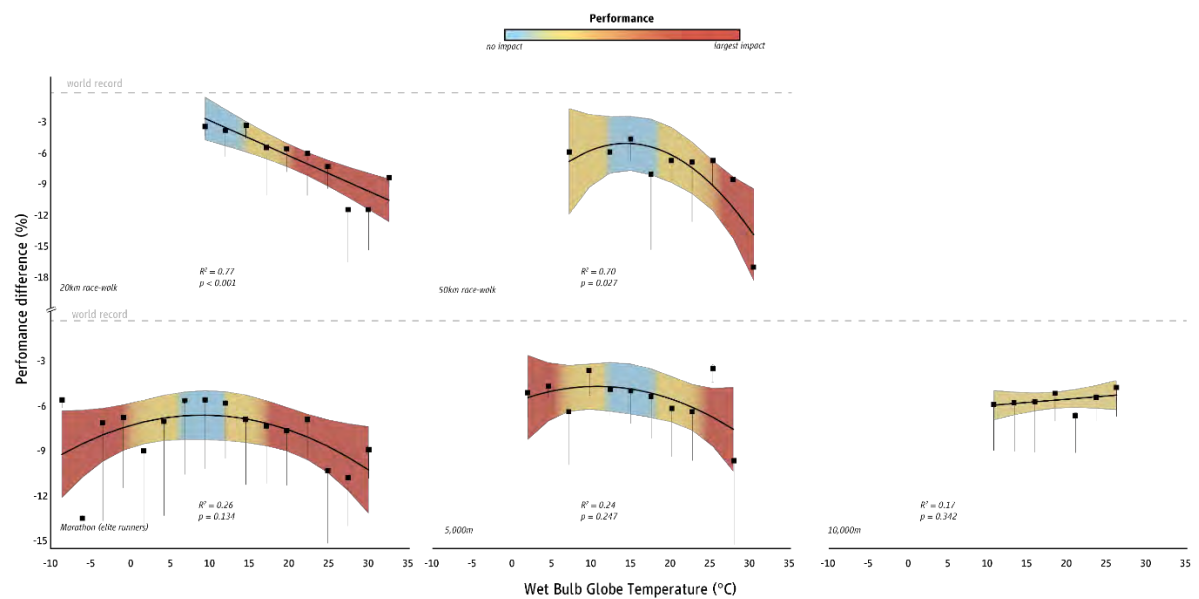


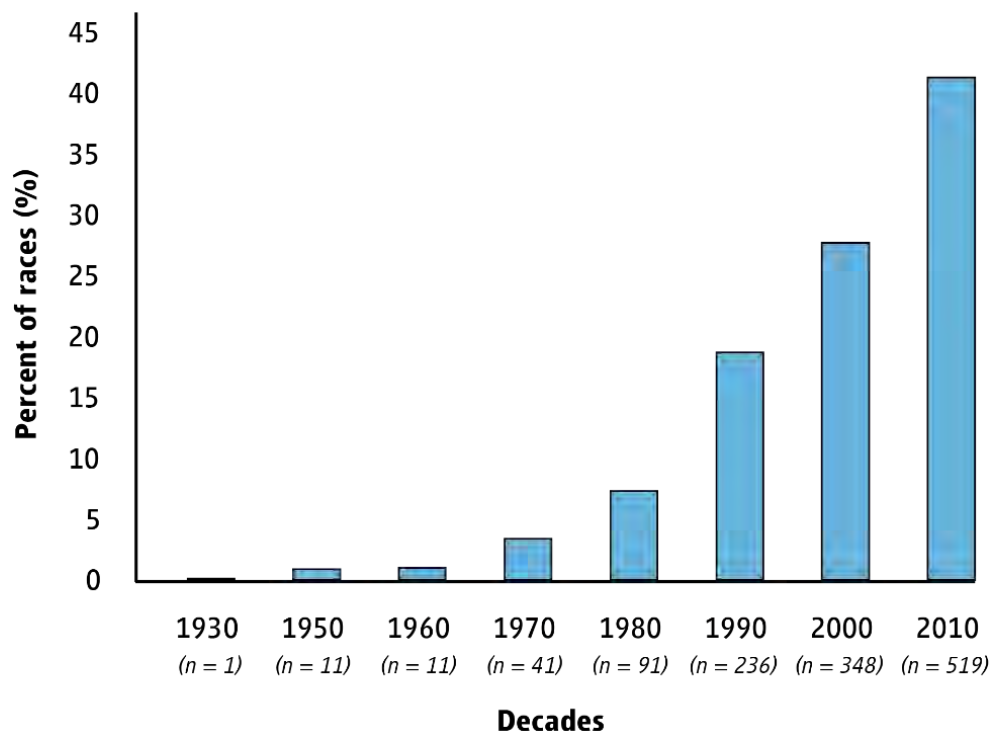
Figure B.3 | Percentage and number of races for 1258 races held between 1936 and 2019.

Figure B.4 | Decision tree (50km race-walk).

Decision tree linking weather conditions and performance in the 50km race-walk. The algorithm is organized in a binary tree: each node asks questions about the weather conditions providing, in the end, an estimate of the performance decrement (since, on average, the percent difference from the standing record was negative, indicating impaired average performance). The values are rounded on the nearest integer and the decision tree is presented at a maximum depth of four.

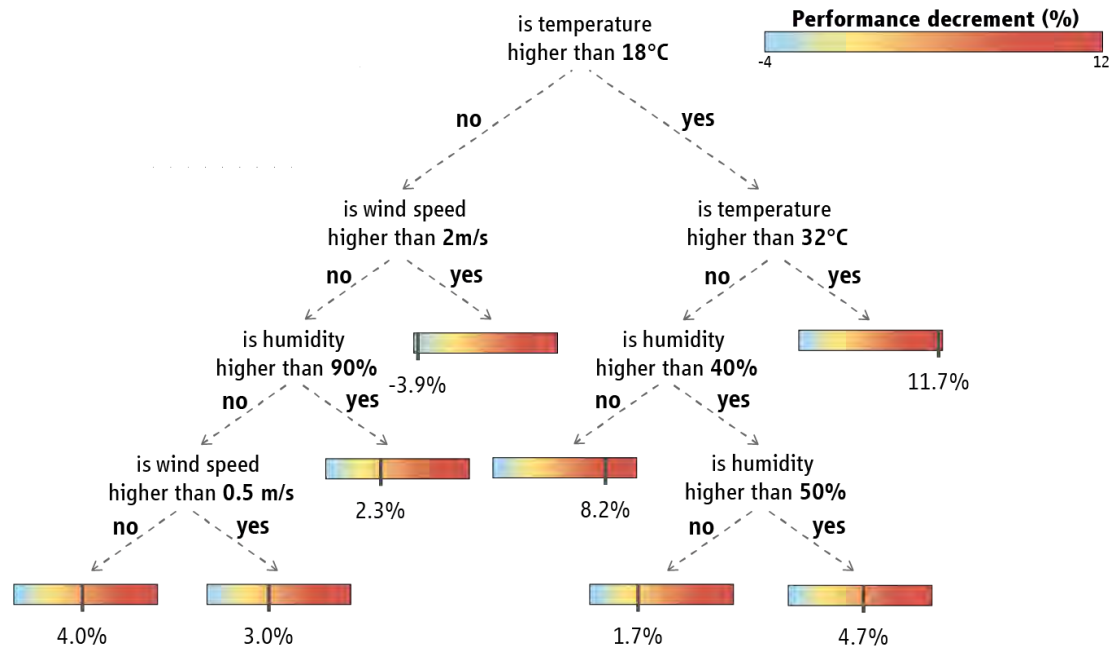


Figure B.5 | Decision tree (20km race-walk).

Decision tree linking weather conditions and performance in the 20km race-walk. The algorithm is organized in a binary tree: each node asks questions about the weather conditions providing, in the end, an estimate of the performance decrement (since, on average, the percent difference from the standing record was negative, indicating impaired average performance). The values are rounded on the nearest integer and the decision tree is presented at a maximum depth of four.

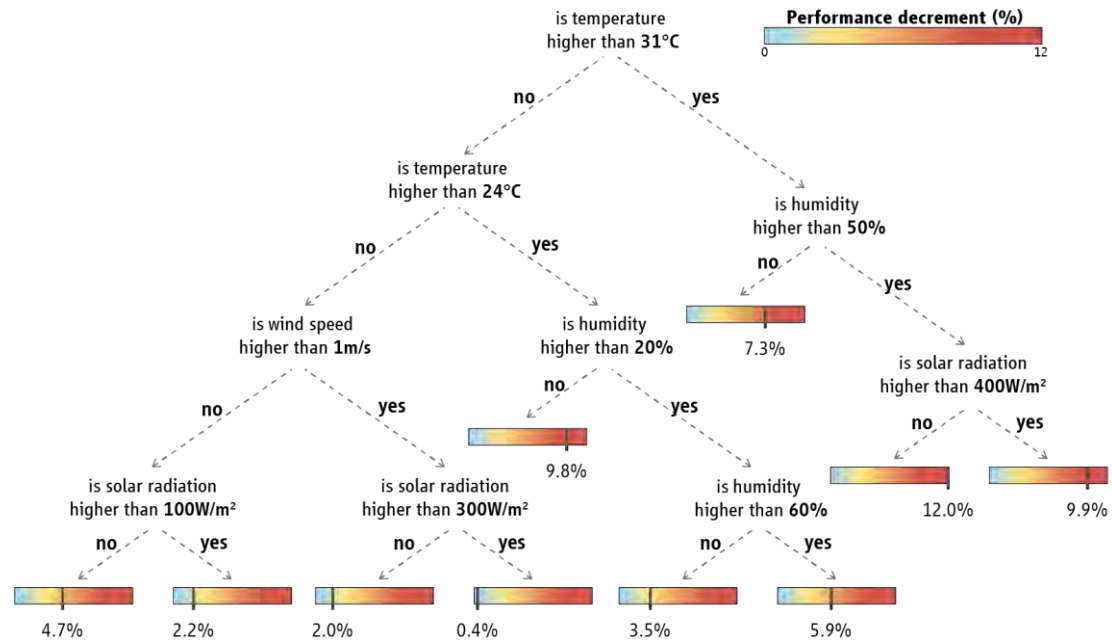


Figure B.6 | Decision tree (10,000m).

Decision tree linking weather conditions and performance in the 10,000m. The algorithm is organized in a binary tree: each node asks questions about the weather conditions providing, in the end, an estimate of the performance decrement (since, on average, the percent difference from the standing record was negative, indicating impaired average performance). The values are rounded on the nearest integer and the decision tree is presented at a maximum depth of four.

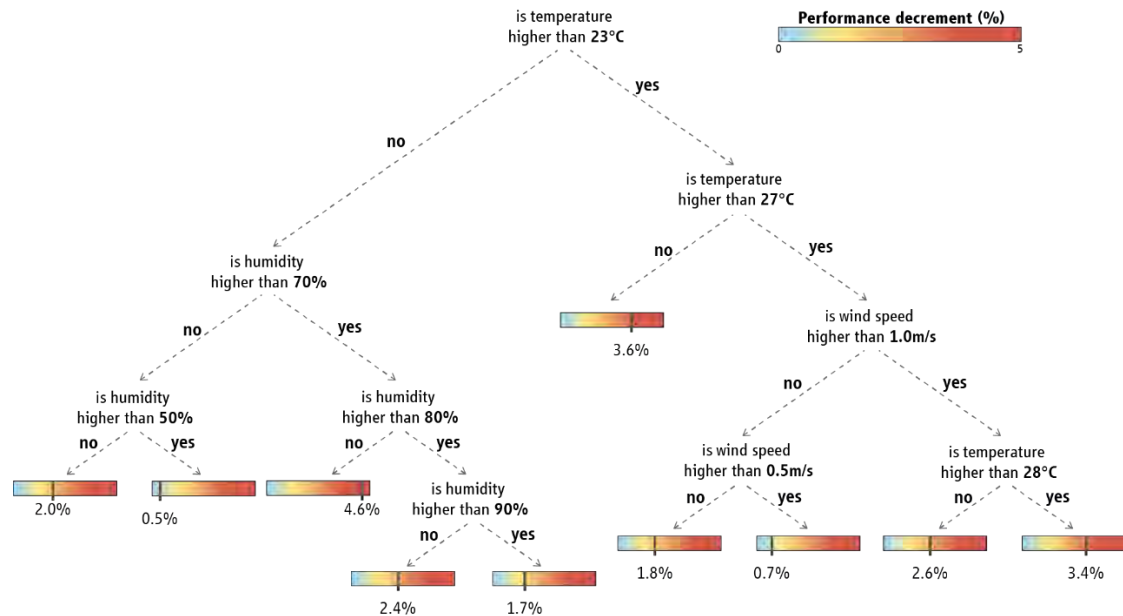


Figure B.7 | Decision tree (5,000m).

Decision tree linking weather conditions and performance in the 5,000m. The algorithm is organized in a binary tree: each node asks questions about the weather conditions providing, in the end, an estimate of the performance decrement (since, on average, the percent difference from the standing record was negative, indicating impaired average performance). The values are rounded on the nearest integer and the decision tree is presented at a maximum depth of four.

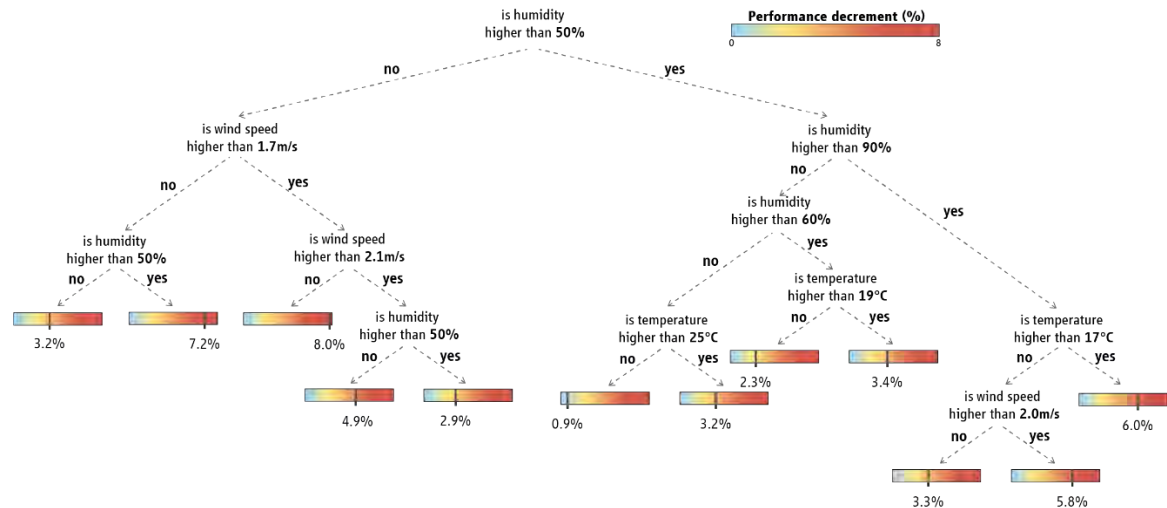


Figure B.8 | Decision tree (3,000m-steeplechase).

Decision tree linking weather conditions and performance in the 3,000m-steeplechase. The algorithm is organized in a binary tree: each node asks questions about the weather conditions providing, in the end, an estimate of the performance decrement (since, on average, the percent difference from the standing record was negative, indicating impaired average performance). The values are rounded on the nearest integer and the decision tree is presented at a maximum depth of four.

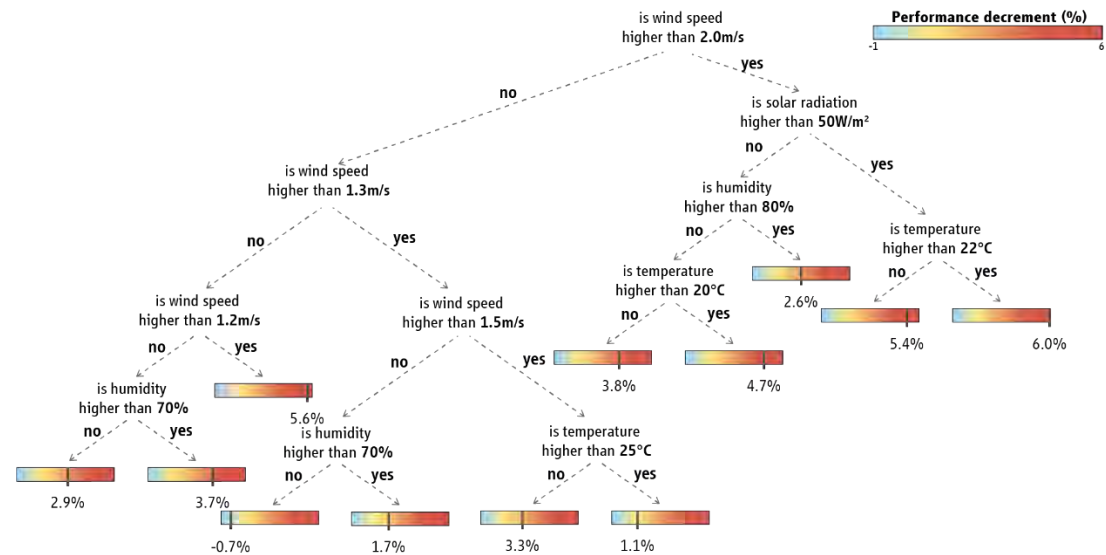


Figure B.10 | Impact of heat stress on 20km race-walk.

The impact of heat stress on 20km race-walk performance for every degree Celsius across a wide range of finishing times. Numbers indicate minutes:seconds of added time to performance based on the air temperature, heat index, simplified WBGT, and WBGT. Colours illustrate the level heat-induced impact on performance. Performance is either unaffected or impaired because, on average, the percent difference from the standing record was negative.

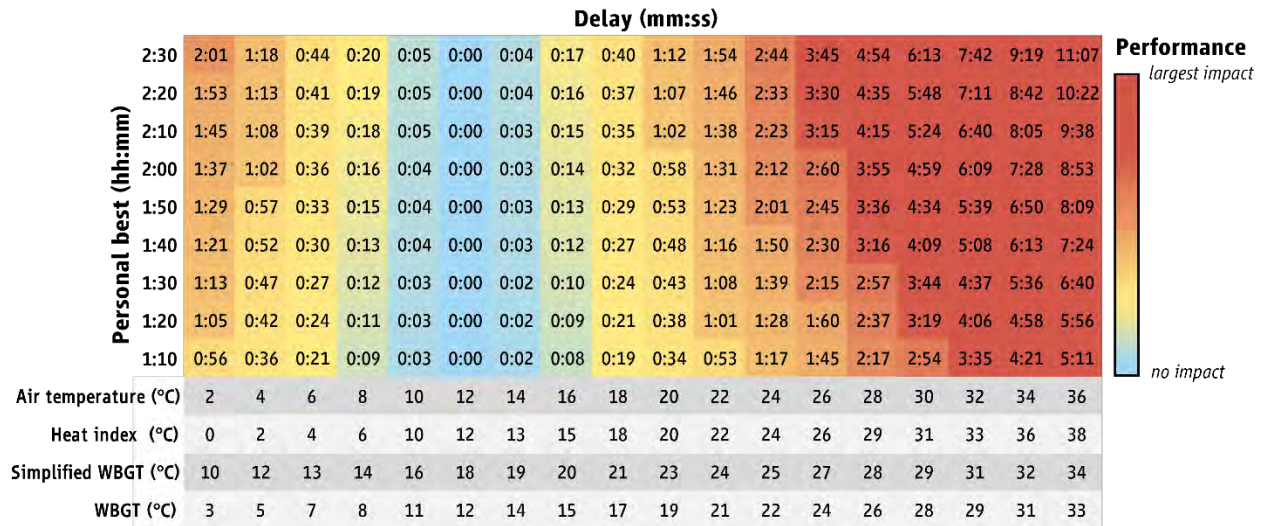


Figure B.11 | Impact of heat stress on 10,000m.

The impact of heat stress on 10,000m performance for every degree Celsius across a wide range of finishing times. Numbers indicate seconds of added time to performance based on the air temperature, heat index, simplified WBGT, and WBGT. Colours illustrate the level heat-induced impact on performance. Performance is either unaffected or impaired because, on average, the percent difference from the standing record was negative.

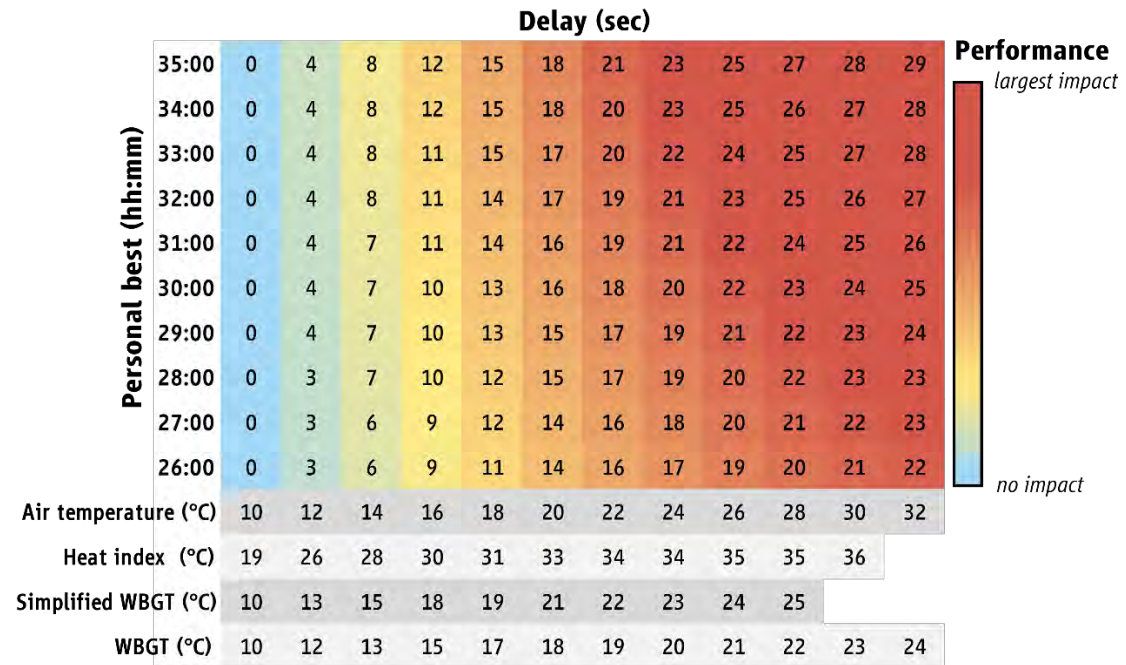
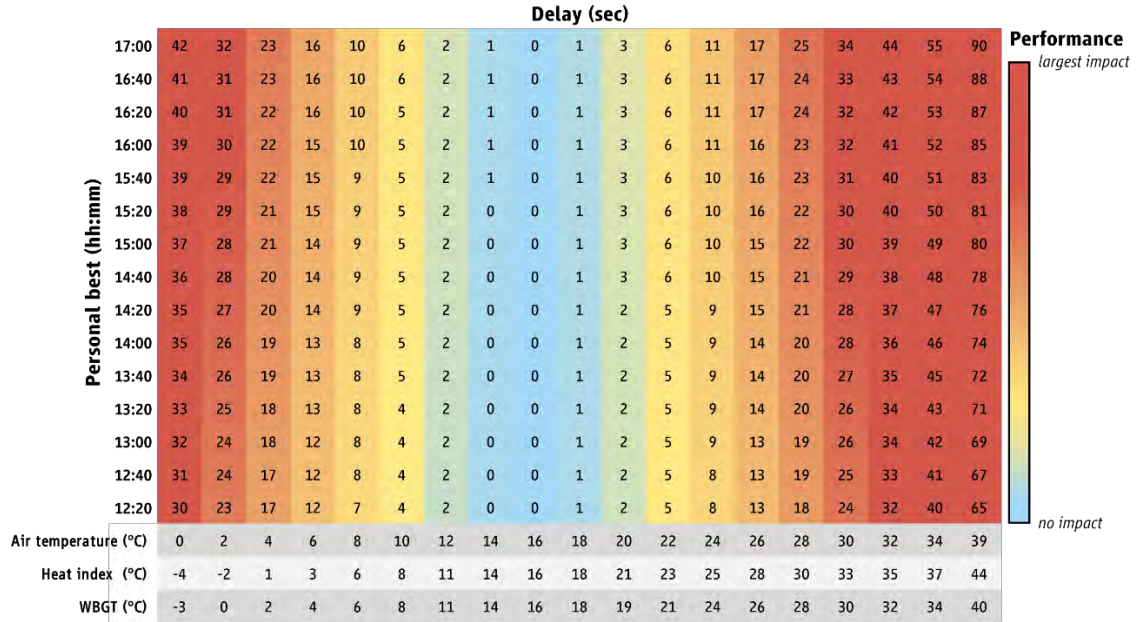


Figure B.12 | Impact of heat stress on 5,000m.

The impact of heat stress on 5,000m performance for every degree Celsius across a wide range of finishing times. Numbers indicate seconds of added time to performance based on the air temperature, heat index, and WBGT. Colours illustrate the level heat-induced impact on performance. Performance is either unaffected or impaired because, on average, the percent difference from the standing record was negative.



Annexes

Annex A: Ethics



Εσωτερική Επιτροπή Δεοντολογίας

Τρίκαλα: 9/6/2021
Αριθμ. Πρωτ:1808

Βεβαίωση έγκρισης της πρότασης για διεξαγωγή Έρευνας με τίτλο: Τεχνολογικές εφαρμογές για την βελτίωση της αθλητικής απόδοσης.

Επιστημονικώς υπεύθυνος / επιβλέπων: Δρ. Ανδρέας Φλουρής
Ιδιότητα: Καθηγητής
Ίδρυμα: Πανεπιστήμιο Θεσσαλίας
Τμήμα: ΤΕΦΑΑ

Κύριος ερευνητής/φοιτητής: Μάντζιος Κωνσταντίνος
Πρόγραμμα Σπουδών: Διδακτορικό
Ίδρυμα: Πανεπιστήμιο Θεσσαλίας
Τμήμα: ΤΕΦΑΑ

Η προτεινόμενη έρευνα θα είναι: Ερευνητικό πρόγραμμα

Τηλ. επικοινωνίας: 6948626874
Email επικοινωνίας: konstantinosmantzios@gmail.com

Η Εσωτερική Επιτροπή Δεοντολογίας του Τ.Ε.Φ.Α.Α., Πανεπιστημίου Θεσσαλίας μετά την υπ. Αριθμ. 3-3/9-6-2021 συνεδρίασή της εγκρίνει τη διεξαγωγή της προτεινόμενης έρευνας.

Ο Πρόεδρος της
Εσωτερικής Επιτροπής
Δεοντολογίας – ΤΕΦΑΑ

Τσιόκανος Αθανάσιος
Καθηγητής



Εσωτερική Επιτροπή Δεοντολογίας

Τρίκαλα: 9/2/2022
Αριθμ. Πρωτ:1890

Βεβαίωση έγκρισης της πρότασης για διεξαγωγή Έρευνας με τίτλο: Επιπτώσεις της θερμοκρασίας πυρήνα σώματος στην αθλητική απόδοση.

Επιστημονικώς υπεύθυνος / επιβλέπων: Δρ. Ανδρέας Φλουρής
Ιδιότητα: Καθηγητής
Ίδρυμα: Πανεπιστήμιο Θεσσαλίας
Τμήμα: ΤΕΦΑΑ

Κύριος ερευνητής/φοιτητής: Μάντζιος Κωνσταντίνος
Πρόγραμμα Σπουδών: Διδακτορικό
Ίδρυμα: Πανεπιστήμιο Θεσσαλίας
Τμήμα: ΤΕΦΑΑ
Η προτεινόμενη έρευνα θα είναι: Ερευνητικό πρόγραμμα

Τηλ. επικοινωνίας: 6948626874
Email επικοινωνίας: konstantinosmantzios@gmail.com

Η Εσωτερική Επιτροπή Δεοντολογίας του Τ.Ε.Φ.Α.Α., Πανεπιστημίου Θεσσαλίας μετά την υπ. Αριθμ. 4-1/9-2-2022 συνεδρίασή της εγκρίνει τη διεξαγωγή της προτεινόμενης έρευνας.

Ο Πρόεδρος της
Εσωτερικής Επιτροπής
Δεοντολογίας – ΤΕΦΑΑ

Τσιόκανος Αθανάσιος
Καθηγητής



University of Thessaly
Department of Physical Education and Sport Science



Internal Ethics Committee

Trikala: 6/4/2016
Protocol Number.: 1095

Approval of research entitled: smartHELMET: effects of different helmets on performance and physiological indices during cycling in varying environmental temperatures.

Scientist responsible – supervisor: Dr. Andreas D. Flouris

Main researcher – student: Dr. Vasilios Sideris

Institution & Department: FAME Laboratory, Department of Physical Education and Sport Science, University of Thessaly; Biomechanical Solutions Ltd.

The proposed research relates to a:

Research grant Postgraduate thesis Undergraduate thesis Independent research

Contact phone: +30 2431 500 601

Contact email: andreasflouris@gmail.com

The Internal Ethics Committee (IEC) of the Department of PE and Sport Science (DPESS), University of Thessaly, examined the proposal in its 1-2/10-2-2016 meeting and approves the implementation of the proposed research.

The Chair of the IEC – DPESS

Athanasios Tsiokanos, PhD

Annex B: Student's Contribution in Paper

Towards Model-Based Online Monitoring of Cyclist's Head Thermal Comfort: Smart Helmet Concept and Prototype

Ali Youssef, Jeroen Colon, Konstantinos Mantzios, Paraskevi Gkiata, Tiago S. Mayor, Andreas D. Flouris, Guido De Bruyne, and Jean-Marie Aerts

I hereby affirm that Konstantinos Mantzios has made significant contributions to the experimental work conducted, as well as the review process of the manuscript for the above paper to be completed.

Author Name: Ali Youssef

Date: 18/05/2023

Signature:



Towards Model-Based Online Monitoring of Cyclist's Head Thermal Comfort: Smart Helmet Concept and Prototype

Ali Youssef, Jeroen Colon, Konstantinos Mantzios, Paraskevi Gkiata, Tiago S. Mayor, Andreas D. Flouris, Guido De Bruyne, and Jean-Marie Aerts

I hereby affirm that Konstantinos Mantzios has made significant contributions to the experimental work conducted, as well as the review process of the manuscript for the above paper to be completed.

Author Name: Jeroen Colon

Date: 22 may 2023

Signature:



Towards Model-Based Online Monitoring of Cyclist's Head Thermal Comfort: Smart Helmet Concept and Prototype

Ali Youssef, Jeroen Colon, Konstantinos Mantzios, Paraskevi Gkiata, Tiago S. Mayor, Andreas D. Flouris, Guido De Bruyne, and Jean-Marie Aerts

I hereby affirm that Konstantinos Mantzios has made significant contributions to the experimental work conducted, as well as the review process of the manuscript for the above paper to be completed.

Author Name: Jean-Marie Aerts

Date: 2 May 2023

Signature:



Towards Model-Based Online Monitoring of Cyclist's Head Thermal Comfort: Smart Helmet Concept and Prototype

Ali Youssef, Jeroen Colon, Konstantinos Mantzios, Paraskevi Gkiata, Tiago S. Mayor, Andreas D. Flouris, Guido De Bruyne, and Jean-Marie Aerts

I hereby affirm that Konstantinos Mantzios has made significant contributions to the experimental work conducted, as well as the review process of the manuscript for the above paper to be completed.

Author Name: Tiago Sotto Mayor Moura Santos

Date: 2023-05-18



Assinado por: Tiago Sotto
Mayor Moura Santos
Identificação: B110510199
Data: 2023-05-18 às 09:57:41
Local: Porto
Motivo: Agreed

Signature:

Towards Model-Based Online Monitoring of Cyclist's Head Thermal Comfort: Smart Helmet Concept and Prototype

Ali Youssef, Jeroen Colon, Konstantinos Mantzios, Paraskevi Gkiata, Tiago S. Mayor, Andreas D. Flouris, Guido De Bruyne, and Jean-Marie Aerts

I hereby affirm that Konstantinos Mantzios has made significant contributions to the experimental work conducted, as well as the review process of the manuscript for the above paper to be completed.

Author Name: Paraskevi Gkiata

Date: 8/5/2023

Signature:



Risk assessment for heat stress during work and leisure

Leonidas G. Ioannou, Giorgos Gkikas, Konstantinos Mantzios, Lydia Tsoutsoubi, Andreas D. Flouris

I hereby affirm that Konstantinos Mantzios has made significant contributions to the experimental work conducted, as well as the review process of the manuscript for the above book chapter to be completed.

Author Name: Leonidas Ioannou

Date: 02/05/2023

Signature:



Risk assessment for heat stress during work and leisure

Leonidas G. Ioannou, Giorgos Gkikas, Konstantinos Mantzios, Lydia Tsoutsoubi, Andreas D. Flouris

I hereby affirm that Konstantinos Mantzios has made significant contributions to the experimental work conducted, as well as the review process of the manuscript for the above book chapter to be completed.

Author Name: Gkikas Georgios

Date: 03/05/2023

Signature:



Risk assessment for heat stress during work and leisure

Leonidas G. Ioannou, Giorgos Gkikas, Konstantinos Mantzios, Lydia Tsoutsoubi, Andreas D. Flouris

I hereby affirm that Konstantinos Mantzios has made significant contributions to the experimental work conducted, as well as the review process of the manuscript for the above book chapter to be completed.

Author Name: Lydia Tsoutsoubi

Date: 02/05/2023

Signature:

